Title
Water Dynamics in Giant Trees

Author
Williams, Cameron B.

Publication Date
2017

Peer reviewed|Thesis/dissertation

Water Dynamics in Giant Trees

by

Cameron B. Williams

A dissertation submitted in partial satisfaction of the

requirements for the degree of

Doctor of Philosophy

in

Integrative Biology

in the

Graduate Division

of the

University of California, Berkeley

Committee in charge:

Professor Todd E. Dawson, Chair
Professor John J. Battles
Professor George Koch
Professor Cynthia Looy

Fall 2017

Water Dynamics in Giant Trees

by

Cameron B. Williams

Abstract

Water Dynamics in Giant Trees

by

Cameron B. Williams

Doctor of Philosophy in Integrative Biology

University of California, Berkeley

Professor Todd E. Dawson, Chair

The Earth's tallest trees tend to grow in geographic regions where water is abundant. An abundance of water in the environment, however, does not by itself enable trees to overcome several inherent challenges with being tall. First, water must be transported over very long distances through tiny conduits, and it adheres to their inside walls. Thus, the progress of water flow is impeded by hydraulic resistance that may accumulate with longer transport distances. Second, gravity pulling down on the water imparts a tension that increases with height in tree at a rate of –0.01 MPa m^{-1}. Therefore, water inside foliage and branches at the top of a 100 m tall tree is under far more tension than foliage emerging from the base, yet normal physiological processes still occur. Third, environmental conditions become increasingly desiccating with height in forest canopy. Relative humidity decreases while sunlight, wind speed, and vapor pressure deficit increase along this vertical gradient. The strategies trees use to overcome these three challenges in part enable them to grow so tall. In order to improve our understanding of the limits to tree height growth, I studied the mechanisms by which tall trees cope with these height-related constraints, using the conifers coast redwood (*Sequoia sempervirens* (D. Don) Endlicher) and giant sequoia (*Sequoiadendron giganteum* (Lindley) J. Buchholz) as well as the angiosperm mountain ash (*Eucalyptus regnans* F. von Mueller).

In *Chapter 1*, I explored two mechanisms that trees use to compensate for the accumulation of hydraulic resistance with height growth. The first mechanism is varying the diameters of the conduits with height in tree according to a theoretical model, wherein a series of conduits from tree top to base widens at a specific minimum rate that is maintained throughout height growth. The premise is based in fluid dynamics. An elongating series of cylindrical conduits with constant diameter is hydraulically less efficient than the same elongating series that also widens. I tested this model in exceptionally tall individuals of coast redwood, giant sequoia, and mountain ash. Data matched the theoretical predictions. However, a decelerating rate of conduit widening was observed in the bottom one-third of the trees suggesting a limit to this hydraulic compensation mechanism that I interpreted as an optimization of carbon investment for a given hydraulic benefit. The second mechanism is a whole-tree increase in the amount of sapwood that provisions the leaves. Across a large range of tree sizes, I quantified the rate of accumulation of sapwood relative to leaf area using data available from the literature. Sapwood accumulated at a faster rate than leaf area in the conifers but the rates were equivalent in mountain ash. Sapwood and leaves serve water supply and demand roles, but they are also

carbon sinks and sources, respectively. I therefore interpreted these results as hydraulic compensation in the conifers that may limit height growth due to carbon balance constraints, whereas the mountain ash appeared to have additional height growth potential. Limits to these two compensation mechanisms may thus be imposed by carbon balance constraints that limit tree height growth.

Chapter 2 investigates water relations of the foliage of giant sequoia, to determine how foliage remains adequately hydrated against height-related constraints. Together with coauthors Rikke Reese Næsborg and Todd E. Dawson, I generated pressure-volume curves on foliage collected crown-wide from 12 large giant sequoia trees up to 95 m tall, to identify the tissue-level drivers responsible for maintenance of sufficient turgor pressures and water contents both with height tree and over time as the dry season progressed. Hydraulic capacitance was about twice as large as reported for other tree species. Maintenance of turgor pressure in all parts of the trees was accomplished by increases in tissue osmotica with height that depressed the turgor loss point at a rate equivalent to the gravitational potential gradient. High relative water contents were sustained with height by building structurally stiffer tissues as well as carrying an increased proportion of water in the symplasm versus apoplasm. Seasonal increases in the fraction of apoplastic water were important for maintaining physiological function when water in the environment may have been more limiting. This suite of foliar water relations traits permits minimum midday water potentials to operate close to the turgor loss point and may also enable the Earth's largest tree species to survive short-term drought.

In *Chapter 3*, I quantify the importance of stem water storage in tall giant sequoia. Water storage in trees is known to contribute substantially to daily transpiration to extend physiological function, but does gravity dampen the dynamics of water storage with height? In the top 5 to 6 m of tall giant sequoia trees I collected detailed architectural information and installed automated sensors that monitored diurnal fluxes in sap flow, stem diameter, and water potential. To provide context for water use at the tree tops, I also installed sap flow gauges at the tree bases. Unsurprisingly, larger stems released larger volumes of stored water. However, tree top water storage contributed a tiny fraction of daily transpired water, and hydraulic capacitance was similarly low, supporting the hypothesis that chronically low water potentials dampen the water storage dynamics with height in tall trees. Lag times among the sensors indicated that a large portion of the stored water was expressed from live secondary phloem tissues of the inner bark. Despite the reliance on seemingly small volumes of stored water, whole-tree sap flow exceeded 3000 L d^{-1}, which is the highest daily water budget reported for any tree on Earth.

These studies together underscore how water use and management in giant trees is truly dynamic over space and time. Over a tree's lifetime, modifications to sapwood anatomy and volume foster efficient water movement along the entire flow path. Seasonal shifts in the compartments where foliar water is held may extend physiological processes during dry periods. The physiological consequences of daily swings in atmospheric conditions are controlled by tissue osmotic and elastic properties, as well as the release of stored water to the transpiration stream. Each of these dynamics varies along a tree's vertical profile to compensate for height-related constraints and enables the tallest trees to support functional leaves well beyond 100 m above the ground.

DEDICATION

To all enthusiasts of big trees.

TABLE OF CONTENTS

ACKNOWLEDGEMENTS

What do family, friends, colleagues, tree climbers, and skateboarders have in common? All provided various kinds of support for the developmental and educational processes leading to this document and degree.

First and foremost, I owe my current position in life to my Dad who inspired curiosity about the natural world, to my Mom who nurtured me in the aftermaths of the many bad decisions I made growing up, and to my sister who provided a source of competition that encouraged me to seek higher education. Without their influences, I'd probably still be working at Subway. And I am indebted to my wife Rikke for providing a foundational psyche from which to operate, for her encouragement to actually finish this ball-and-chain dissertation, for navigating the complicated logistics of tree-climbing fieldwork, and for generating hundreds of pressure-volume curves that surely would have driven any other woman to seek divorce. I promise to provide chocolate, ice cream, strawberries, and warm clothing into perpetuity!

Several colleagues engaged in mind-blowing conversations and hilarious field expeditions that continue to fill my sails. Anthony Ambrose and Wendy Baxter are particularly outstanding in this regard, and I can't wait for our next research adventure. Others include Marie Antoine, Matiss Castorena, Alberto Echeverria, Paul Fine, Greg Goldsmith, Sybil Gotsch, Jesse Hahm, George Koch, Stefania Mambelli, Mark Olson, Aaron Ramirez, Adam Roddy, Steve Sillett, Andrew Weitz, Chris Wong, and Bob Van Pelt. Steve and Bob are especially noteworthy for infecting me with the "big tree bug". Insightful and high-level dialogs with Tommaso Anfodillo as well as committee members John J. Battles, George Koch, and Cynthia Looy were critical for my professional development and deeper understanding of trees and forests.

Pioneering giant trees is an extremely challenging endeavor that demands a special kind of focus and creativity, and there are very few individuals that can calmly, safely, and efficiently install access ropes in such trees. I am fortunate to have essentially apprenticed with several of the world's most talented climbers, including Anthony Ambrose, Jim Campbell-Spickler, Tim Kovar, and Steve Sillett. Without their knowledge and skills, I might not be writing this acknowledgement.

The Dawson Lab is a positive, engaging, and enriching atmosphere within which to explore science, and Todd Dawson deserves a *Sequoiadendron*-sized BRAVO for being the orchestrator. Fellow graduate student lab-mates Roxy Cruz, Clarissa Fontes, Greg Goldsmith, Allison Kidder, Adam Roddy, Ilana Stein, and Claire Willing also contributed wonderfully to this atmosphere. Special thanks to Allison and Claire for eagerly assisting with the final paperwork while I was in Costa Rica.

Long-lasting, non-academic friendships are pivotal to stabilizing life trajectories. Those friends who played major roles include Sabrina & Dave, EJ, Klinger, the Rhinos, James & Robi, Erik Elstrom, Otto, Lucy & Nick, Christina & Becket, and Allison & Doug. Finally, thanks to all my skateboarding buddies from 1988 to 2017, who value the exchange of blood and sweat for exhilaration. It was this rule-less activity that facilitated the urge to explore the vast crowns of giant trees!

CHAPTER 1

Constraints on hydraulic compensation in the Earth's tallest trees

ABSTRACT

Hydraulic limitations to tree height growth may be mitigated by basipetal conduit widening and by increasing investment in the amount of sapwood relative to leaf area (LA). However, limits to conduit size may restrict basipetal widening, and maintaining an increasing ratio of carbon investment into plumbing versus photosynthetic capacity is unsustainable. These hydraulic compensation mechanisms may therefore become progressively constrained with height growth. In the conifers *Sequoia sempervirens* and *Sequoiadendron giganteum* and the angiosperm *Eucalyptus regnans*, axial variation in conduit diameter was measured to assess size limitations. I also quantified proportional increases in LA and sapwood volume (SV) across a broad range of tree sizes to evaluate carbon balance constraints. Conduits widened basipetally at a decelerating rate consistent with hydraulic compensation, but approached an asymptote well above the ground. With increasing tree size, SV accumulated at a faster rate than LA in the conifers, while in *Eucalyptus* this relationship was isometric. Conduit size in exceptionally tall trees may be a constraint for maintaining an efficient hydraulic system. In the conifers, an increased investment in SV versus LA suggests an imbalanced carbon budget that limits height growth, while the *Eucalyptus* appeared to maintain height growth potential.

INTRODUCTION

As trees grow taller, their rates of height growth decrease. The hydraulic limitation hypothesis (Ryan & Yoder, 1997) proposed that taller trees experience slower height growth due to two compounding factors: (1) the greater effect of the gravitational potential gradient that imposes –0.01 MPa per meter of height, and (2) longer water transport paths and thus more hydraulic resistance (*r*) through the xylem conduits. Both factors constrain height growth via reduced minimum leaf water potentials that inhibit turgor pressure (Woodruff *et al*., 2004), leaf expansion (Oldham *et al*., 2010), and photosynthesis (Tezara *et al*., 1999). Indeed, maximum height in the tallest conifers *Sequoia sempervirens* and *Pseudotsuga menziesii*, as estimated via limits to shoot functional characteristics imposed by gravity and *r*, were consistent with historical height records (Koch *et al*., 2004; Domec *et al*., 2008). Evaluation of the hydraulic limitation hypothesis revealed compensation mechanisms that mitigate the accumulation of *r* with tree height growth, including varying the dimensions of the xylem conduits along the hydraulic pathway (Anfodillo *et al*., 2013) and adjusting the relative investments in hydraulic supply versus transpirational demand (Ryan *et al*., 2006), but constraints on these two mechanisms have not been evaluated in the Earth's tallest trees.

Contrary to the pipe model where the diameters of xylem conduits are constant along a tree's hydraulic pathway (Shinozaki *et al*., 1964), it has long been known that each conduit in the series is slightly wider than the next, such that the series widens basipetally (i.e., increases in diameter towards the roots; Sanio, 1872; Fegel, 1941; Zimmermann, 1978). Because increasing diameter so strongly affects *r* relative to increasing path length as described by laminar flow in the Hagen-Poiseuille equation (Tyree & Zimmermann, 2002), basipetal conduit widening is an effective compensatory mechanism that mitigates the increase of *r* with tree height growth (Anfodillo *et al*., 2013). Although water typically

travels distally along the plant hydraulic pathway, I prefer the term 'basipetal widening' to its synonym 'acropetal tapering' because it is possible to add conduits in series without generating much extra *r* as long as the new conduits are wider than those to which they are connected.

Basipetal conduit widening is also a central tenet of metabolic scaling theory (MST), a theoretical framework mechanistically linking organism size to individual, community, and ecosystem attributes (West *et al*., 1999). For individual vascular plants adhering to MST, metabolic processes are optimized if certain assumptions—a volume-filling, fractal-like hierarchical branching architecture; invariantly sized leaves; uniform biomechanical constraints; and minimization of *r*—are met (Enquist, 2002). This framework yielded the prediction that basipetal conduit widening should follow a power function with a characteristic exponent (Anfodillo *et al*., 2006),

$$D = \alpha L^{\beta} \qquad \text{(Equation 1)}$$

where D = conduit diameter, L = distance from tree top, α = scaling coefficient (i.e., y-intercept), and β = scaling exponent (i.e., slope). The rate of basipetal widening is described by β. A zero value indicates conduits of uniform diameter while larger values indicate greater rates of widening. At $\beta \geq 0.20$, *r* becomes nearly independent of *L* (Anfodillo *et al.*, 2006). Therefore, $\beta = 0.20$ can be considered a minimum threshold above which metabolic efficiency may be maintained throughout tree height growth (Enquist, 2003).

An important implication of MST is that a tree could grow taller without accumulating much additional *r*, which is inconsistent with the hydraulic limitation hypothesis (Ryan & Yoder, 1997). Due in part to several challenging assumptions (Kozłowski & Konarzewski, 2004) MST has been vigorously debated (Coomes, 2006; Martinez del Rio, 2008), and its underlying premise has even been questioned (Glazier, 2015). Despite some skepticism about a specific threshold for basipetal conduit widening to minimize hydraulic resistance with height growth (e.g., Hacke *et al*., 2016; Pfautsch, 2016), axial variation in conduit diameter across broad array of woody angiosperms and conifers fits well to a power function and yields β converging to about 0.20 (Anfodillo *et al*., 2013). Correct or not, attention to MST has elucidated several functional implications of axial variation in conduit dimensions. Basipetal conduit widening cannot fully render *r* independent of hydraulic path length (Mäkelä & Valentine, 2006), but it does compensate by reducing the accumulation of *r* (Becker *et al*., 2000). However, it concentrates the vast majority of *r* toward a tree's top where conduits are narrowest (Tyree & Zimmermann, 2002; Petit *et al*., 2008, 2010). In addition, larger β values (e.g., 0.30) markedly reduce total *r* (Becker *et al*., 2000), but limitations to minimum tree top and maximum tree base conduit diameters may constrain β.

Constraints to β should be apparent in limits to conduit widths at the tree top and base, such that apical conduits either increase or do not correlate with total tree height (*H*) and that basal conduits either decrease or do not correlate with *H*. At tree tops, minimum conduit diameter is likely limited by *r* since even a slight narrowing of the conduits would dramatically increase the total *r* (Tyree & Zimmermann, 2002). Minimum conduit width at the tops of tall conifers is likely controlled by smaller pits that increase safety from cavitation but also excessively retard water flow (Domec *et al*., 2008; Lazzarin *et al*., 2016). Indeed, taller angiosperms produce wider, not narrower, tree top conduits presumably to maintain low whole-tree *r* (Olson *et al*., 2014). Maximum conduit widths at tree tops is likely influenced by the gravitational potential gradient which imposes low water potentials and consequently low turgor pressures that may limit cell expansion (Woodruff *et al*., 2004). At tree bases, maximum conduit size is sometimes evident as their diameters appear to approach

an asymptote both radially from inner to outer growth rings (Spicer & Gartner, 2001; Leal, 2007) as well as axially from tree top to base (Becker *et al*., 2003; James *et al*., 2003; Anfodillo *et al*., 2006; Mencuccini *et al.*, 2007; Petit *et al*., 2010). In taller trees the shape of the vertical profile of conduit diameters could be revealing of a limit to tree base conduit widths. Reasons for the upper limits to tree base conduit diameter remain unclear but may be related to increasing carbon costs associated with building larger conduits that yield negligible hydraulic benefits (Hacke *et al*., 2004; Mencuccini *et al.*, 2007; Hölttä *et al.*, 2011), minimizing fluid volume to maintain an efficient distribution network (Banavar *et al*., 1999), or low temperatures that limit cell expansion (Petit *et al*., 2011). Limits to tree top and tree base conduit diameters have implications for basipetal conduit widening as a hydraulic compensation mechanism because they translate to increased r via smaller β as trees grow taller. Thus, data describing axial variation in conduit widths in exceptionally tall trees are needed to further evaluate constraints on this compensation mechanism.

Measurements of conduit diameter and path length provide estimates of lumen r along a hydraulic pathway, but perforation plates and pits are ignored even though these end-wall constrictions contribute substantially to r (Choat *et al*., 2008). However, constant proportionality between lumen versus end-wall r (Lancashire & Ennos, 2002; Hacke *et al*., 2006; Wheeler *et al*., 2005; Pittermann *et al*., 2006; Lazzarin *et al*., 2016) facilitates investigations into the implications of axial variation in conduit diameter on r because lumen diameter is much easier to quantify than pit structure. Moreover, combined measurements of conduit diameter and r not only prove that basipetal conduit widening mitigates path-length r, but also show that the rate of r accumulated with path length is indeed predictable from anatomical measurements (Petit *et al*., 2008).

In addition to basipetal conduit widening, adjusting relative investments in hydraulic supply versus transpirational demand has also been proposed as a hydraulic compensation mechanism (Ryan *et al.*, 2006). An increasing ratio of sapwood area to leaf area (LA) as trees grow represents hydraulic compensation as a shift in the water balance towards supply and away from transpiration because a larger sapwood cross-sectional area improves conductivity with the addition of conduits in parallel (Tyree & Zimmermann, 2002). However, cases in which this ratio increases or decreases with height growth have been about equally reported, which could indicate that maximization of growth potential via increased LA and therefore photosynthetic capacity may override maintenance of hydraulic supply in some species (Buckley & Roberts, 2006; Koch *et al*., 2015).

A potential oversimplification of using sapwood area as a proxy for investment in hydraulic supply is that this two-dimensional metric may not be representative of a three-dimensional vascular tissue. Thus assessments of hydraulic compensation mechanisms may be improved by using the scaling of total sapwood volume (SV) instead of sapwood area. This volume better represents the metabolic investment in building and maintaining the active xylem tissue as a whole, including the living parenchyma cells responsible for repairing embolized conduits (Zwieniecki & Holbrook, 2009). The main challenge in using SV is that it is much more difficult to measure than sapwood area, and thus reliable data are scarce.

While such a shift in investment toward hydraulic supply and away from transpirational demand may indicate hydraulic compensation, this shift should in principle tradeoff with a sustainable carbon balance because it would increase the carbon costs of plumbing relative to assimilation as trees enlarge. For example, a tree conforming to MST where each leaf is supplied by an invariant number of conduits such that LA is predicted to scale with tree size to the ¾ power (West *et al*., 1999) would incur increasing costs of sapwood construction and maintenance with height growth, leading to a source-sink carbon imbalance. Indeed, *Sequoia sempervirens*, *Sequoiadendron giganteum*, and *Eucalyptus*

regnans trees with higher respiratory demand per unit of leaf area grew slower than those with lower respiratory demand, and higher ratios of SV to LA were a component of reduced aboveground vigor (Sillett *et al.,* 2010, 2015a). Therefore, sustaining carbon balance for indefinite growth may require isometry between the amounts of sapwood and leaves with tree enlargement as proposed by Olson *et al*. (2014). The relationships between investments in hydraulic supply versus photosynthetic capacity are needed for a broad range of tree sizes to clarify this apparent tradeoff between hydraulic compensation and carbon balance.

I had two objectives in this study of constraints on hydraulic compensation mechanisms. The first objective was to quantify axial variation in xylem conduit diameter for exceptionally tall individuals of the Earth's tallest species to explore limits to basipetal conduit widening. Study species included the 1st and 4th tallest conifers *Sequoia sempervirens* and *Sequoiadendron giganteum* as well as the tallest angiosperm *Eucalyptus regnans*. I predicted the rate of basipetal conduit widening to be ≥0.20 as an indicator of hydraulic compensation with height growth, and evaluated how apical and basal conduit dimensions might influence whole-tree hydraulic efficiency. The second objective was to quantify the relative investments in LA versus SV across a broad range of tree sizes, using published data for these species. I hypothesized that LA would scale isometrically with SV to maintain carbon balance at the expense of hydraulic compensation, such that a negative allometric relationship (i.e., increasing investment in SV compared to LA) would indicate constrained height growth.

MATERIALS & METHODS

Study sites and trees

Study sites were selected based on the abundance of exceptionally tall trees for a given species. Humboldt Redwoods State Park, California, along the floodplain of Bull Creek (40°N, 124°W; 45–65 m elevation) contains a high proportion of the Earth's tallest trees (Sawyer *et al*., 2000). Four *Sequoia sempervirens* (D. Don) Endlicher ranging in height from 99 to 105 m were selected for study there in 2013; three supported healthy twin leaders of which the subdominant was selected for study, while the fourth had a single dominant leader that died shortly before collection. Tall *Sequoiadendron giganteum* (Lindley) J. Buchholz occur in scattered groves in California's Sierra Nevada Mountains (Willard, 2000). In 2013 I selected three *Sequoiadendron* that were 87 m tall from Calaveras Big Trees State Park (38°N, 120°W; 1450–1470 m elevation) as well as three additional trees that were 90 to 95 m tall from Kings Canyon National Park and neighboring Whitaker's Forest Research Station (37°N, 119°W; 1670–1780 m elevation). Wallaby Creek on the Hume Plateau in Kinglake National Park, Victoria, Australia (37°S, 145°E; 450–500 m elevation) hosted the tallest angiosperm forest before the stand-replacing Black Saturday Fire (Cruz *et al*., 2012) swept through the understory on 7 February 2009, killing all overstory trees but leaving their fine twigs intact (Sillett *et al*., 2015b). I selected five of these dead *Eucalyptus regnans* F. von Mueller that were 86 to 93 m tall for collection of wood specimens in 2010. All study tree heights were >85% of the tallest known individual for a given species and included the second tallest known *Sequoiadendron* and *Eucalyptus* (Table 1).

Wood specimen collection

I climbed each study tree using nondestructive arborist methods, including single rope and doubled rope techniques (Jepson, 2000) to access the entire length of the primary stem axis (i.e., trunk). Total tree height (*H*) was established by lowering a 100 m fiberglass measuring tape from the tree top to average ground level. All heights were recorded to cm

Table 1. Names, locations, and sizes of 15 *Sequoia sempervirens*, *Sequoiadendron giganteum*, and *Eucalyptus regnans* study trees.

Name	Species	Location	DBH (m)	Height (m)
SESE 1	*Sequoia sempervirens*	Humboldt Redwoods State Park	3.31	104.8
SESE 2	*Sequoia sempervirens*	Humboldt Redwoods State Park	3.39	104.6
SESE 3	*Sequoia sempervirens*	Humboldt Redwoods State Park	2.30	101.1
SESE 4	*Sequoia sempervirens*	Humboldt Redwoods State Park	2.42	99.3
SEGI 1	*Sequoiadendron giganteum*	Kings Canyon National Park	4.21	94.8
SEGI 2	*Sequoiadendron giganteum*	Whitaker Forest Research Station	4.99	90.7
SEGI 3	*Sequoiadendron giganteum*	Whitaker Forest Research Station	2.93	90.0
SEGI 4	*Sequoiadendron giganteum*	Calaveras Big Trees State Park	4.73	86.7
SEGI 5	*Sequoiadendron giganteum*	Calaveras Big Trees State Park	4.22	86.6
SEGI 6	*Sequoiadendron giganteum*	Calaveras Big Trees State Park	6.21	86.5
EURE 1	*Eucalyptus regnans*	Kinglake National Park	2.65	92.6
EURE 2	*Eucalyptus regnans*	Kinglake National Park	3.12	91.5
EURE 3	*Eucalyptus regnans*	Kinglake National Park	2.74	87.7
EURE 4	*Eucalyptus regnans*	Kinglake National Park	2.98	86.8
EURE 5	*Eucalyptus regnans*	Kinglake National Park	2.70	85.7

resolution. In *Sequoia* and *Sequoiadendron* a 12 mm diameter increment borer was used to extract cores from the trunk of each tree, while in the dead *Eucalyptus* chainsaws were used to extract wedges. Cores and wedges captured the outermost approximately five annual rings. I avoided the swollen bases of the trees as well as branch junctions, burls, and other structural anomalies to reduce the probability of encountering reaction wood. Wood specimens were collected at 5 to10 m intervals along the lower half of the trunk and at increasing frequencies closer to the tree top to capture the rapid change in conduit diameters expected near the apex. In *Sequoia* and *Eucalyptus* I also collected the topmost approximately 1 m of the dead dominant leader or live subdominant twin leader. Collection heights were later converted to distance from tree top (L) to enable comparisons among trees of different heights during analyses.

Extraction of wood anatomical data

Quantitative data describing conduit size along the trunks were extracted using a rigid, standardized protocol to minimize measurement errors (von Arx *et al*., 2016). Transverse sections of each core or wedge were carved from the field specimens, softened in hot water, and sectioned (12-15 μm) using a disposable blade mounted to a sliding Reichert microtome. These thin sections were then stained with 1% safranin and permanently mounted to glass microscope slides using Eukitt (Bioptica, Milan, Italy). Each mounted section was focused under a light microscope (Eclipse 80i; Nikon Instruments Inc., Tokyo, Japan) through which the outermost annual ring was photographed with a digital camera. The digital images were analyzed with ImageJ v. 1.45d (Rasband, 1997–2017) to quantify the areas of at least 20 vessels (in *Eucalyptus*) and 100 tracheids (in *Sequoia* and *Sequoiadendron*) with 0.0001 μm^2 resolution in a zone of the transverse section that included the outer complete growth ring between two rays. Lumen areas (A) were converted to diameters (D) by assuming circular cross sections and using the formula $D=(A/\pi)^{1/2}$.

Data analysis

Before analyzing variation in conduit diameter, I reduced the probability of including the tapered ends of xylem conduits by removing those with a diameter less than half of the largest lumen within each annual ring's radial profile (James *et al*., 2003). I then calculated hydraulic mean diameter (D_h), which accounts for each conduit's contribution to hydraulic conductance for the N conduits within an annual ring:

$$D_h = \frac{\sum_{n=1}^{N} D_n^5}{\sum_{n=1}^{N} D_n^4} \qquad \text{(Equation 2)}$$

where D = diameter of lumen n (Sperry & Saliendra, 1994). Equation 2 is a superior representation of hydraulic conductivity compared to the unweighted mean vessel diameter (Hacke *et al*., 2016).

All statistical analyses were performed in R (R Development Core Team, 2015). I used both ordinary least squares (OLS) regression as well as reduced major axis (RMA) regression to establish the scaling relationships between each set of pairwise comparisons of D_h and L. While the primary choice was OLS regression because it more appropriately enabled predictions of D_h from L (Smith, 2009), I repeated the analysis using RMA to facilitate comparisons with the vast majority of literature in which estimates of basipetal conduit widening were reported. These two variables were $\log_{10}$-transformed to comply with assumptions of normality and homoscedasticity prior to regression analyses (Sokal & Rohlf, 1995). OLS and RMA regression analyses yielded a scaling exponent (β; i.e., slope), scaling coefficient (α; i.e., y-intercept), and 95% confidence intervals, taking the form $\log_{10}Y=\log_{10}\alpha+\beta\log_{10}X$, where $X=L$ and $Y=D_h$. $\text{Log}_{10}\alpha$ and its associated 95% confidence interval were then retransformed into the linear scale for reporting as components of a power function with β, taking the form $Y=\alpha X^{\beta}$ that was fit to each tree's set of pairwise comparisons. Thus β represents the rate of change in D_h along the trunk, while α (hereafter, $D_{h\text{-}top}$) represents D_h at 1 cm from the tree top. In addition to calculating $D_{h\text{-}top}$, β, and 95% confidence intervals separately for each tree, I also calculated species-level $D_{h\text{-}top}$ and β to narrow confidence intervals and reduce the uncertainty of fit for each species. Confidence intervals that overlapped with $\beta \geq 0.20$ were considered evidence of hydraulic compensation and in agreement with MST (Anfodillo *et al*., 2006, 2013).

To evaluate limits to conduit size, relationships between H and $D_{h\text{-}top}$ as well as between H and extrapolated tree base conduit diameter ($D_{h\text{-}base}$) were analyzed using OLS regression. Shapiro-Wilk tests and plots of observed versus predicted values validated assumptions of normality and homoscedasticity, respectively, for these linear models. Additional anatomical data were available from *Eucalyptus regnans* (Petit *et al*., 2010) which enabled me to compare $D_{h\text{-}top}$ from three medium-sized trees (average H=57.3 m) with the three tallest *Eucalyptus* using a t-test on the scaling coefficients derived via RMA regression.

Finally, data describing LA and SV across a broad range of tree sizes for *Sequoia*, *Sequoiadendron*, and *Eucalyptus regnans* were extracted from the literature (Sillett *et al*., 2010; Coonen & Sillett 2015; Sillett *et al*., 2015a, b) to interpret the pattern of change in the proportions of photosynthetic capacity versus hydraulic supply as trees enlarge. Only fully mapped trees and revised estimates from duplicate reports were used, yielding a total of 84 *Sequoia*, 32 *Sequoiadendron*, and 27 *Eucalyptus* trees. The scaling relationships between LA and SV were analyzed using RMA regression on $\log_{10}$-transformed data. This method was appropriate for determining whether isometry was maintained between LA and SV with increasing tree size because neither variable was considered dependent nor independent such

that a symmetric relationship was desired (Warton *et al*., 2006; Smith, 2009). 95% confidence intervals that overlapped a slope value of 1.00 were considered isometric and interpreted as maintenance of carbon balance to sustain indefinite growth at the expense of hydraulic compensation, while slopes less than 1.00 were considered negative allometric and interpreted as hydraulic compensation at the expense of carbon balance. RMA regression was performed using the R package 'smatr' (Warton *et al*., 2015).

RESULTS

Axial variation in conduit diameter

In all study trees D_h was narrowest near the tree top where a rapid rate of widening occurred basipetally, and widest near the tree base where the conduit diameters increased gradually toward the ground (Fig. 1). Measured values of tracheid D_h in *Sequoia* and *Sequoiadendron* were similar for a given L, ranging from 9.0 μm at L=0.20 m to 67.5 μm at L=84.80 m. Vessel elements in *Eucalyptus regnans* were much larger, ranging from a minimum of 28.0 μm at L=0.01 m to a maximum of 260.7 μm at L=47.70 m.

A power function fit well to each set of pairwise comparisons of D_h and L (Fig. 1), explaining 81 to 98% of the variation when trees were analyzed separately, and 89 to 95% when grouped by species (Table 2). However, beginning approximately 60 m from the tree tops the rate of basipetal widening progressively declined below the power function as D_h approached an early asymptote (Fig. 1, insets). Scaling exponents (β) describing the rate of D_h widening with L ranged from 0.17 to 0.28 (Table 2) and were within the range commonly reported. Consistent with MST, 95% confidence intervals for β included values ≥0.20 for each of the 15 study trees as well as for each of the three species when data were analyzed intraspecifically (Table 2), supporting the prediction that basipetal conduit widening serves a hydraulic compensation function with height growth in the tallest trees. Scaling coefficients ($D_{h\text{-}top}$) representing D_h at 1 cm from tree top positions were indistinguishable between *Sequoia* and *Sequoiadendron* (two-tailed t-test; P=0.62) and ranged from 3.9 to 9.6 μm, while those for *Eucalyptus* were much larger and ranged from 20.5 to 30.8 μm. Extrapolating D_h to tree base positions ($D_{h\text{-}base}$) yielded larger average values for *Sequoia* than *Sequoiadendron* and averaged 58.2 and 46.1 μm, respectively, while *Eucalyptus* averaged 264.1 μm. Data analyzed using RMA regression yielded similar results (Table S1).

Conduit diameter and total tree height

Constraints to β should be apparent in limits to $D_{h\text{-}top}$ and $D_{h\text{-}base}$, such that $D_{h\text{-}top}$ either increases or does not correlate with H and that $D_{h\text{-}base}$ either decreases or does not correlate with H. Since I found no differences in $D_{h\text{-}top}$ or β between *Sequoia* and *Sequoiadendron*, these two conifers were combined into a single group to expand the range of H among trees to test for changes in $D_{h\text{-}top}$ and $D_{h\text{-}base}$ with H (Fig. 2). OLS regression revealed that H was not correlated with $D_{h\text{-}top}$ (P=0.98). However, H was positively correlated with $D_{h\text{-}base}$ as expected (P<0.01, R^2=0.80). Thus across the conifers of different H, apical conduit diameters maintained constant width while those among tree bases increased. Within the narrow range of H for *Eucalyptus*, I found no correlation between $D_{h\text{-}top}$ and H (P=0.86) or between $D_{h\text{-}base}$ and H (P=0.62). However, a t-test comparing average $D_{h\text{-}top}$ derived via RMA regression from three medium-sized *Eucalyptus* (Petit *et al*., 2010) versus the three tallest revealed significantly wider average $D_{h\text{-}top}$ in the taller trees (19.9 μm versus 27.1μm; P=0.02).

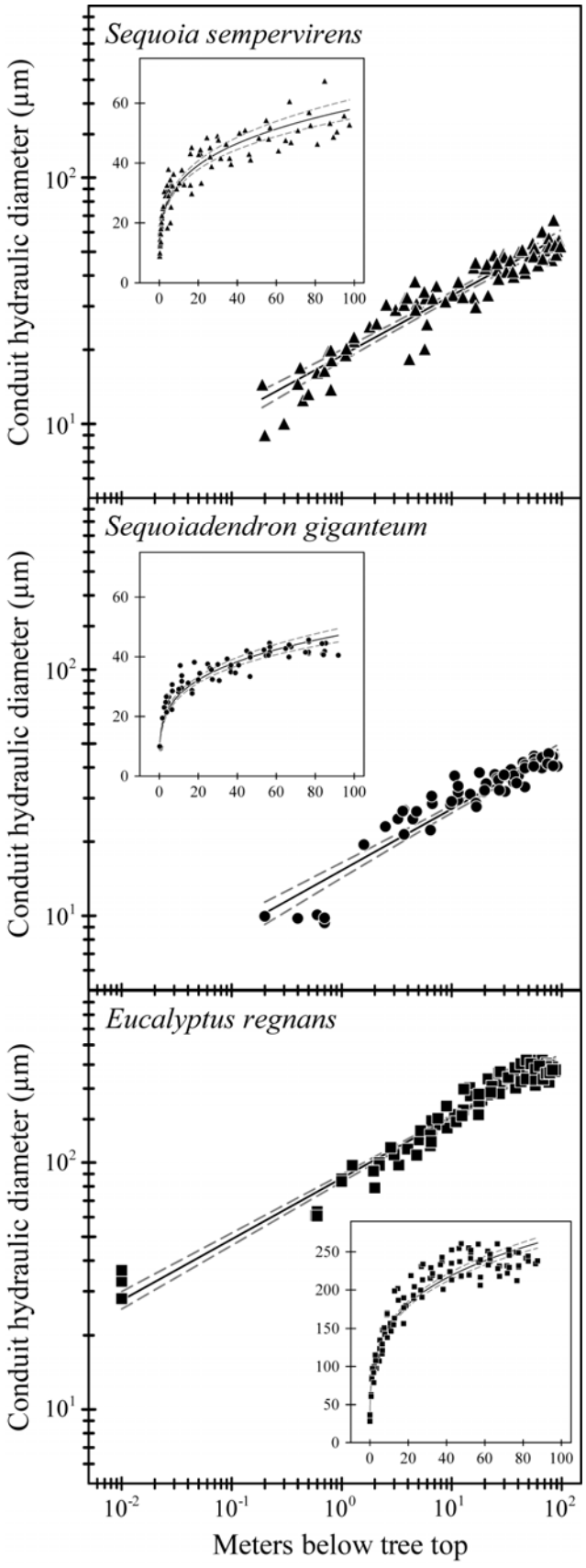

Figure 1. Scaling relationships between tracheid or vessel element hydraulically weighted diameter and distance from tree top for *Sequoia sempervirens*, *Sequoiadendron giganteum*, and *Eucalyptus regnans* trees 86–105 m tall. Each panel is a composite of multiple individuals: *Sequoia*, n=4; *Sequoiadendron*, n=6; *Eucalyptus*, n=5. Inset figures show the same data plotted onto untransformed axes. Dashed envelopes represent 95% confidence intervals. Relationships were derived via ordinary least squares regression.

Table 2. Summary statistics for scaling relationships between tracheid or vessel element hydraulically weighted diameter and distance from tree top for 15 tall *Sequoia sempervirens*, *Sequoiadendron giganteum*, and *Eucalyptus regnans* trees. The relationships were derived via ordinary least squares regression.

			Intercept (μm)		Slope	
ID	**# points**	**R^2**	**α**	**95% CI**	**β**	**95% CI**
SESE 1	23	0.96	5.58	4.67 to 6.66	0.27	0.24 to 0.29
SESE 2	18	0.83	8.27	5.69 to 12.01	0.21	0.16 to 0.26
SESE 3	17	0.93	7.11	5.58 to 9.05	0.22	0.18 to 0.25
SESE 4	20	0.90	5.20	3.86 to 7.00	0.26	0.22 to 0.30
All *Sequoia sempervirens*	78	0.90	6.17	5.40 to 7.06	0.24	0.22 to 0.26
SEGI 1	15	0.91	3.94	2.70 to 5.75	0.27	0.22 to 0.32
SEGI 2	10	0.89	4.14	2.26 to 7.60	0.27	0.19 to 0.35
SEGI 3	9	0.98	5.17	4.16 to 6.43	0.24	0.21 to 0.27
SEGI 4	10	0.87	9.64	6.41 to 14.49	0.17	0.11 to 0.22
SEGI 5	12	0.86	4.65	2.68 to 8.07	0.26	0.18 to 0.33
SEGI 6	11	0.81	7.65	4.38 to 13.34	0.19	0.12 to 0.26
All *Sequoiadendron giganteum*	67	0.89	4.85	4.10 to 5.74	0.25	0.23 to 0.27
EURE 1	22	0.98	25.47	22.10 to 29.35	0.26	0.24 to 0.27
EURE 2	23	0.97	30.83	26.85 to 35.40	0.24	0.22 to 0.26
EURE 3	19	0.92	28.47	21.37 to 37.93	0.24	0.21 to 0.28
EURE 4	22	0.94	20.46	16.02 to 26.12	0.28	0.25 to 0.32
EURE 5	22	0.95	30.33	25.07 to 36.69	0.24	0.21 to 0.26
All *Eucalyptus regnans*	108	0.95	27.58	25.42 to 29.92	0.25	0.24 to 0.26

The scaling coefficient (α) is the intercept and the scaling exponent (β) is the slope of a power function taking the form $Y=\alpha X^{\beta}$.

Scaling of leaf area with sapwood volume

The relationship between LA and SV across a broad range of tree sizes can be used to evaluate the metabolic cost invested during growth for maintaining hydraulic supply to the whole crown. This relationship explained 91% of the variation (Fig. 3, Table 3) suggesting that the amount of sapwood tissue that must be kept functional is a consequence of metabolic activity of the leaves. Combining all three species in this analysis yielded a negative allometric (i.e., $\beta<1.00$) scaling exponent ($\beta=0.81$, 95% CI=0.77–0.85) indicating that SV accumulates at faster rate than LA among trees and species. Analyzing these data separately for each species revealed a similar trend for *Sequoia* ($\beta=0.87$, 95% CI=0.82–0.91) and *Sequoiadendron* ($\beta=0.64$, 95% CI=0.57–0.70). However, I observed an isometric relationship between LA and SV for *Eucalyptus* ($\beta=1.09$, 95% CI=0.88–1.31).

DISCUSSION

Basipetal conduit widening (β) in tall trees

The convergence of β≥0.20 across a diverse array of woody plants now including some of Earth's tallest trees indicates a functional relationship between conduit diameter and height in tree that minimizes the accumulation of hydraulic resistance (*r*) with height growth, independent of size, age, and climate (West *et al*., 1999; Anfodillo *et al*., 2006, 2013; Olson *et al.*, 2014). Comparing conduit diameters at 1 cm from the tree tops ($D_{h\text{-}top}$) with those at tree bases ($D_{h\text{-}base}$) yielded a 10-fold relative increase that was substantially larger than predicted by MST, in which a factor of three is expected for a 100 m tall tree (West *et al*., 1999; Anfodillo *et al*., 2006). This discrepancy was caused by an unrealistic number of about 18 branching levels that was assumed for a 100 m tree by West *et al*. (1999) and shows that variation in conduit size is actually much higher. Moreover, including the distal-most leaf veins and fine roots (Zwieniecki *et al*., 2002; Petit *et al.*, 2009) should lead to relative increases even larger than a factor of 10, and consequently more than a 100-fold increase in lumen area. Considering the Hagen-Poiseuille equation, such a dramatic increase in conduit width explains why *r* is negligible in the basal compared to the distal portion of the hydraulic pathway (Petit *et al*., 2010) as demonstrated by the steep and nonlinear decrease in water potentials distally along the flow path of some trees (Tyree & Zimmermann, 2002).

Constraints on conduit widths

The degree of basipetal conduit widening depends on the sizes of apical and basal conduits. Conduits at both positions typically widen with *H*, but those at the apex widen at a slower rate (Olson *et al*., 2014). Since the vast majority of *r* is concentrated near the tree tops where the conduits are narrowest (Petit *et al.*, 2010), increasing $D_{h\text{-}top}$ by just a few microns would substantially improve whole-tree hydraulic efficiency. However, a

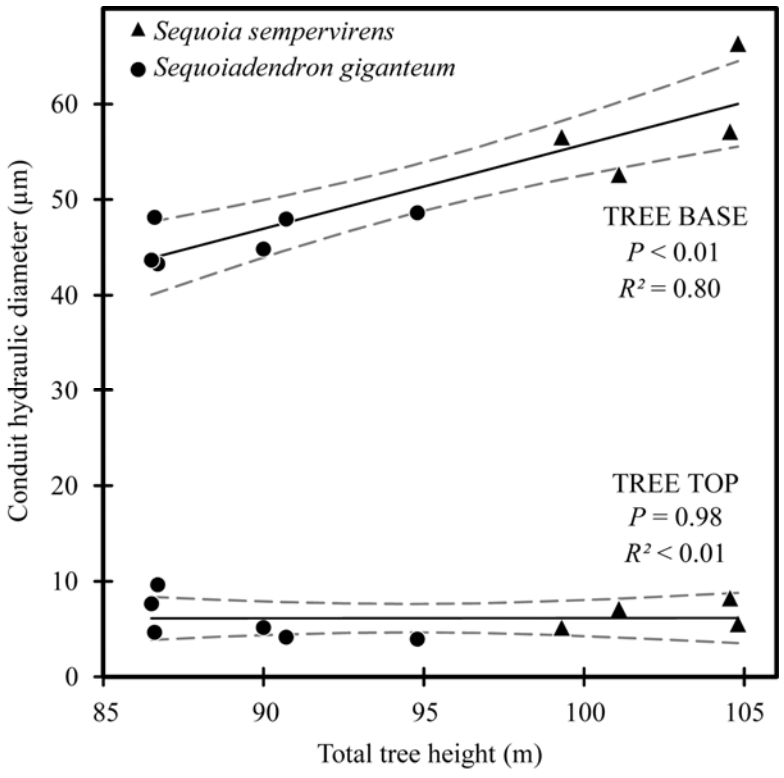

Figure 2. Relationships between tree top or tree base tracheid diameter and total tree height for *Sequoia sempervirens* and *Sequoiadendron giganteum* combined. Dashed envelopes represent 95% confidence intervals. *P*-values refer to significance of slope. Relationships were derived via ordinary least squares regression.

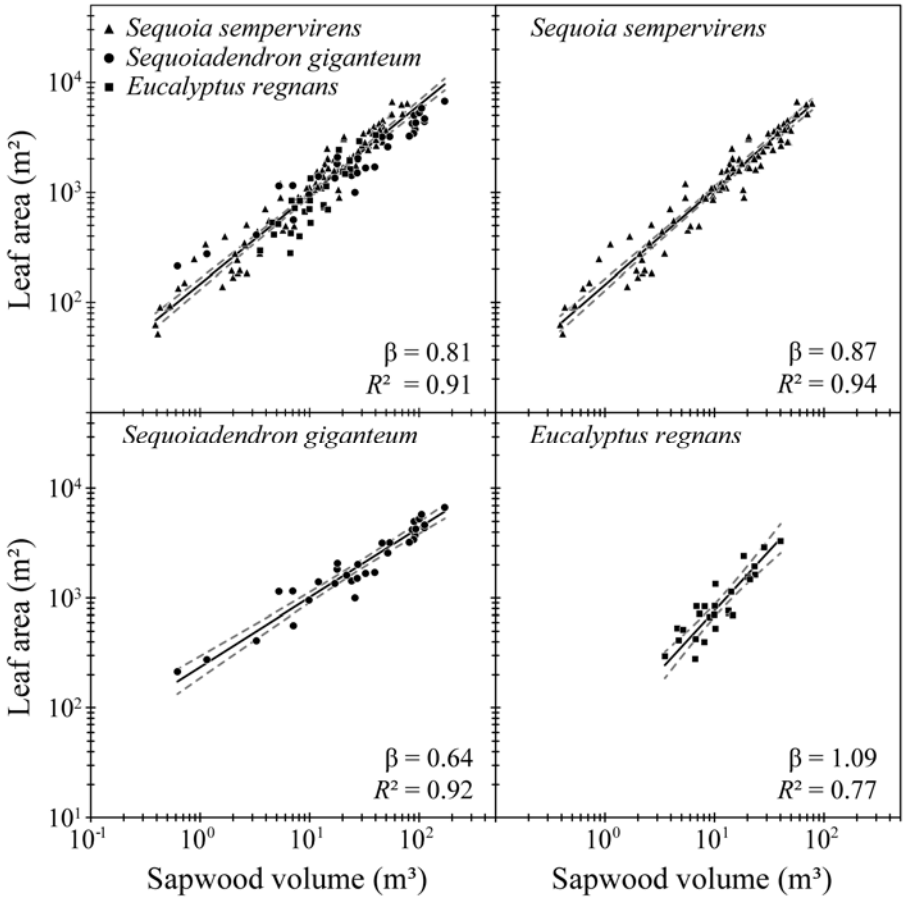

Figure 3. Scaling relationships between sapwood volume and leaf area across a broad range of sizes for 143 *Sequoia sempervirens*, *Sequoiadendron giganteum*, and *Eucalyptus regnans* trees. β is the slope of the relationship. Dashed envelopes are 95% confidence intervals. Relationships were derived via reduced major axis regression. Data from Sillett et al. (2010), Coonen & Sillett (2015), Sillett et al. (2015a, b).

Table 3. Summary statistics for scaling relationships between sapwood volume and leaf area for 143 individual *Sequoia sempervirens*, *Sequoiadendron giganteum*, and *Eucalyptus regnans* spanning a broad range of tree sizes. Data from Sillett *et al*. (2010), Coonen & Sillett (2015), Sillett *et al*. (2015a, b). The relationships were derived via reduced major axis regression.

			Intercept (m^2)		Slope	
Species	**# trees**	**R^2**	**α**	**95% CI**	**β**	**95% CI**
Sequoia sempervirens	84	0.94	144.67	128.08 to 163.42	0.87	0.82 to 0.91
Sequoiadendron giganteum	32	0.92	234.87	186.35 to 296.01	0.64	0.57 to 0.70
Eucalyptus regnans	27	0.77	62.04	36.46 to 105.57	1.09	0.88 to 1.31
All species	143	0.91	146.90	130.49 to 165.38	0.81	0.77 to 0.85

The scaling coefficient (α) is the intercept and the scaling exponent (β) is the slope of a power function taking the form $Y=\alpha X^{\beta}$.

disproportionate increase of apical compared to basal conduits as reported in *Acer pseudoplatanus* (Petit *et al*., 2008) could yield smaller β. In *Eucalyptus regnans*, the larger $D_{h\text{-}top}$ I observed in taller individuals did not compromise β, suggesting improved hydraulic efficiency over longer transport paths consistent with other angiosperms (Olson *et al.*, 2014). In the conifers, constant $D_{h\text{-}top}$ with H suggests that the size of tree top conduits may have limited capacity to vary, probably due to excessive r through the small pits (Domec *et al*., 2008; Lazzarin *et al*., 2016) and low turgor pressures that limit cell expansion (Woodruff *et al*., 2004). This conduit size limitation in the conifers, however, also did not compromise β. Therefore, the results for $D_{h\text{-}top}$ provide no evidence for constraints to β.

Constraints to β were clearer at tree bases. $D_{h\text{-}base}$ increased with H across the conifers, which I interpret as a mechanism allowing the maintenance of high β within individual trees as they grow taller. Admittedly, this trend was observed only after the *Sequoia* and *Sequoiadendron* data were combined, but the interpretation is supported by the fact that $D_{h\text{-}top}$ was not different between the two species and that they are closely related sister taxa (Farjon, 2005). While this trend supports the notion of H driving variation in conduit diameter (Olson *et al*., 2014), a closer look at the data also suggests that diameter may be limited. An upper limit to $D_{h\text{-}base}$ is evident in the untransformed plots of D_h and L (Fig. 1), where beginning approximately 60 m from the tree tops, the rate of basipetal conduit widening decelerated below the power function as D_h approached an early asymptote well above the tree bases. The apparent contradiction between these asymptotes in the untransformed plots of D_h and L and increasing $D_{h\text{-}base}$ with H (Fig. 2) may be explained by height growth potential within a hydraulic limitation framework. The *Sequoia* trees I sampled had a larger $D_{h\text{-}base}$ and appeared further from an asymptote, whereas *Sequoiadendron* had a smaller $D_{h\text{-}base}$ and appeared closer to an asymptote, suggesting less accumulation of r with additional height growth in *Sequoia* compared to *Sequoiadendron*. Indeed, the *Sequoia* I sampled were further from the height record of 116 m for this species while the *Sequoiadendron* were closer to the 96 m record (Sillett *et al*., 2015a). Thus I predict the positive slope in the relationship between $D_{h\text{-}base}$ and H (Fig. 2) would steepen to the left and flatten to the right with the inclusion of shorter and taller individuals, respectively, of these two species. Radial increases in tracheid and vessel diameters that approach a maximum in outermost annual rings at tree bases (Spicer & Gartner, 2001; Leal, 2007) support this explanation. I hypothesize that early asymptotes are caused by an optimized balance between hydraulic efficiency and carbon investment. Widening the conduits toward a tree's base minimally benefits whole-tree hydraulic efficiency (Petit *et al.*, 2010), adds fluid volume that may reduce network efficiency (Banavar *et al*., 1999), and incurs the progressively increasing cost of building and maintaining larger conduits (Hacke *et al.*, 2004; Mencuccini *et al.*, 2007; Hölttä *et al.*, 2011). Therefore, the optimal balance between hydraulic efficiency and carbon investment may determine the degree to which basipetal conduit widening serves as a hydraulic compensation mechanism. Although β values were consistent with MST predictions, the early asymptotes in these scaling relationships suggest that alternative models maximizing hydraulic efficiency while minimizing carbon allocation may better describe axial variation of conduit dimensions in tall trees.

Hydraulic compensation may tradeoff with carbon balance

The results confirm that basipetal conduit widening is a universal hydraulic compensation mechanism among woody plants that maintains hydraulic supply independent of tree size. I now evaluate the carbon cost constraints associated with building and maintaining such a hydraulic network by considering a framework that combines this anatomical structure with whole-tree allometries.

With increasing H, supplying each unit of LA with a fixed number of conduits as in MST (West *et al.*, 1999) would require building and maintaining an elongating and therefore increasingly costly vascular system. This problem may be bypassed by reducing the number of conduits per unit of LA while simultaneously increasing $D_{h\text{-}top}$ where the vast majority of r is concentrated and maintaining $\beta \geq 0.20$. Thus, leaf-specific conductance and a source-sink carbon balance may be maintained as trees enlarge. The expectation is that wider apical conduits with height growth should allow isometry between LA and SV so that the cost of maintaining hydraulic conductance becomes independent of tree size. The increase in $D_{h\text{-}top}$ with H across angiosperms up to 60 m (Olson *et al.*, 2014) provides empirical support for this source-sink carbon balance mechanism. If, however, cell expansion is hindered by low turgor pressures at the tree tops where water potentials are lowest (Koch *et al*., 2004; Woodruff *et al*., 2004; Williams *et al*., 2017), an upper limit to $D_{h\text{-}top}$ may be reached in exceptionally tall trees. This limit would reduce leaf-specific conductance with height growth, but could be offset by additional lateral investment in SV relative to LA. The consequence of such a mechanism would be an imbalanced carbon budget that limits growth potential, manifest as a negative allometric relationship between LA and SV. This hydraulic compensation mechanism may, therefore, tradeoff with carbon balance.

Interpreting the results within this framework suggests that specific anatomical and allometric adjustments may enable maintenance of high leaf-specific conductance throughout tree growth. In *Sequoia* and *Sequoiadendron* I observed no variation in $D_{h\text{-}top}$ with H, and the relationships between LA and SV were negative allometric. These results are consistent with maintenance of leaf-specific conductance by accelerating investment in SV relative to LA. Conversely, in *Eucalyptus* I observed larger $D_{h\text{-}top}$ in taller trees. The fact that wider conduits increase hydraulic conductance at a faster rate than conduit volume is added (Tyree & Zimmermann, 2002) may explain why taller *Eucalyptus* exhibited wider $D_{h\text{-}top}$ without an allometric adjustment in the relationship between LA and SV. That is, the improvement in conductance provided by wider $D_{h\text{-}top}$ sufficiently compensated for the increase in r caused by height growth, without the need for a costly increase in SV relative to LA. Therefore, the capacity to increase the diameter of apical conduits with height growth while sustaining $\beta \geq 0.20$ may allow *Eucalyptus* to maintain isometry between LA and SV, and could indicate that the individuals studied had additional height growth potential.

A tradeoff between hydraulic compensation and maintaining carbon balance may limit tree height growth. For *Sequoiadendron*, $LA \propto SV^{0.64}$, which I believe is close to a theoretical minimum scaling exponent (Notes S1), while for *Sequoia* the scaling exponent had a slightly larger value. In *Eucalyptus* the relationship was isometric. This rank order of the scaling relationships between LA and SV, and by extension degrees of tradeoff between hydraulic compensation and carbon balance, may explain why *Sequoiadendron* reached a plateau of maximum height at a basal trunk diameter (DBH) smaller than *Sequoia*, while *Eucalyptus* appeared to be further from its maximum height (Fig. 4).

Conclusions and future directions

Basipetal conduit widening and the capacity to adjust $D_{h\text{-}top}$ with H are two compensation mechanisms that mitigate hydraulic limitations to height growth. Across a wide array of woody plants, now including the some of Earth's tallest trees, the rate of basipetal conduit widening is consistent with minimizing the accumulation of r with height growth (West *et al*., 1999; Anfodillo *et al*., 2006, 2013). However, these data also suggest that $D_{h\text{-}base}$ may be limited by an optimal balance between hydraulic efficiency and carbon investment, which may impose a constraint on basipetal conduit widening. The evaluation of the relative investments in LA and SV allowed interpretation of why *Sequoiadendron* appears to peak in height well before reaching maximum DBH, while *Eucalyptus regnans* appears

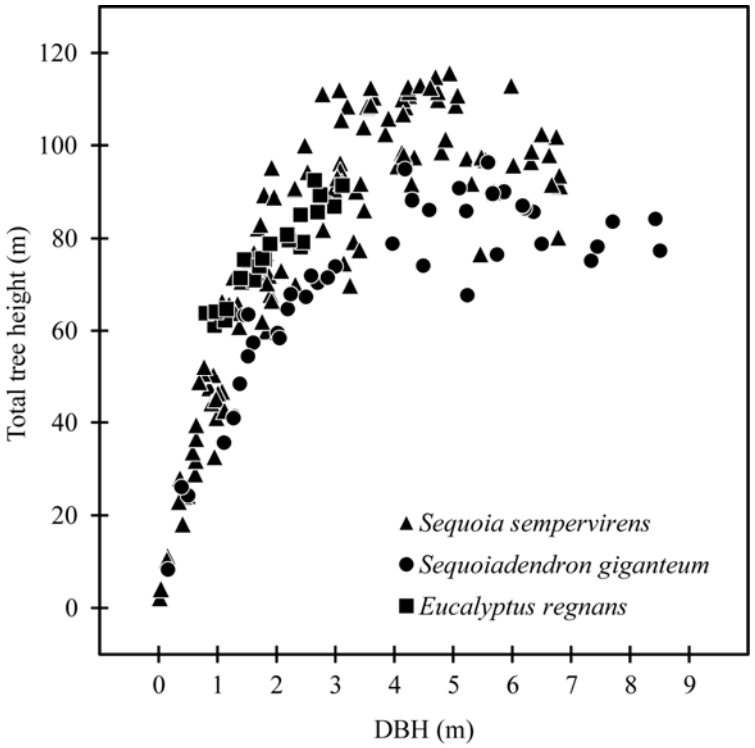

Figure 4. Graphical relationships between total tree height and diameter at breast height (DBH) for 196 *Sequoia sempervirens*, *Sequoiadendron giganteum*, and *Eucalyptus regnans* trees spanning a broad range of tree sizes. Note that *Eucalyptus* appears to have additional height growth potential compared to *Sequoia* and *Sequoiadendron*, which peak in height at approximately 3 m DBH. Data from Sillett et al. (2010), Coonen & Sillett (2015), Sillett et al. (2015a, b).

to have additional height growth potential. These results encourage the development of alternative models that optimize the balance between hydraulic compensation and carbon investment as trees enlarge. Such models may help explain constraints to hydraulic compensation mechanisms and improve our understanding of the limits to tree height.

ACKNOWLEDGEMENTS

This research was supported by a grant from the National Science Foundation (IOS-1010769). Collaborators Tomasso Anfodillo, Alan Crivalero, George Koch, and Todd Dawson provided critical guidance and assistance at multiple stages and will be coauthors when this manuscript is published. Anthony Ambrose, Wendy Baxter, Tom Greenwood, Joe Harris, Rikke Reese Næsborg, and Giacomo Renzullo helped collect wood specimens. Anthony Ambrose, John Battles, Cindy Looy, and Stefania Mambelli provided constructive comments on the manuscript. I am grateful to Ion Maher and Tony Fitzgerald of Kinglake National Park, Jay Harris of California State Parks, Koren Nydick of Sequoia and Kings Canyon National Parks, and Rob York of Whitaker's Forest Research Station for research permissions.

REFERENCES

Anfodillo T, Carraro V, Carrer M, Fior C, Rossi S. 2006. Convergent tapering of xylem conduits in different woody species. *New Phytologist* 169: 279–290.

Anfodillo T, Petit G, Crivellaro A. 2013. Axial conduit widening in woody species: a still neglected anatomical pattern. *IAWA Journal* 34: 352–364.

Banavar JR, Maritan A, Rinaldo A. 1999. Size and form in efficient transportation networks. *Nature* 6732: 130–132.

Becker P, Gribben RJ, Lim CM. 2000. Tapered conduits can buffer hydraulic conductance from path-length effects. *Tree Physiology* 20: 965–967.

Becker P, Gribben RJ, Schulte PJ. 2003. Incorporation of transfer resistance between tracheary elements into hydraulic resistance models for tapered conduits. *Tree Physiology* 23: 1009–1019.

Buckley TN, Roberts DW. 2006. How should leaf area, sapwood area, and stomatal conductance vary with tree height to maximize growth? *Tree Physiology* 26: 145–157.

Choat B, Cobb AR, Jansen S. 2008. Structure and function of bordered pits: new discoveries and impacts on whole-plant hydraulic function. *New Phytologist* 177: 608–626.

Coomes, D. 2006. Challenges to the generality of WBE theory. *Trends in Ecology and Evolution* 21: 593–596.

Coonen EJ, Sillett SC. 2015. Separating effects of crown structure and competition for light on trunk growth of Sequoia sempervirens. *Forest Ecology and Management* 358: 26–40.

Cruz MG, Sullivan AL, Gould JS, Sims NC, Bannister AJ, Hollis JJ, Hurley RJ. 2012. Anatomy of a catastrophic wildfire: the Black Saturday Kilmore East fire in Victoria, Australia. *Forest Ecology and Management* 284: 269–85.

Domec JC, Lachenbruch B, Meinzer FC, Woodruff DR, Warren JM, McCulloh KA. 2008. Maximum height in a conifer is associated with conflicting requirements for xylem design. *Proceedings of the National Academy of Sciences* 105: 12069–12074.

Enquist BJ. 2002. Universal scaling in tree and vascular plant allometry: toward a general quantitative theory linking plant form and function from cells to ecosystems. *Tree Physiology* 22: 1045–1064.

Enquist BJ. 2003. Cope's Rule and the evolution of long-distance transport in vascular plants: allometric scaling, biomass partitioning and optimization. *Plant, Cell & Environment* 26: 151–61.

Farjon A. 2005. *A Monograph of Cupressaceae and Sciadopitys*. Kew, UK: Royal Botanic Gardens.

Fegel AC. 1941. Comparative anatomy and varying physical properties of trunk, branch and root wood in certain northeastern trees. *Bulletin of the New York State College of Forestry at Syracuse University, Technical Publication* 55: 1–20.

Glazier DS. 2015. Is metabolic rate a universal ‘pacemaker’ for biological processes? *Biological Reviews* 90: 377–407.

Hacke U.G., Sperry J.S. & Pittermann J. 2004. Analysis of circular bordered pit function. II. Gymnosperm tracheids with torus-margo pit membranes. *American Journal of Botany* 91: 386–400.

Hacke UG, Sperry JS, Wheeler JK, Castro, L. 2006. Scaling of angiosperm xylem structure with safety and efficiency. *Tree Physiology* 26: 689–701.

Hacke UG, Spicer R, Schreiber SG, Plavcová L. 2016. An ecophysiological and developmental perspective on variation in vessel diameter. *Plant, Cell and Environment*. 40: 831–845.

Hölttä T, Mencuccini M, Nikinmaa E. 2011. A carbon cost-gain model explains the observed patterns of xylem safety and efficiency. *Plant, Cell and Environment* 34: 1819–1834.
James SA, Meinzer FC, Goldstein G, Woodruff D, Jones T, Restom T, Mejia M, Clearwater M, Campanello P. 2003. Axial and radial water transport and internal water storage in tropical forest canopy trees. *Oecologia* 134: 37–45.
Jepson J. 2000. *The tree climber's companion: a reference and training manual for professional tree climbers.* Longville, MN, USA: Beaver Tree Publishing.
Koch GW, Sillet SC, Jennings GM, Davis SV. 2004. The limits to tree height. *Nature* 428: 851–854.
Koch GW, Sillett SC, Antoine ME, Williams CB. 2015. Growth maximization trumps maintenance of leaf conductance in the tallest angiosperm. *Oecologia* 177: 321–331.
Kozłowski J, Konarzewski M. 2004. Is West, Brown and Enquist's model of allometric scaling mathematically correct and biologically relevant? *Functional Ecology* 18: 283–289.
Lazzarin M, Crivellaro A, Mozzi G, Williams C, Dawson T, Anfodillo T. 2016. Tracheid and pit anatomy vary in tandem in a tall giant sequoia. *IAWA Journal* 37: 172–185.
Lancashire JR, Ennos AR. 2002. Modelling the hydrodynamic resistance of bordered pits. *Journal of Experimental Botany* 53: 1485–1493.
Leal S, Sousa VB, Pereira H. 2007. Radial variation of vessel size and distribution in cork oak wood (*Quercus suber* L.). *Wood Science and Technology* 41: 339–350.
Mäkelä A & Valentine HT. 2006. The quarter-power scaling model does not imply size-invariant hydraulic resistance in plants. *Journal of theoretical biology* 243: 283–285.
Martinez del Rio C. 2008. Metabolic theory or metabolic models? *Trends in Ecology and Evolution* 23: 256–260.
Mencuccini M, Hölttä T, Petit G, Magnani F. 2007. Sanio's laws revisited. Size-dependent changes in the xylem architecture of trees. *Ecology Letters* 10: 1084–1093.
Oldham AR, Sillett SC, Tomescu AM, Koch GW. 2010. The hydrostatic gradient, not light availability, drives height-related variation in *Sequoia sempervirens* (Cupressaceae) leaf anatomy. *American Journal of Botany* 97: 1087–1097.
Olson ME, Anfodillo T, Rosell JA, Petit G, Crivellaro A, Isnard S, Castorena M. 2014. Universal hydraulics of the flowering plants: vessel diameter scales with stem length across angiosperm lineages, habits and climates. *Ecology Letters* 17: 988–997.
Petit G, Anfodillo T, Mencuccini M. 2008. Tapering of xylem conduits and hydraulic limitations in sycamore (*Acer pseudoplatanus*) trees. *New Phytologist* 177: 653–664.
Petit G, Anfodillo T, De Zan C. 2009. Degree of tapering of xylem conduits in stems and roots of small *Pinus cembra* and *Larix decidua* trees. *Botany* 87: 501–508.
Petit G, Pfautsch S, Anfodillo T, Adams MA. 2010. The challenge of tree height in *Eucalyptus regnans*: when xylem tapering overcomes hydraulic resistance. *New Phytologist* 187: 1146–1153.
Petit G, Anfodillo T, Carraro V, Grani F, Carrer M. 2011. Hydraulic constraints limit height growth in trees at high altitude. *New Phytologist* 189: 241–252.
Pfautsch S. 2016. Hydraulic anatomy and function of trees—basics and critical developments. *Current Forestry Reports* 2: 236–248.
Pittermann J, Sperry JS, Hacke UG, Wheeler JK, Sikkema EH. 2006. Inter-tracheid pitting and the hydraulic efficiency of conifer wood: the role of tracheid allometry and cavitation protection. *American Journal of Botany* 93: 1265–1273.
R Development Core Team. 2015. R: *A language and environment for statistical computing*. Vienna, Austria: R Foundation for Statistical Computing. URL http://www.R-project.org/.

Rasband WS. 1997–2017. ImageJ, U. S. National Institutes of Health, Bethesda, Maryland, USA. URL http://imagej.nih.gov/ij/.
Ryan MG, Yoder BJ. 1997. Hydraulic limits to tree height and tree growth. *Bioscience* 47: 235–242.
Ryan MG, Phillips N, Bond BJ. 2006. The hydraulic limitation hypothesis revisited. *Plant, Cell & Environment* 29: 367–381.
Sanio K. 1872. Über die Größe der Holzzellen bei der gemeinen Kiefer (*Pinus sylvestris*). *Jahrbuch Wissenschaftlichen Bot* 8: 401–420.
Sawyer JO, Sillett S, Libby WJ, Dawson TE, Popenoe JH, Largent DL, Van Pelt R, Veirs SD Jr, Noss RF, Thornburgh DA, Del Tredici P. 2000. Redwood trees, communities, and ecosystems: a closer look. In: Noss RF, ed. *The redwood forest: history, ecology, and conservation of the coast redwoods*. Covelo, CA, USA: Island Press, 81–118.
Shinozaki K, Yoda K, Hozumi K, Kira T. 1964. A quantitative analysis of plant form – The pipe model theory I. Basic analyses. *Japanese Journal of Ecology* 14: 94–105.
Sillett SC, Van Pelt R, Koch GW, Ambrose AR, Carroll AL, Antoine ME, Mifsud BM. 2010. Increasing wood production through old age in tall trees. *Forest Ecology and Management* 259: 976–994.
Sillett SC, Van Pelt R, Carroll AL, Kramer RD, Ambrose AR, Trask D. 2015a. How do tree structure and old age affect growth potential of California redwoods? *Ecological Monographs* 85: 181–212.
Sillett SC, Van Pelt R, Kramer RD, Carroll AL, Koch GW. 2015b. Biomass and growth potential of *Eucalyptus regnans* up to 100 m tall. *Forest Ecology and Management* 348: 78-91.
Smith RJ. 2009. Use and misuse of the reduced major axis for line-fitting. *American Journal of Physical Anthropology* 140: 476–486.
Sokal RR, Rohlf FJ. 1995. *Biometry (3rd edition)*. New York, USA: WH Freeman and Company.
Sperry JS, Saliendra NZ. 1994. Intra-and inter-plant variation in xylem cavitation in *Betula occidentalis*. *Plant, Cell and Environment* 17: 1233–1241.
Spicer R, Gartner BL. 2001. The effects of cambial age and position within the stem on specific conductivity in Douglas-fir (*Pseudotsuga menziesii*) sapwood. *Trees* 15: 222–229.
Tezara W, Mitchell VJ, Driscoll SD, Lawlor DW. 1999. Water stress inhibits plant photosynthesis by decreasing coupling factor and ATP. *Nature* 401: 914–917.
Tyree MT & Zimmermann MH. 2002. *Xylem structure and the ascent of sap, 2nd edition*. Berlin, Germany: Springer.
von Arx G, Crivellaro A, Prendin AL, Čufar K, Carrer M. 2016. Quantitative wood anatomy-practical guidelines. *Frontiers in Plant Science* 7.
Warton D, Duursma R, Falster D, Taskinen S. 2015. smatr: (Standardized) major axis estimation and testing routines. R package version 3.2.0. [WWW document] URL http://CRAN.R-project.org/package=smatr. [accessed 17 April 2015].
Warton DI, Wright IJ, Falster DS, Westoby M. 2006. Bivariate line-fitting methods for allometry. *Biological Reviews* 81: 259–291.
West GB, Brown JH, Enquist BJ. 1999. A general model for the structure and allometry of plant vascular systems. *Nature* 400: 664–667.
Wheeler JK, Sperry JS, Hacke UG, Hoang N. 2005. Inter-vessel pitting and cavitation in woody Rosaceae and other vesselled plants: a basis for a safety versus efficiency trade-off in xylem transport. *Plant, Cell & Environment* 28: 800–812.
Willard D. 2000. *A Guide to the Sequoia Groves of California*. Yosemite National Park, CA, USA: Yosemite Natural History Association.

Williams CB, Reese Næsborg R, Dawson TE. 2017. Coping with gravity: the foliar water relations of giant sequoia. *Tree Physiology* doi:10.1093/treephys/tpx074.
Woodruff DR, Bond BJ, Meinzer FC. 2004. Does turgor limit growth in tall trees? *Plant, Cell & Environment* 27: 229–236.
Zimmermann MH. 1978. Hydraulic architecture of some diffuse-porous trees. *Canadian Journal of Botany* 56: 2286–2295.
Zwieniecki MA, Holbrook NM. 2009. Confronting Maxwell's demon: biophysics of xylem embolism repair. *Trends in plant science* 14: 530–534.
Zwieniecki MA, Melcher PJ, Boyce CK, Sack L, Holbrook NM. 2002. Hydraulic architecture of leaf venation in *Laurus nobili*s L. *Plant, Cell & Environment* 25: 1445–1450.

SUPPORTING INFORMATION

Table S1. Summary statistics for scaling relationships between tracheid or vessel element hydraulically weighted diameter and distance from tree top for 15 tall *Sequoia sempervirens*, *Sequoiadendron giganteum*, and *Eucalyptus regnans* trees. The relationships were derived via reduced major axis regression.

			Intercept (μm)		Slope	
ID	**# points**	**R^2**	**α**	**95% CI**	**β**	**95% CI**
SESE 1	23	0.96	5.36	4.49 to 6.40	0.27	0.25 to 0.30
SESE 2	18	0.83	7.12	4.90 to 10.34	0.23	0.18 to 0.29
SESE 3	17	0.93	6.70	5.26 to 8.54	0.23	0.19 to 0.26
SESE 4	20	0.90	4.73	3.51 to 6.37	0.27	0.23 to 0.32
All *Sequoia sempervirens*	78	0.90	5.62	4.92 to 6.43	0.26	0.24 to 0.28
SEGI 1	15	0.91	3.59	2.46 to 5.25	0.29	0.24 to 0.34
SEGI 2	10	0.89	3.65	1.99 to 6.70	0.29	0.22 to 0.37
SEGI 3	9	0.98	5.09	4.10 to 6.33	0.24	0.21 to 0.27
SEGI 4	10	0.87	8.79	5.84 to 13.22	0.18	0.13 to 0.24
SEGI 5	12	0.86	4.00	2.31 to 6.95	0.28	0.21 to 0.36
SEGI 6	11	0.81	6.47	3.71 to 11.29	0.21	0.15 to 0.29
All *Sequoiadendron giganteum*	67	0.89	4.33	3.66 to 5.12	0.26	0.24 to 0.29
EURE 1	22	0.98	24.90	21.61 to 28.70	0.26	0.24 to 0.28
EURE 2	23	0.97	30.09	26.20 to 34.55	0.24	0.22 to 0.26
EURE 3	19	0.92	26.25	19.71 to 34.98	0.25	0.22 to 0.29
EURE 4	22	0.94	19.22	15.05 to 24.54	0.29	0.26 to 0.33
EURE 5	22	0.95	29.01	23.98 to 35.10	0.24	0.22 to 0.27
All *Eucalyptus regnans*	108	0.95	26.35	24.29 to 28.58	0.25	0.24 to 0.26

The scaling coefficient (α) is the intercept and the scaling exponent (β) is the slope of a power function taking the form $Y=\alpha X^{\beta}$.

Notes S1. Derivation of scaling exponents between leaf area and sapwood volume.

Here I derive theoretical scaling exponents predicting the relationships between leaf area (LA) and sapwood volume (SV). Metabolic scaling theory (MST; West *et al*., 1999) predicts $LA \propto M^{3/4}$, where M is total plant mass excluding metabolically inactive components. Using an analogy to MST I rely on relationships between total tree height (H), the volume of a single conduit (V_i) extending from tree base to top, and the total number of these conduits (N_c). The approach is best applied to conifers in which the sapwood is composed of almost entirely of conduits with minimal non-conductive tissue. For this derivation, I replace M with SV because I are interested in proportional increases in photosynthetic capacity and hydraulic supply as trees enlarge. This replacement was validated by the nearly isometric relationship I found between M and SV via reduced major axis (RMA) regression on $\log_{10}$-transformed data (slope=0.97, 95% CI=0.95–0.99, R^2=0.97) after heartwood was excluded from 84 *Sequoia sempervirens* and 32 *Sequoiadendron giganteum* spanning a broad range of tree sizes and assuming heartwood densities of 407 and 378 kg m^{-3}, respectively (Sillett *et al*., 2010, 2015; Coonen & Sillett 2015). Note that I applied intraspecific trunk heartwood densities to all heartwood, including branches; applying trunk and branch heartwood densities separately to trunks versus branches would have resulted in a slightly steeper slope in the scaling relationship between M and SV.

MST predicts that $LA \propto H^3$, $N_c \propto LA^1$, and $V_i \propto H^1$. This latter relationship is based on the architecture of the idealized MST tree, wherein uniformly-sized conduits are embedded within cylindrical stem segments whose total cross-sectional area is preserved among branching levels (i.e., the Da Vinci rule). This structure translates into an external conduit diameter (D) that is constant with H, yielding $D \propto H^0$. Combined with the scaling relationship for a cylinder $V_i \propto D^2 H$ gives $V_i \propto (H^0)^2 H$, which simplifies to $V_i \propto H^1$. Total SV, which is the sum of all V_i or $SV = N_c V_i$ is therefore equivalent to $SV = H^3 H^1$, so $SV \propto H^4$. Rearranging $LA \propto H^3$ and $SV \propto H^4$ gives $H \propto LA^{1/3}$ and $H \propto SV^{1/4}$, respectively. Thus $LA^{1/3} \propto SV^{1/4}$, which is equivalent to $LA \propto SV^{3/4}$. This scaling relationship is analogous to Kleiber's law relating metabolic rate to body size in animals (Kleiber 1932).

I now derive a minimum scaling exponent by replacing two relationships inherent within the MST with empirical relationships for the conifers *Sequoia* and *Sequoiadendron*. First $LA \propto H^{2.61}$ for the aforementioned 116 trees using RMA regression on $\log_{10}$-transformed data (95% CI=2.39–2.83, R^2=0.59). Second, the rate of basipetal conduit widening I estimated from exceptionally tall individuals of these species was β=0.23, so $D \propto H^{0.23}$. Following the same procedure as above with the scaling relationship for a cylinder gives $V_i \propto (H^{0.23})^2 H$ which simplifies to $V_i \propto H^{1.46}$. Total $SV = H^{2.61} H^{1.46}$, so $SV \propto H^{4.07}$. Finally, combining $LA \propto H^{2.61}$ with $SV \propto H^{4.07}$ gives $LA \propto SV^{0.64}$, which matches the empirical scaling relationship $LA \propto SV^{0.64}$ I observed for the *Sequoiadendron*.

References

Coonen EJ, Sillett SC. 2015. Separating effects of crown structure and competition for light on trunk growth of Sequoia sempervirens. *Forest Ecology and Management* 358: 26–40.

Kleiber M. 1932. Body size and metabolism. *Hilgardia* 6: 315–353.

Sillett SC, Van Pelt R, Koch GW, Ambrose AR, Carroll AL, Antoine ME, Mifsud BM. 2010. Increasing wood production through old age in tall trees. *Forest Ecology and Management* 259: 976–994.
Sillett SC, Van Pelt R, Carroll AL, Kramer RD, Ambrose AR, Trask D. 2015. How do tree structure and old age affect growth potential of California redwoods? *Ecological Monographs* 85: 181–212.
West GB, Brown JH, Enquist BJ. 1999. A general model for the structure and allometry of plant vascular systems. *Nature* 400: 664–667.

CHAPTER 2

Coping with gravity: the foliar water relations of giant sequoia

Originally published by Oxford University Press as: Cameron B. Williams, Rikke Reese Næsborg, and Todd E. Dawson. 2017. Coping with gravity: the foliar water relations of giant sequoia. *Tree Physiology* 37: 1312–1326. doi:10.1093/treephys/tpx074

ABSTRACT

In tall trees, the mechanisms by which foliage maintains sufficient turgor pressure and water content against height-related constraints remain poorly understood. Pressure-volume curves generated from leafy shoots collected crown-wide from 12 large *Sequoiadendron giganteum* (giant sequoia) trees provided mechanistic insights into how the components of water potential vary with height in tree and over time. The turgor loss point (TLP) decreased with height at a rate indistinguishable from the gravitational potential gradient and was controlled by changes in tissue osmotica. For all measured shoots, total relative water content at the TLP remained above 75%. This high value has been suggested to help leaves avoid precipitous declines in leaf-level physiological function, and in giant sequoia was controlled by both tissue elasticity and the balance of water between apoplasm and symplasm. Hydraulic capacitance decreased only slightly with height, but importantly this parameter was nearly double in value to that reported for other tree species. Total water storage capacity also decreased with height, but this trend essentially disappeared when considering only water available within the typical range of water potentials experienced by giant sequoia. From summer to fall measurement periods we did not observe osmotic adjustment that would depress the TLP. Instead we observed a proportional shift of water into less mobile apoplastic compartments leading to a reduction in hydraulic capacitance. This collection of foliar traits allows giant sequoia to routinely, but safely, operate close to its TLP, and suggests that gravity plays a major role in the water relations of Earth's largest tree species.

INTRODUCTION

California's giant sequoia (*Sequoiadendron giganteum*) is the first largest and fifth tallest tree species on Earth, with massive trunks and immense crowns that can support 1400 m^3 of wood, 6700 m^2 of leaf area, and grow to 95 m tall (Van Pelt, 2001; Tng *et al*., 2012; Sillett *et al*., 2015). This magnificent tree species is a component of mixed conifer forests in the Sierra Nevada Mountains, and can be characterized as a paleoendemic whose water requirements restrict the species to basin-like topographies containing abundant subsurface snowmelt (Rundel, 1972; Anderson, 1995; Willard, 2000).

Recent concerns have been raised that *Sequoiadendron* may be vulnerable to projected changes in climate (York *et al*., 2013). Both fossil and genetic evidence indicate the species range fluctuated with changes in precipitation and temperature over the past 2.3 million years; wet intervals coincided with slight expansions, and dry conditions drove contractions that were exacerbated by warmer temperatures (Anderson & Smith, 1994; Davis, 1999a, 1999b; Dodd &

DeSilva, 2016). Global temperatures are now warmer than during 75% of the last 11,300 years, and projections indicate warmer California temperatures will be common in the coming decades (Cayan *et al*., 2008; Marcott *et al*., 2013). In the Sierra Nevada Mountains, warmer temperatures will diminish deep water storage and water availability to mixed conifer forests containing *Sequoiadendron* (Bales *et al*., 2011; Goulden *et al*., 2012; Hunsaker *et al*., 2012). Despite these concerns, there is some evidence that *Sequoiadendron* may be relatively resilient to drought. The fact that individual trees may live beyond 3,200 years indicates the ability to survive multiyear droughts (Sillett *et al*., 2015; Rocky Mountain Tree-Ring Research, 2016). Indeed, the 2012-2017 drought recorded recently across California has been linked to the widespread death of more than 100 million trees in the Sierra Nevada Mountains (Griffin & Anchukaitis, 2014; Belmecheri *et al*., 2015; USDA, 2016), but *Sequioadendron* did not immediately appear to be dying (personal observation). This ability to survive drought in part reflects a relatively conservative hydraulic architecture, with dense branch wood that retains 95% hydraulic conductivity at minimum midday water potentials, and dense leaves with efficient water use and tight stomatal regulation (Ambrose *et al*., 2009; Pittermann *et al*., 2012; Ambrose *et al*., 2015). However, the physiological mechanisms responsible for maintaining foliar water content above damaging levels are needed if we are to understand how *Sequoiadendron* may be resistant to drought.

Foliage is the primary physiological interface between plants and atmosphere. According to the cohesion-tension theory, water travels skyward via a free-energy gradient of sequentially lower pressures along the soil-plant-atmosphere continuum (Dixon & Joly, 1895; Philip, 1966). Therefore, foliar water potential (Ψ_w) must remain lower than the soil in order to transport water to the leaves, but there are thresholds beyond which low Ψ_w will lead to dysfunction (Tyree & Sperry, 1989). Water potential can be defined as the sum of its component parts. For short-statured plants such as shrubs and herbs,

$$\Psi_w = \Psi_\pi + \Psi_p \qquad \text{(Equation 1)}$$

where Ψ_π is the osmotic potential and a negative value, and Ψ_p is the turgor pressure and is either zero or positive (Lambers *et al*., 2008). Turgor loss stops key processes, including cell expansion, stomatal conductance, and leaf hydraulic conductivity (Kramer & Boyer, 1995; Brodribb *et al*., 2003; Blackman *et al*., 2010). Setting osmotic concentration to obtain sufficiently low Ψ_π is therefore critical to prevent Ψ_w from reducing Ψ_p to zero. This turgor loss point (TLP) can be an indicator of drought tolerance both within and among species as well as over space and time (Dawson, 1990; Bartlett *et al*., 2012, 2014). In addition, maintaining relative water content (RWC) above about 75% prevents metabolic inhibition of photosynthesis and destabilization of cell membranes by excessively high osmotic concentrations (Lawlor & Cornic, 2002; Steponkus, 1984).

Maintaining positive Ψ_p and high RWC in foliage may be accomplished by managing osmotic concentration, tissue elasticity, and capacitive discharge of stored water (Scholz *et al*., 2011; Bartlett *et al*., 2012). Osmotic concentration exerts the strongest control over TLP. A higher concentration (lower Ψ_π) increases the range between Ψ_π and Ψ_p thus allowing more negative Ψ_w before turgor pressure is lost. Active synthesis or translocation of osmotica can further depress TLP seasonally as droughts intensify (Kozlowski & Pallardy, 2002; Sanders & Arndt, 2012). Higher osmotic concentrations, however, also drive lower RWC, but this effect may be counteracted by adjusting tissue elasticity (Bartlett *et al*., 2012). Structurally stiffer

tissues conserve water content by limiting cell contraction under extremely low Ψ_w (Cheung *et al*., 1975). Hydraulic capacitance and water storage capacity together offer an additional layer of protection for Ψ_p and RWC, although they do not themselves depress the TLP (Bartlett *et al*., 2012). Hydraulic capacitance reflects the ability to discharge stored water into the transpiration stream, while water storage capacity is that quantity of water stored (Scholz *et al*., 2011). Both hydraulic capacitance and water storage capacity stabilize Ψ_w against rapid fluctuations in vapor pressure deficits (Sack *et al*., 2003; Scholz *et al*., 2011; Edwards *et al*., 1986; Martins *et al*., 2016). They may also replenish evaporative losses through the lamina after stomata close (Lamont & Lamont, 2000, Hao *et al*., 2010).

In addition to maintaining positive Ψ_p in a desiccating environment, tall trees must also cope with a physiognomy that imparts vertical challenges. Acceleration due to gravity adds another component to the Ψ_w equation,

$$\Psi_w = \Psi_\pi + \Psi_p + \Psi_g \qquad \text{(Equation 2)}$$

where Ψ_g is the gravitational potential that imposes a gradient of –0.0098 MPa per meter of height above the ground (Nobel, 1983; Hinckley *et al*., 2011). Long hydraulic pathways additionally impede conductance (Tyree & Zimmermann, 2002; Mencuccini, 2003; Petit *et al*., 2010), and microclimatic conditions such as sunlight, humidity, and wind become increasingly desiccating with height in forest canopy (Parker, 1995). These height-related constraints can lead to decreasing Ψ_w with height in tall trees at a rate that is steeper than expected from the gravitational potential gradient alone (Koch *et al*., 2004; Woodruff *et al*., 2004; Ishii *et al* 2008; Ambrose *et al*., 2016).

In tall trees, the tissue-level mechanisms by which foliage maintains sufficient turgor pressure and water content against height-related constraints remain poorly understood. Given the strong control that osmotic concentration has over TLP, the consistent decrease in Ψ_w with height, and the fact that plants exhibiting more negative TLP are routinely more tolerant of lower Ψ_w (Kubuske & Abrams, 1994; Bucci *et al*., 2004), one might predict increasing foliar osmotic concentrations to depress TLP with height in tree. However, osmotic concentrations increase with height in some tall trees while in others there is no relationship, and TLP does not consistently decrease with height (Connor *et al*., 1977; Meinzer *et al*., 2008; Ishii *et al*., 2014; Azuma *et al*., 2016). The scarcity of studies, especially those reporting variation in hydraulic capacitance and water storage capacity with height, constrains our understanding of how foliar water relations help to maintain sufficient turgor pressure and water content against height-related constraints in tall trees.

Studying foliar water relations in *Sequoiadendron* provides an opportunity to evaluate the drought tolerance of a nationally iconic species whose 2.3 million year history suggests it may be vulnerable to a warmer and drier climate in the long term, but whose ability to live beyond 3,200 years suggests that it may be resilient in the short term. The tall stature and immense crowns of this species offer ideal conditions for studying strategies that help maintain Ψ_p above TLP against height-related constraints. Our primary objectives in this study of foliar water relations in *Sequoiadendron* were to: (1) quantify variation in TLP with height in tree; (2) determine the cellular controls over maintenance of turgor pressure and water content, and how they change seasonally from summer to fall; and (3) evaluate the importance of variation in water relations parameters with height as Ψ_w changes over the course of a day.

MATERIALS & METHODS

Study sites and field measurements

We selected 12 study trees in California, USA, from South Calaveras Grove in Calaveras Big Trees State Park (38.25°N, 120.24°W), Redwood Mountain Grove in Kings Canyon National Park (36.69°N, 118.91°W), Mountain Home State Demonstration Forest (36.21°N, 118.67°W), and Freeman Creek Grove (36.14°N, 118.52°W). Study trees ranged from 1.4-8.4 m in diameter, 48-95 m tall, and 230-2,510 years old (Sillett *et al*., 2015), and they grew on relatively rich alluvial soils close to perennial watercourses. Tree crowns were accessed using tree-climbing techniques (Jepson, 2000). Within each tree crown, 14-29 shoots were selected using randomly generated heights above ground, horizontal distances from main trunk, and azimuths from tree center. A selected shoot was cut at a stem diameter of approximately 2.0 cm, sealed into a plastic bag, and shielded from sunlight in an opaque container during transport to a laboratory. We harvested 300 shoots from the 12 study trees in summer (Jun-Jul) 2012, and in the fall (Sep-Oct) we harvested an additional 185 shoots that grew from the same branches and within 0.5 m of the original collections in order to detect seasonal changes in water relations. A measuring tape extending from average ground level to the tree top enabled each shoot's height to be recorded to 0.1 m resolution.

Pressure-volume curves

Within 3 hours of collection, each field-harvested shoot was submerged in tap water in which three (1 primary plus 2 back-up) smaller shoots 3-4 mm diameter were excised with a sharp razor blade. Maintaining submersion, a shoot's base was pushed through a slit in the foil cap of a water-filled test tube which was then placed into a dark humidity chamber to encourage overnight rehydration. Pressure-volume (PV) curves were generated the next morning using bench-drying and repeat-pressurization methods (Tyree & Hammel, 1972; Hinckley *et al*., 1980). A shoot was prepared for measurements by removing approximately 0.5 mm of the basal end with a sharp razor blade and blotting the leaves dry with a lint-free towelette. Mass of each shoot was measured on an analytical balance to 0.0001 g resolution immediately before and after a measurement of Ψ_w (MPa) made with a Scholander pressure chamber (Model 1000, PMS Instrument Co., Corvallis, OR). The two masses were averaged and paired with the Ψ_w. This process was repeated to generate a series of paired mass and Ψ_w comprising a PV curve for each shoot as it desiccated in ambient air. The rate of chamber pressurization used to quantify water potential was about 0.01 MPa s^{-1}, and measurements proceeded until about 85% of the initial shoot mass remained. Each shoot was then oven-dried at 60° to obtain dry mass necessary to calculate RWC (decimal),

$$\text{RWC} = \frac{\text{mass} - \text{dry mass}}{\text{fully hydrated mass} - \text{dry mass}} \qquad \text{(Equation 3)}$$

(Koide *et al*., 2000) for each point of the PV curve. Pressure-volume curves that failed due to shoot breakage or that yielded multiple outlying estimates were excluded from further analyses, reducing the final water relations dataset to 260 summer and 180 fall PV curves.

Rehydration of a shoot sometimes caused oversaturation which was visualized in a scatterplot of H_2O mass on Ψ_w as water content approached an asymptote at high Ψ_w. We removed points contributing to this "plateau effect" in each PV curve to avoid overestimation of water content (Kubiske & Abrams, 1991). We then used an iterative process to objectively separate the remaining points into pre-turgor loss and post-turgor loss from which water relations variables were estimated using linear regressions. Starting with three points taken at the lowest water potentials, which represented the first iteration's post-turgor loss points, an osmotic potential at full turgor ($\Psi_{\pi ft}$, MPa) was extrapolated as –1/y-intercept of a linear regression of $-1/\Psi_w$ on 1–RWC (Richter 1978), while saturated water content (SWC, g) was extrapolated from the remaining points (pre-turgor loss points) as the x-intercept of a linear regression of Ψ_w on H_2O mass (Ladiges, 1975). These two relationships allowed Ψ_π (MPa) and Ψ_p (MPa) to be calculated for each point in the PV curve (Equations 1, 3). A TLP (MPa) was then extrapolated as the x-intercept of a linear regression of Ψ_p on Ψ_w using the pre-turgor loss points. If this TLP was not between the two consecutive Ψ_w measurements that separated the pre- from post-turgor loss points, the solution was rejected and the next iteration initiated. The next iteration included a fourth post-turgor loss point, and a new TLP was calculated. This iterative process continued until a TLP was successfully bracketed between two consecutive Ψ_w measurements. The bracketed value was used as the final TLP as well as to separate pre- from post-turgor loss points that we then used to calculate the remaining final water relations variables. The final pre-turgor loss points contained an average of eight points and were well represented by linear regressions (average $R^2 = 0.9980$).

Pre-turgor loss points were used to infer total RWC at the TLP (total RWC_{TLP}, decimal) as the corresponding x-value from the $-1/\Psi_w$ on 1–RWC relationship, as well as to calculate bulk tissue elastic modulus (ε, MPa),

$$\varepsilon = \frac{\Delta\Psi_p}{\Delta RWC} \bullet SWF \qquad \text{(Equation 4)}$$

(Tyree & Hammel, 1972; Koide *et al*., 2000), where SWF is the symplastic water fraction. We also used the pre-turgor loss points to calculate three metrics of water storage. Hydraulic capacitance normalized by dry mass (C_{mass}, g g^{-1} MPa^{-1}) was the change in water content per change in Ψ_w (Scholz *et al*., 2011),

$$C_{mass} = \frac{\Delta RWC}{\Delta\Psi_w} \bullet \frac{SWC}{\text{dry mass}} \qquad \text{(Equation 5)}$$

Total water storage capacity normalized by dry mass (S_{mass}, g g^{-1}) was used as an index of succulence (Bacelar *et al*., 2004),

$$S_{mass} = \frac{SWC}{\text{dry mass}} \qquad \text{(Equation 6)}$$

Finally, we developed a new measure of storage capacity as water available within the typical range of Ψ_w and normalized by dry mass (W_{mass}, g g^{-1}), defined as the change in water content between Ψ_g and TLP,

$$W_{mass} = (TLP - \Psi_g) \bullet \frac{\Delta H_2O}{\Delta \Psi_w} \bullet \frac{1}{\text{dry mass}} \quad \text{(Equation 7)}$$

where $\Delta H_2O / \Delta \Psi_w$ is the slope of linear regression of Ψ_w on H_2O mass before turgor loss. Although we favor expressing these three metrics of water storage by dry mass due to the highly three-dimensional configuration of *Sequoiadendron* foliage, we also normalize them by total shoot fresh area (C_{area}, S_{area}, W_{area}) predicted from a power function fit to 267 pairs of dry mass (g) and fresh area (cm^2),

$$\text{fresh area} = 13.1392 \bullet \text{dry mass}^{0.7920} \quad \text{(Equation 8)}$$

($R^2 = 0.93$; Anthony Ambrose, unpublished data), to facilitate comparisons with other reports. Post-turgor loss points were used to calculate $\Psi_{\pi ft}$, AWF (decimal) as the x-intercept of $-1/\Psi_w$ on 1–RWC, and SWF (decimal) as 1–AWF. Symplastic water fractions were incorporated into the calculation of ε (Tyree & Hammel, 1972; Koide *et al*., 2000) and also used to compute symplastic RWC at TLP (symplastic RWC_{TLP}, decimal). See Table 1 for a list of water relations variables and their units used in this study.

Sensitivity analyses

We performed three sensitivity analyses to determine the cellular drivers of TLP, symplastic RWC_{TLP}, and total RWC_{TLP}. The relative sensitivity (Φ_i) for an independent variable was calculated from the partial derivative of the dependent variable with respect to the independent variable ($\Phi_i = \partial Y/\partial X_i \bullet |X_i/Y|$), where $|X_i/Y|$ normalizes the absolute sensitivity to allow relative comparisons among independent variables irrespective of their units (Hamby, 1994; Smith *et al*., 2008). The partial differential equations provided by Bartlett *et al*. (2012) allowed us to quantify the influences that $\Psi_{\pi ft}$ and ε had over TLP and symplastic RWC_{TLP}. Using the same methodology to determine the cellular drivers of total RWC_{TLP}, we used the underlying equation,

$$\text{total } RWC_{TLP} = (1 - AWF) \bullet \frac{\varepsilon + \Psi_{\pi ft}}{\varepsilon} + AWF \quad \text{(Equation 9)}$$

(Bartlett *et al*., 2012) to derive three new partial differential equations that quantified the absolute sensitivity of total RWC_{TLP} to ε, $\Psi_{\pi ft}$, or AWF:

$$\frac{\partial \text{ total } RWC_{TLP}}{\partial \varepsilon} = \Psi_{\pi ft} \bullet \frac{(AWF - 1)}{\varepsilon^2} \quad \text{(Equation 10a)}$$

$$\frac{\partial \text{ total } RWC_{TLP}}{\partial \Psi_{\pi ft}} = \frac{(AWF - 1)}{\varepsilon} \quad \text{(Equation 10b)}$$

$$\frac{\partial \text{ total } RWC_{TLP}}{\partial AWF} = 1 - \frac{(\varepsilon + \Psi_{\pi ft})}{\varepsilon} \quad \text{(Equation 10c)}$$

Table 1. Water relations variables, their symbols, units, and derivations.

Symbol	Definition	Unit	Derivation
AWF	Apoplastic water fraction	decimal	x-intercept from $-1/\Psi_w$ on 1 – RWC regression
C_{mass}	Hydraulic capacitance, normalized by dry mass	g g^{-1} MPa^{-1}	(ΔRWC / $\Delta\Psi_w$) • (SWC / dry mass)
C_{area}	Hydraulic capacitance, normalized by fresh arrea	g m^{-1} MPa^{-1}	(ΔRWC / $\Delta\Psi_w$) • (SWC / fresh area)
ε	Bulk tissue elastic modulus	MPa	($\Delta\Psi_p$ / ΔRWC) • SWF
Ψ_g	Gravitational potential	MPa	–0.0098 • H
Ψ_p	Turgor pressure	MPa	$\Psi_w - \Psi_\pi - \Psi_g$
Ψ_π	Osmotic potential	MPa	–1/y-value from $-1/\Psi_w$ on 1 – RWC regression
$\Psi_{\pi ft}$	Osmotic potential at full turgor	MPa	–1/y-intercept from $-1/\Psi_w$ on 1 – RWC regression
Ψ_w	Bulk shoot water potential	MPa	$\Psi_p + \Psi_\pi + \Psi_g$
RWC	Relative water content	decimal	(mass – dry mass) / (fully hydrated mass – dry mass)
total RWC_{TLP}	Total relative water content at the turgor loss point	decimal	corresponding RWC for TLP
symplastic RWC_{TLP}	Symplastic portion of relative water content at the turgor loss point	decimal	SWF • total RWC_{TLP}
S_{mass}	Water storage capacity, normalized by dry mass	g g^{-1}	SWC / dry mass
S_{area}	Water storage capacity, normalized by area	g m^{-1}	SWC / fresh area
W_{mass}	Water storage capacity prior to TLP, corrected for gravity, normalized by dry mass	g g^{-1}	(TLP – Ψ_g) • (ΔH_2O / $\Delta\Psi_w$) / dry mass
W_{area}	Water storage capacity prior to TLP, corrected for gravity, normalized by fresh area	g m^{-1}	(TLP – Ψ_g) • (ΔH_2O / $\Delta\Psi_w$) / fresh area
SWC	Saturated water content	g	x-intercept from Ψ_w on H_2O mass
SWF	Symplastic water fraction	decimal	1 – AWF
TLP	Turgor loss point	MPa	x-intercept from Ψ_p on Ψ_w regression

The parameter estimates from a PV curve (e.g., ε, $\Psi_{\pi ft}$, AWF) were used to solve these equations, and the outputs were normalized to relative sensitivities. The relative sensitivities for an independent variable were averaged across all 260 summertime PV curves to yield a measure of the strength of influence that variable had over the dependent variable. To visualize the relative sensitivity of total RWC_{TLP} to $\Psi_{\pi ft}$, ε, or AWF, we performed a "one-at-a-time" sensitivity analysis wherein one independent variable was allowed to vary over its measured range while the other two were held constant at their minimum, average, or maximum values.

Importance of foliar water storage

We quantified the importance of foliar water storage capacity based on our average estimates of S_{mass} and W_{mass}. This metric was averaged across all 260 summertime PV curves and then scaled up to whole-tree levels using estimates of foliar dry mass published for each of the 12 study trees (Sillett *et al*., 2015). Daily water use per crown dry mass was then calculated as 1.62 L day^{-1} kg^{-1} using an estimate derived from summertime sap flow measurements reported for a large *Sequoiadendron* (Ambrose *et al*., 2016). Finally, the importance of stored water was expressed as the quotient of whole-crown water storage per daily summertime water use.

Diurnal courses of Ψ_w, Ψ_p, and Ψ_π

Pressure-volume curves can be combined with measurements of Ψ_w made periodically over a day to estimate diurnal courses of Ψ_p as well as Ψ_π (after Robichaux, 1984). Using a batch of PV curves generated from shoots growing within a 2.0 m height range in a tree, we developed a composite linear regression of Ψ_p on Ψ_w from pre-turgor loss points (Fig. 1) that was then used to predict changes in Ψ_p from periodic measurements of Ψ_w made with a pressure chamber. These courses of Ψ_w and Ψ_p combined with Ψ_g for a given height allowed calculation of Ψ_π for each field measurement of Ψ_w (Equation 2). We used this approach to estimate diurnal changes in the components of Ψ_w at upper crown and lower crown positions for the tallest study tree at each of the four sites. The eight composite Ψ_p on Ψ_w relationships were each developed

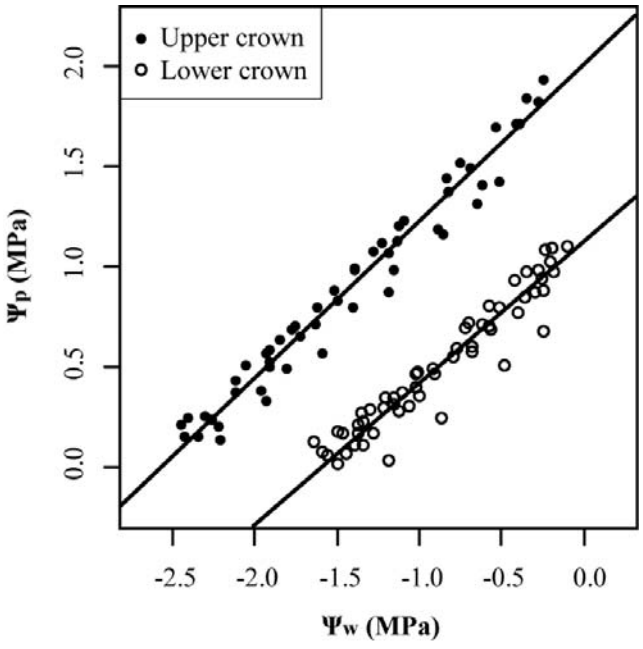

Figure 1. Linear regression relationships between turgor pressure (Ψ_p) and water potential (Ψ_w) prior to turgor loss derived from pressure-volume curves generated separately for eight upper crown (83.0 m) shoots and six lower crown (14.7 m) shoots that were collected from a *Sequoiadendron* in Mountain Home State Demonstration Forest. The relationships were used to predict Ψ_p from diurnal courses of Ψ_w for this tree.

from 3-8 PV curves. Within one week after generating the PV curves, we measured Ψ_w at 1.5-hour intervals from pre-dawn to post-dusk using 3-10 replicate shoots that were 3-4 mm diameter and collected at random from each crown position.

Statistical analyses

Water relations estimates were computed from the PV curves using reduced major axis regression because the variables each had their own error, were co-dependent, and were of different types (Sokal & Rohlf, 1995). Relationships between height above ground and water relations variables were evaluated using ordinary least squares regression, and the slopes of TLP and $\Psi_{\pi ft}$ on height were compared using ANCOVA. Paired two-tailed t-tests were used to compare the relative sensitivities of TLP or symplastic RWC_{TLP} to ε or $\Psi_{\pi ft}$, as well as the relative sensitivities of total RWC_{TLP} to ε, $\Psi_{\pi ft}$, or AWF. Summer versus fall water relations estimates were also compared using paired t-tests. Statistical analyses were performed in R (R Development Core Team, 2016).

RESULTS

Water relations correlates with height

Ordinary least squares regression between height above ground and each of the water relations variables revealed several significant relationships (Table 2). Turgor loss point decreased with height at a rate that was indistinguishable from the gravitational potential gradient of –0.0098 MPa m^{-1} (95% CI –0.0122 to –0.0093; $R^2 = 0.45$; Fig. 2). Osmotic potential at full turgor decreased with height at a slower rate (ANCOVA, $F(1, 516) = 6.0725$, $p = 0.01$).

Table 2. Statistical relationships between water relations variables and height in *Sequoiadendron* tree using ordinary least squares regression.

Water relations variable	slope	intercept	R^2	*p* -value
AWF	-0.0034	0.7186	0.27	<0.01
$\Psi_{\pi ft}$	-0.0083	-0.9801	0.39	<0.01
TLP	-0.0107	-1.3316	0.45	<0.01
$\Psi_{\pi ft}$ – TLP	0.0024	0.3514	0.23	<0.01
total RWC_{TLP}	-0.0008	0.9250	0.44	<0.01
symplastic RWC_{TLP}			0.00	0.41
ε	0.0351	3.6795	0.16	<0.01
C_{mass}	-0.0002	0.0899	0.06	<0.01
C_{area}			0.01	0.06
S_{mass}	-0.0040	1.5261	0.14	<0.01
S_{area}	-1.3052	763.2557	0.07	<0.01
W_{mass}	-0.0002	0.1192	0.03	<0.01
W_{area}			0.00	0.47

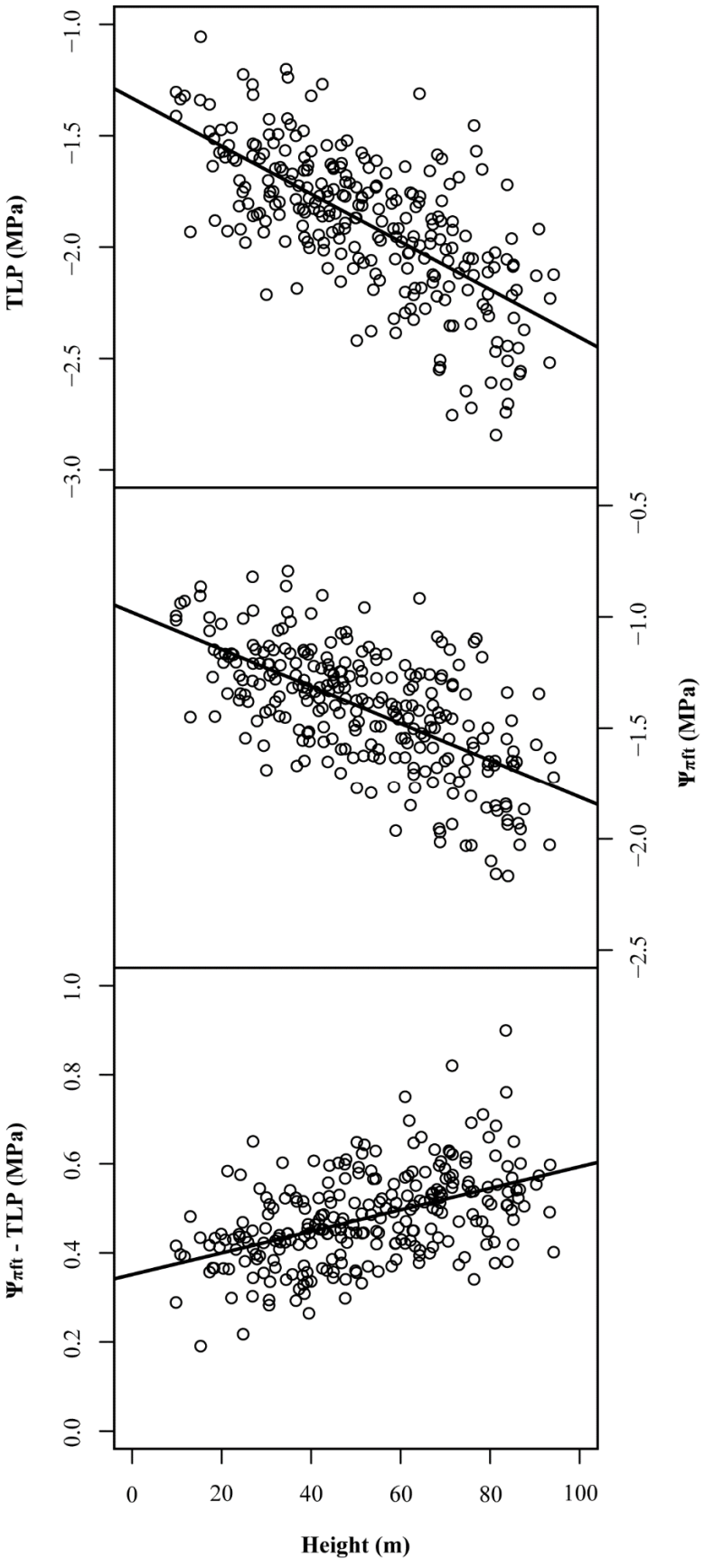

Figure 2. Turgor loss point (TLP) and osmotic potential at full turgor pressure ($\Psi_{\pi ft}$) both decreased with height in *Sequoiadendron* tree, while the difference between these two water relations variables increased with height. Trendlines represent ordinary least squares regressions.

The difference in slopes caused TLP and $\Psi_{\pi ft}$ to diverge with height and may indicate declining turgor pressures toward the tree tops. Bulk tissue elastic modulus increased with height (R^2 = 0.16; Fig. 3). Apoplastic water fraction was negatively correlated with height (R^2 = 0.27) and varied widely from 17 to 80%. Total RWC_{TLP} was also negatively correlated with height (R^2 = 0.44), but symplastic RWC_{TLP} was uncorrelated. Several water storage parameters exhibited weak negative correlations with height (Fig. 4). Although S_{mass} decreased, this trend essentially disappeared when substituting our more conservative estimate of water storage, W_{mass}.

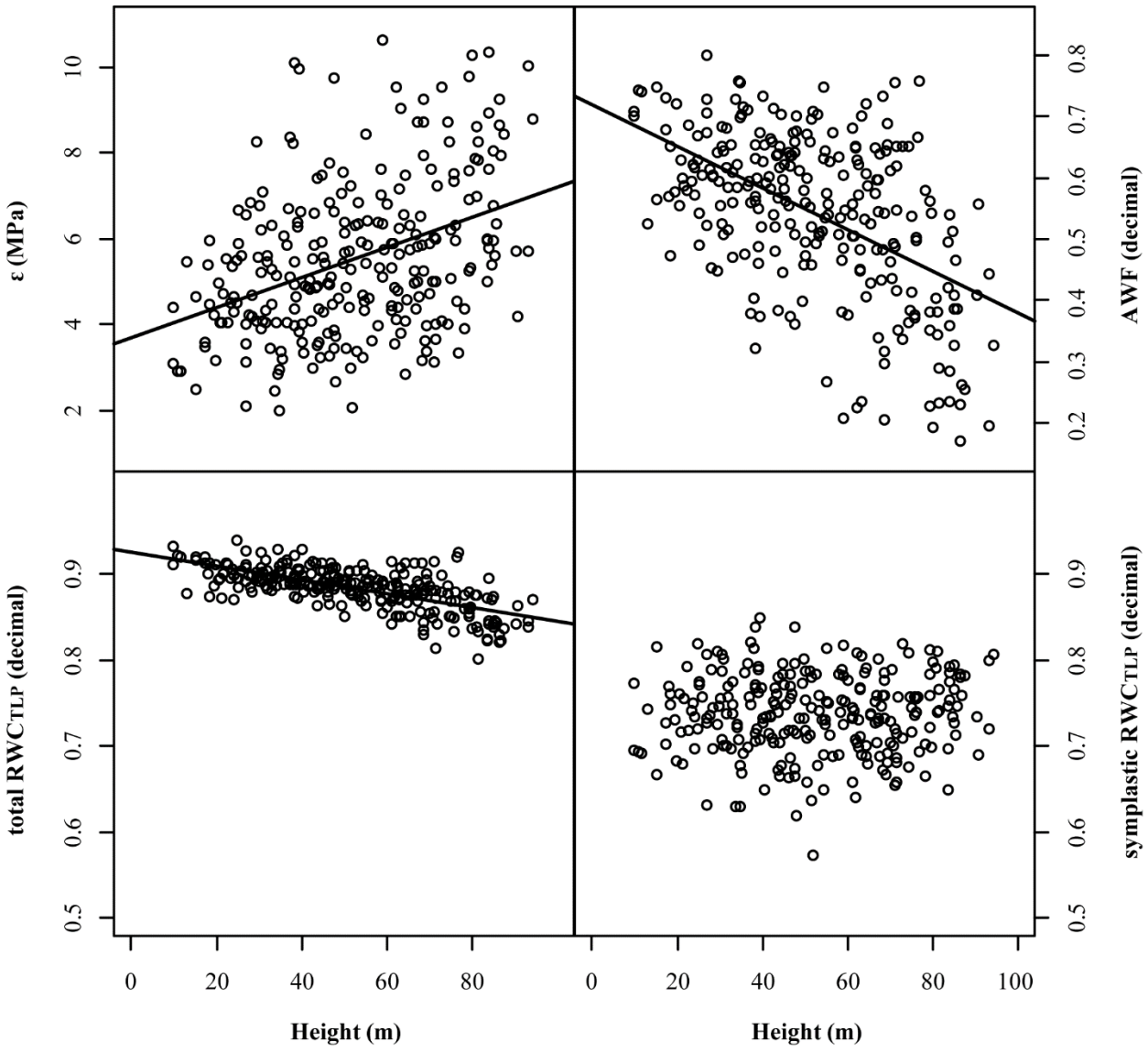

Figure 3. Relationships between four foliar water relations variables and height in *Sequoiadendron* using ordinary least squares regression. The four water relations variables are bulk tissue elastic modulus (ε), apoplastic water fraction (AWF), total relative water content at the turgor loss point (total RWC_{TLP}), and symplastic RWC_{TLP}.

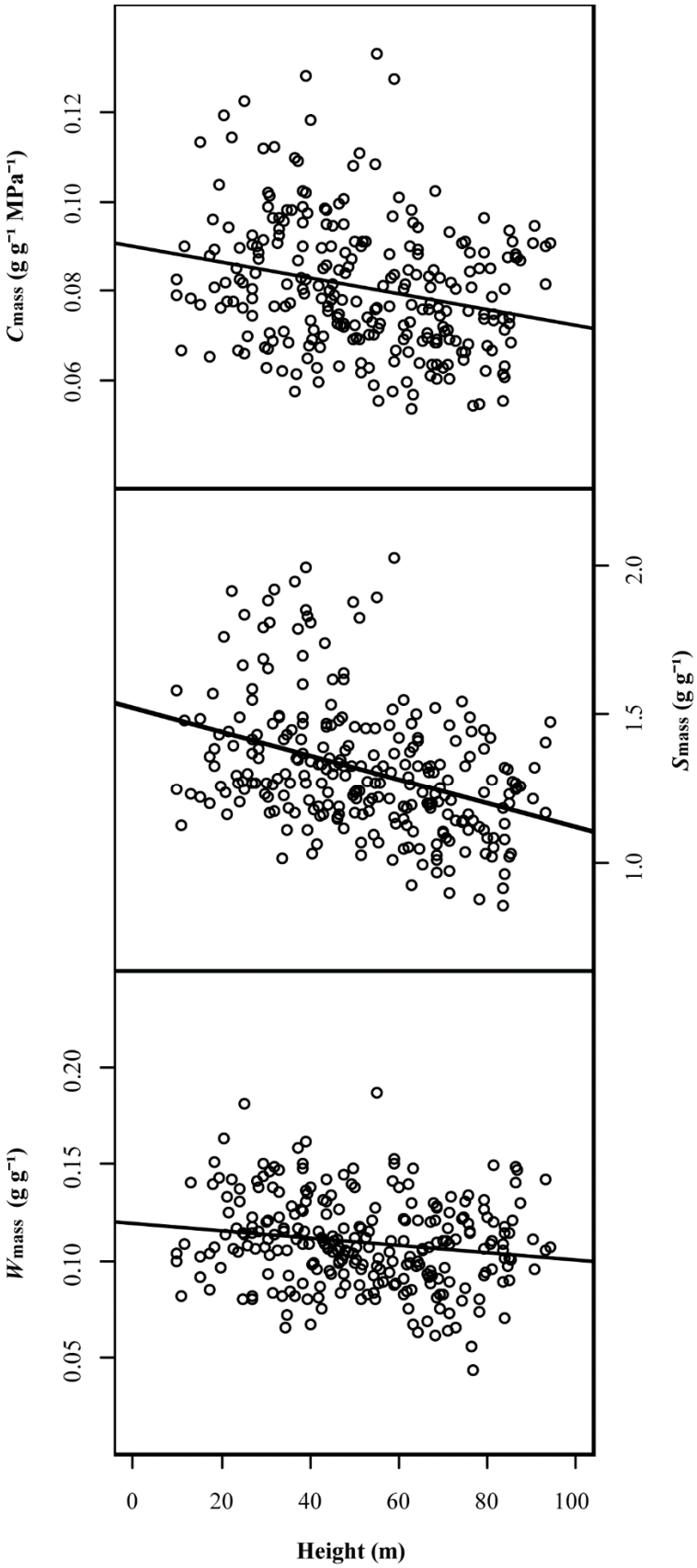

Figure 4. Relationships between three foliar water relations variables and height in *Sequoiadendron* tree using ordinary least squares regression. The three water relations variables are mass-normalized hydraulic capacitance (C_{mass}), total water storage capacity (S_{mass}), and water storage that was available within the typical range of water potentials (W_{mass}).

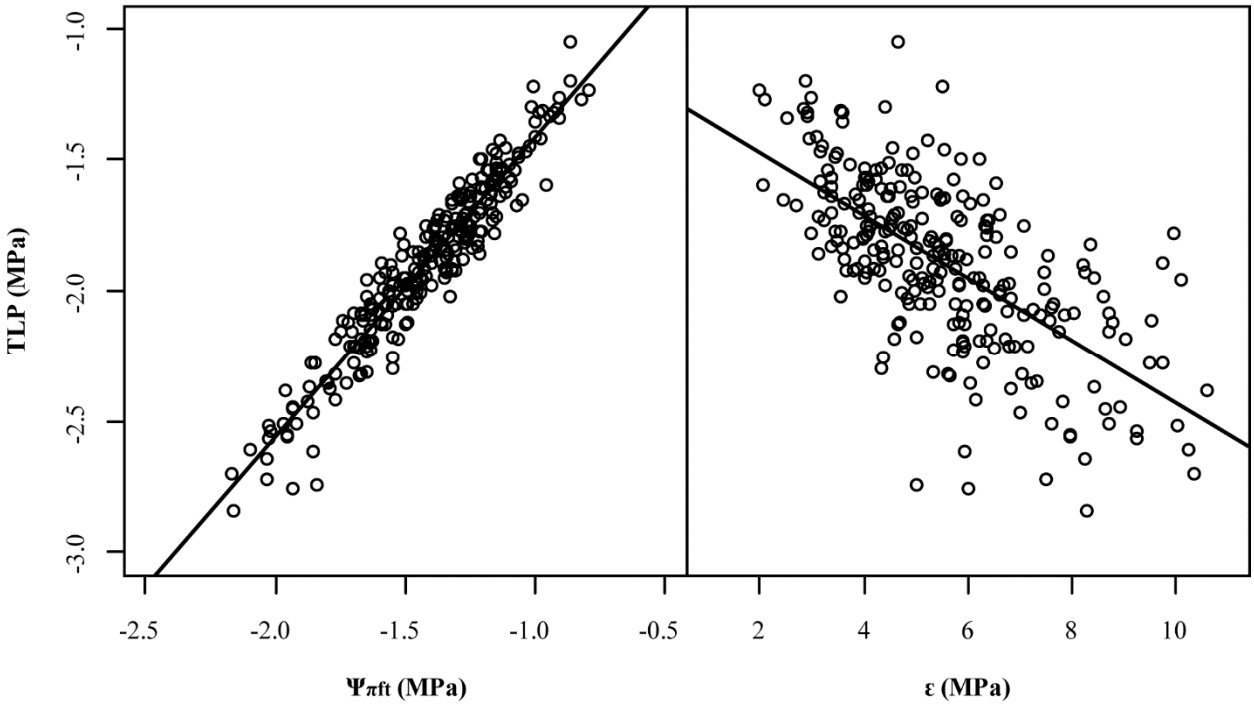

Figure 5. Relationships between three foliar water relations variables in *Sequoiadendron* using ordinary least squares regression. The three water relations variables are turgor loss point (TLP), osmotic potential at full turgor ($\Psi_{\pi ft}$), and bulk tissue elastic modulus (ε).

Controls over TLP and RWC_{TLP}

We found a strong positive correlation between TLP and $\Psi_{\pi ft}$ ($p < 0.01$; $R^2 = 0.91$) and a negative correlation with ε ($p < 0.01$; $R^2 = 0.43$; Fig. 5). Our differential sensitivity analysis indicated that TLP was more responsive to changes in $\Psi_{\pi ft}$ than ε ($p < 0.01$; Table 3). Symplastic RWC_{TLP} was equally sensitive to $\Psi_{\pi ft}$ and ε, indicating that the decline in symplastic water content driven by osmotica was counteracted by stiffer tissues. This analysis also revealed that total RWC_{TLP} was more sensitive to AWF than to ε or $\Psi_{\pi ft}$ ($p < 0.01$ for both), and the sensitivity ratio of total RWC_{TLP} to AWF versus ε decreased with height ($p < 0.01$; $R^2 = 0.22$; Fig. 6). These results indicate that the proportion of symplastic versus apoplastic water was an important driver of changes in total RWC_{TLP}. Our "one-at-a-time" sensitivity analysis for total RWC_{TLP} provided visualizations of the potential responsiveness to $\Psi_{\pi ft}$, ε, and AWF (Fig. 7). Reductions in total RWC_{TLP} that were driven by high osmotic concentrations could be offset by shifting water to the apoplasm without varying tissue elasticity. Increasing AWF also had a strong potential to counteract a precipitous decline in total RWC_{TLP} that occurred with more flexible tissues at constant osmotic concentration. Likewise, stiffer tissues could offset the linear decline in total RWC_{TLP} that was driven by lower AWF. Overlaying real data points onto these sensitivity visualizations revealed that a balance between ε and AWF successfully maintained total RWC_{TLP} above 75% across the entire range of osmotic concentrations.

Table 3. Results from a sensitivity analysis using partial differentiation to evaluate the relative importance of variables underlying foliar water relations traits in *Sequoiadendron*. Absolute sensitivities quantify the responsiveness of turgor loss point (TLP), symplastic relative water content at the TLP (symplastic RWC_{TLP}), and total RWC_{TLP} to their underlying variables, bulk tissue elastic modulus (ε), osmotic potential at full turgor ($\Psi_{\pi ft}$), or apoplastic water fraction (AWF). Absolute sensitivities were normalized to enable relative comparisons among input variables.

Function	Absolute sensitivity	Standard error	Normalized sensitivity	Standard error
∂ TLP / ∂ ε	0.153	0.006	0.378	0.006
∂ TLP / $\partial \Psi_{\pi ft}$	1.909	0.018	1.378	0.006
∂ symplastic RWC_{TLP} / ∂ ε	0.058	0.002	0.378	0.006
∂ symplastic RWC_{TLP} / $\partial \Psi_{\pi ft}$	0.202	0.004	0.378	0.006
∂ total RWC_{TLP} / ∂ ε	0.023	0.000	0.136	0.002
∂ total RWC_{TLP} / $\partial \Psi_{\pi ft}$	0.085	0.001	0.136	0.002
∂ total RWC_{TLP} / ∂ AWF	0.270	0.003	0.171	0.004

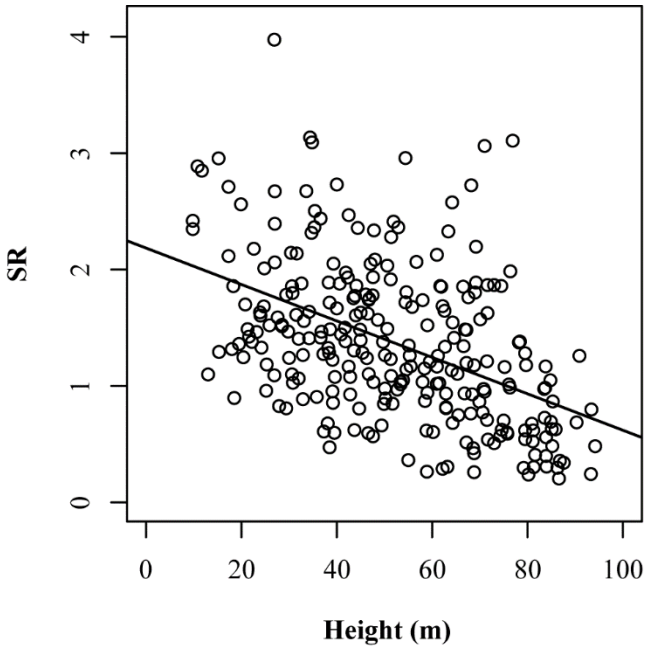

Figure 6. Total relative water content at the turgor loss point (total RWC_{TLP}) is controlled by three underlying variables: osmotic potential at full turgor ($\Psi_{\pi ft}$), bulk tissue elastic modulus (ε), and apoplastic water fraction (AWF). The relative sensitivity of total RWC_{TLP} to changes in AWF declined with height in *Sequoiadendron* tree while the relative sensitivity to ε increased. The result is borne out in this ordinary least squares regression in which the relative sensitivity ratio (SR) of AWF to ε decreased with height in tree.

Water storage

Estimates for area-normalized hydraulic capacitance (C_{area}) in *Sequoiadendron* foliage were quite large with a mean of 42.7 g m^{-2} MPa^{-1} (range 26.0-62.8). Scaling our two metrics of water storage capacity, S_{mass} and W_{mass}, to whole-crown levels yielded very different estimates for the importance of water storage capacity. We estimated the importance of S_{mass} to be 85.1% ± SE 11.5% of daily transpiration, whereas the importance of W_{mass} was far less at only 6.8% ± 0.9%.

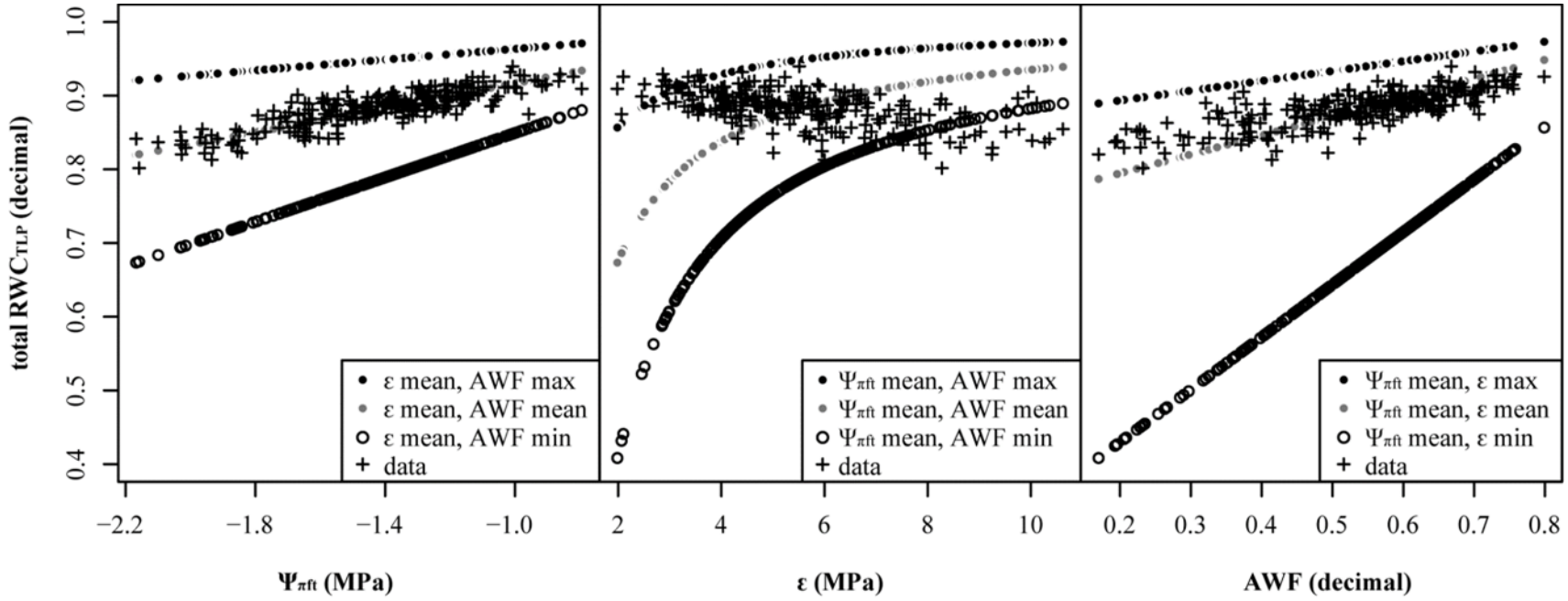

Figure 7. A "one-at-a-time" sensitivity analysis portraying the responsiveness of total relative water content at the turgor loss point (total RWC_{TLP}) to changes in three underlying variables: osmotic potential at full turgor ($\Psi_{\pi ft}$), bulk tissue elastic modulus (ε), and apoplastic water fraction (AWF). In each panel, one underlying variable was allowed to vary over its measured range while the other two were held constant at their minimum, average, or maximum value. Real data points (+) from *Sequoiadendron* are superimposed to aid interpretation.

Temporal changes in foliar water relations

Comparing water relations variables from the 180 shoot harvest locations measured in both summer and fall revealed seasonal differences (Table 4). The largest percent changes from summer to fall were increases in AWF (27.2%) and S_{area} (20.8%). Area-normalized water storage parameters exhibited larger seasonal differences than their mass-normalized counterparts. Total RWC_{TLP} increased while symplastic RWC_{TLP} decreased. We did not observe seasonal changes in $\Psi_{\pi ft}$, TLP or ε.

Daily courses of Ψ_w were overall more negative in upper crown than in lower crown positions, decreasing at first direct sunlight, reaching minimum values at midday with an occasional short recovery period, and then recovering to nearly pre-dawn values after the last direct light (Fig. 8). Minimum Ψ_w at a given position did not surpass its TLP, but subjecting any tree's lower crown foliage to Ψ_w experienced in the upper crown would have resulted in turgor loss. Diurnal courses of Ψ_p and Ψ_π mimicked the trajectories of Ψ_w; Ψ_p approached zero while Ψ_π decreased toward midday, followed by recovery as daylight diminished. The range of Ψ_π was consistently equal to or greater than the range of Ψ_g at any upper or lower crown position.

Table 4. Paired, two-tailed t-tests were used to compare summer versus fall foliar water relations variables in *Sequoiadendron*. Negative percent differences indicate significant summer-to-fall decreases in the average value while positive differences indicate increases.

Water relations variable	*P*-value	% Change
AWF	<0.01	+27.2
$\Psi_{\pi ft}$	0.84	
TLP	0.29	
total RWC_{TLP}	<0.01	+1.5
symplastic RWC_{TLP}	0.02	-1.4
ε	0.06	
C_{mass}	0.02	-1.2
C_{area}	0.02	+6.6
S_{mass}	<0.01	+11.7
S_{area}	<0.01	+20.8
W_{mass}	0.45	
W_{area}	<0.01	+11.5

DISCUSSION

Our results suggest that gravity plays a major role in shaping the water relations of *Sequoiadendron*. Height-related increases in osmotic concentration, apoplastic water fraction, and bulk tissue elastic modulus enabled tight control over turgor pressure and water content. Together with seasonal adjustments in water content and exceptionally large hydraulic capacitance, these foliar water relations traits allow *Sequoiadendron* to regularly function close to the turgor loss point.

Gravity explains variation in TLP

Recent meta-analyses revealed that the turgor loss point (TLP) can be an indicator of drought tolerance both within and among species (Bartlett *et al*., 2012, 2014). In tall trees,

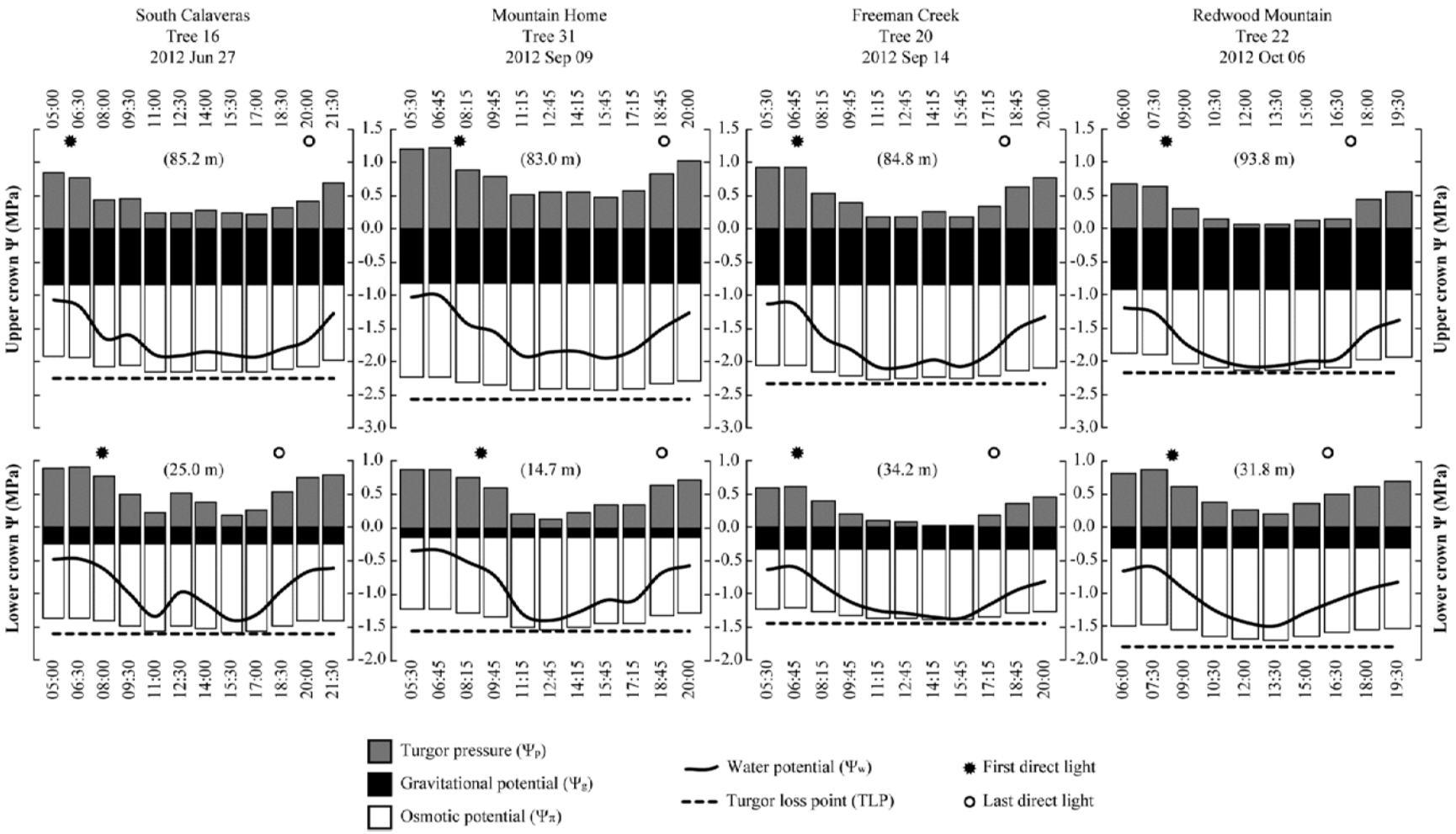

Figure 8. Diurnal courses of water potential (Ψ_w) and its three components, turgor pressure (Ψ_p), gravitational potential (Ψ_g), and osmotic potential (Ψ_π), at upper crown and lower crown positions in four tall *Sequoiadendron* trees. The turgor loss point (TLP) is also shown for each of the eight diurnal courses, as is the timing of direct sunlight exposure. Note that Ψ_w approaches but does not surpass TLP, and that subjecting lower crown foliage to Ψ_w experienced in the upper crown would result in turgor loss.

several environmental factors potentially contribute to variation in the TLP with height, including the standing –0.01 MPa per meter of height imposed by gravity, the accumulation of hydraulic resistance with path length (Petit *et al*., 2010), and overall drier microclimatic conditions toward the tree tops (Parker, 1995). Therefore, one might expect the TLP to decrease with height at a rate equivalent to or more extreme than the gravitational potential gradient. However, factors associated with hydraulic constraints, not light, are consistently more important to variation in leaf structure in *Sequoia* and *Sequoiadendron* (Koch *et al*., 2004; Ishii *et al*., 2008, Ambrose *et al*., 2009; Oldham *et al*., 2010; Chin & Sillett 2016). Moreover, the slope of TLP on height extracted from PV curves generated across all 12 study trees was indistinguishable from that of the gravitational potential gradient. These results together suggest that gravity, not path length or microclimate, was the primary environmental factor explaining variation in the TLP.

Tissue osmotic and elastic properties have both been reported to control variation in TLP (Niinemets, 2001; Merchant *et al*., 2007; Mitchell *et al*., 2008), but a global meta-analysis of water relations research implicated osmotica as the primary control (Bartlett *et al*., 2012). Consistent with this, our sensitivity analysis showed that TLP was more responsive to variation in osmotica than to tissue elasticity across the range of values in *Sequoiadendron*. Moreover, separating the components of water potential (Ψ_w) over diurnal courses revealed that the range of osmotic potential (Ψ_π) was equivalent to or greater than the gravitational potential (Ψ_g) at a given height (Fig. 8). These results clearly demonstrate that variation in TLP in *Sequoiadendron* is primarily controlled by tissue osmotica. The decreasing osmotic potential at full turgor ($\Psi_{\pi ft}$) with height also supports this assertion. However, the widening difference between $\Psi_{\pi ft}$ and TLP with height (Fig. 2) suggests that turgor pressure (Ψ_p) also decreases with height as observed for other tall conifers (Koch *et al*., 2004; Woodruff *et al*., 2004; Meinzer *et al*., 2008). An increasing influence of osmotica with height was also recorded in *Eucalyptus regnans* and *Pseudotsuga menziesii* (Connor *et al*., 1977; Meinzer *et al*., 2008), a trend that we too inferred from reported slopes of Ψ_w and Ψ_p with height in *Sequoia sempervirens* (Koch *et al*., 2004). In *Pseudotsuga menziesii*, a concomitant decrease in TLP has also been observed (Woodruff *et al*., 2004). This research collectively points to a potentially common strategy of coping with the gravitational potential gradient via osmotica that reduce TLP with height.

Maintaining sufficient water content

Higher osmotic concentrations clearly drive lower TLP, but the tradeoff is a concomitant reduction in symplastic RWC_{TLP} in the absence of elastic compensation (Bartlett *et al*., 2012). The primary function of variation in elasticity may be a structural stiffening of tissues to limit cell contraction under extremely low Ψ_π so that sufficient water content can be maintained (Cheung *et al*., 1975). We observed no difference in the relative sensitivity of symplastic RWC_{TLP} to $\Psi_{\pi ft}$ versus ε, confirming that the reduction in symplastic RWC_{TLP} associated with lower $\Psi_{\pi ft}$ was offset by stiffer tissues. The fact that symplastic RWC_{TLP} throughout our study trees remained above about 60% against height-related constraints is well explained by increased tissue rigidity with height (Fig. 3). The regulation of tissue elastic properties with height in *Sequoiadendron* may be accomplished by increasing the number of fibers and hypodermal layers as well as the ratio of leaf vascular area to shoot area (Chin & Sillett, 2016).

Total RWC_{TLP} appears to be controlled by an additional underlying variable—the balance of water between the apoplasm and symplasm. Our sensitivity analysis revealed that total RWC_{TLP} was more responsive to variation in AWF than ε. As with symplastic RWC_{TLP}, higher osmotic concentrations caused a reduction in total RWC_{TLP} when ε was held constant, but this

trend was offset by an increase in AWF (Fig. 7). At constant osmotic concentration, the same change in AWF also relieved the dependence of total RWC_{TLP} on ε, thus allowing tissue structure to range from rigid to flexible without compromising total RWC_{TLP}. With height in tree, we observed a shift in the drivers that maintain total RWC_{TLP}. Stiffer foliage was associated with lower AWF, and the relative sensitivity of total RWC_{TLP} to AWF decreased while the sensitivity to ε increased along this vertical gradient (Fig. 6). This shift in the relative importance of these drivers may serve two functions. First, stiffer foliage physically constrains tissue contraction under low water potentials to conserve water content, which was sustained above the 75% required to avoid metabolic inhibition and cell membrane destabilization (Lawlor & Cornic, 2002; Steponkus, 1984). Second, we speculate that the concomitant increase in more mobile symplastic water may better buffer swings in vapor pressure deficits experienced in the upper crowns.

Defining apoplastic water—a brief note

Foliage is structurally complex and contains several pathways for water transport. Apoplastic transport occurs through cell walls (and intercellular spaces) outside of the protoplast while symplastic transport occurs through cell protoplasm including plasmodesmata that connect adjoining cells. The PV curve technique assumes apoplastic water remains constant over the course of the measurements (Tyree, 1976; Turner, 1988). However, recent research indicates that a substantial proportion of leaf hydraulic conductance outside the xylem is apoplastic (Buckley, 2014; Scoffoni, 2015; Yaaran & Moshelion, 2016). Moreover, the hollow lumens of tracheary elements carry water through leaf veins, yet these conduits are treated as part of the apoplastic pathway since they lack protoplasm (Tyree & Hammel, 1972; Hacke, 2015). Therefore, the apoplastic pathway is absolutely part of the transpiration stream, and we do not consider apoplastic water (or its fraction, AWF) to be constant over the course of generating a PV curve. This contradiction does not undermine the validity of PV curves, but it does call for a more accurate anatomical portrayal of where the less mobile "apoplastic" water is stored.

Succulent giant sequoia shoots

Both hydraulic capacitance and water storage capacity have the potential to stabilize tree physiological functions against fluctuations in environmental conditions within a diurnal cycle (Edwards *et al*., 1986; Sack *et al*., 2003; Scholz *et al*., 2011; Martins *et al*., 2016). Height in forest canopy is associated with increasingly desiccating microclimatic conditions (Parker, 1995), so one might expect an increase in hydraulic capacitance with height in tree as reported for *Sequoia sempervirens* (Ishii *et al*., 2014). Instead we observed weak evidence for declining C_{mass} in *Sequoiadendron* and no trend in C_{area}, similar to that reported for tall *Pseudotsuga menziesii* (Woodruff *et al*., 2007). However, our exceptionally large values of C_{area} were nearly double that reported for a wide taxon sampling of tree species including other Cupressaceae (Scholz *et al*., 2011; Ishii *et al*., 2014; Azuma *et al*., 2016). Such large C_{area} may be explained by an abundance of leaf transfusion tissue, which can deform under low Ψ_w to release stored water (Brodribb & Holbrook, 2005; Oldham *et al*., 2010; Azuma *et al*., 2016). *Sequoiadendron* has about three times the cross-sectional area of transfusion tissue per leaf compared to *Sequoia* and *Cryptomeria* (Ishii *et al*., 2014; Azuma *et al*., 2016; Chin & Sillett, 2016). The capacity to release large quantities of water over small changes in Ψ_w may allow *Sequoiadendron* to delay stomatal closure as humidity falls and demand for water by a drying atmosphere increases (Martins *et al*., 2016). Rapid and full recharge of transfusion tissue and other capacitors may be

fostered by abundant summertime snowmelt that supplies very large daily summertime demands for water (Ambrose *et al*., 2016).

While hydraulic capacitance represents the ability for stored water to be released to the transpiration stream, water storage capacity is the actual quantity of water available for release (Scholz *et al*., 2011). We found a decrease in foliar water storage capacity with height in *Sequoiadendron* in contrast to the increase found in both *Sequoia* and *Cryptomeria* that has been proposed to lessen the severity of height-related hydraulic constraints (Ishii *et al*., 2014; Azuma *et al*., 2016). Compared to S_{area} or S_{mass} which represent total water storage, the amount of water storage that is actually "available" to the transpiration stream is that which can be used (depleted) over some typical range of water potential (Zweifel *et al*., 2001). Here we define this available water storage as the symplastic water fraction between Ψ_g and TLP and calculated as W_{area} or W_{mass} (Equation 7). Using this definition, the negative correlation between water storage capacity and height essentially disappeared, suggesting that water storage does not play a role in coping with the gravitational potential gradient in *Sequoiadendron*.

Scaling S_{mass} versus W_{mass} to whole-crown levels provided dramatically different estimates for the importance of water storage capacity. We computed a 12.5-fold difference between these two storage metrics, with S_{mass} representing 85.1% and W_{mass} only 6.8% of daily water use. This latter estimate is very comparable to the 5.5% estimated for a mature *Thuja occidentalis* using a modeling approach (Tyree, 1988) but smaller than the 25% estimated for foliated branches of *Picea abies* seedlings using a suite of direct measurements (Zweifel *et al*., 2001). There is no doubt that these estimates will vary widely due to weather-dependent variation in daily transpiration (e.g., Ambrose *et al*., 2010). However, the importance given to S_{area} in estimating over 500% of the potential daily transpiration as reported for *Sequoia* tree tops does not reflect available water even though hydraulic capacitance was also highest in the upper crowns (Ishii *et al*., 2014). The difference of nearly two orders of magnitude is primarily a reflection of how water storage is calculated. The area-normalized succulence reported by Ishii *et al*. (2014) contains all shoot water, including the less mobile AWF, rather than water that is available over the typical range of water potential as represented by W_{area} or W_{mass}. Given the general pattern of leaf water storage contributing less to daily transpiration than stems (Scholz *et al*., 2011), the enormous stems of *Sequoiadendron* and *Sequoia* have great potential to stabilize water potential over longer time scales.

Seasonal water relations

Seasonal changes in osmotica and TLP with height are seldom quantified for tall trees, but reports from *Eucalyptus regnans* and *Pseudotsuga menziesii* suggest that osmotic adjustment may be a common strategy to maintain Ψ_p against gravity (Connor *et al*., 1977; Woodruff *et al*., 2004). In *Pseudotsuga menziesii*, osmotic adjustment steepened the relationship between TLP and height from a slope of essentially zero in spring to a slope approaching the gravitational potential gradient in summer (Woodruff *et al*., 2004). In contrast, we observed neither a shift in $\Psi_{\pi ft}$ nor a steeper slope in the relationship between $\Psi_{\pi ft}$ and height from summer to fall, indicating that sufficient Ψ_p was maintained between the measurement periods without the need for osmotic adjustment. The lack of osmotic adjustment in *Sequoiadendron* may result from the species occupying basin-like topographies containing abundant groundwater (Rundel, 1972; Anderson, 1995). Indeed, our study trees grew on alluvial soils close to perennial watercourses, and surface water flowed through each of our study sites throughout the measurement periods. Alternatively, the fact that $\Psi_{\pi ft}$ decreased with height in some but not all *Sequoia* (Koch *et al*.,

2004; Ishii *et al*., 2014) suggests that seasonal osmotic adjustment could be induced by spatial or temporal variation in environmental conditions.

Our seasonal estimates of water storage that were normalized by mass versus area yielded very different results; mass-normalized estimates exhibited smaller differences than their area-normalized counterparts. This discrepancy can be explained by developmental changes in shoot anatomy combined with the nonlinear function we used to predict shoot areas from their masses. Shoot density increases over time as new xylem is added, so late-season shoots tend toward a region of relatively gentle slope in our predictive relationship where increases in mass occur with little increase in area. Age-related increases in shoot density may therefore have driven a reduction in fall estimates of mass-normalized water storage. Nonetheless, S_{mass} which represents shoot saturated water content including both available and unavailable components, increased 11.7% over the course of the season and was likely associated with the increase in total RWC_{TLP}. These increases in water content, however, may not actually be available to the transpiration stream because W_{mass} did not change and C_{mass} declined, together indicating that the vast majority of this stored water was held outside the typical range of water potential. Reductions in C_{mass} and symplastic RWC_{TLP} appear to be caused by a proportional shift of shoot water from more mobile symplastic to less mobile apoplastic compartments as indicated by the concomitant 27.2% increase in AWF. Seasonal changes in anatomy that increase the ratio of apoplasm to symplasm as shoots age may be responsible for this shift. Tracheid walls should thicken relative to their lumen areas as seasonally drier conditions prevail. In *Sequoiadendron*, the leaf fibers exhibit concentric lamellae that may enhance water storage over time as these hydrophilic and high-capacity cell walls thicken (Célino *et al*., 2014; Zwieniecki & Boyce, 2014; Chin & Sillett, 2016). It therefore appears that the seasonal increase in total RWC_{TLP} we observed is carried by anatomical changes that promote water storage, but that this stored water is not available to the transpiration stream within the typical range of water potential. We speculate that this seasonal increase of less mobile water storage may function as a reserve that maintains water content above dangerous thresholds to avoid precipitous declines in physiological function during peak dry season.

Does giant sequoia exhibit risky behavior?

Diurnal courses of water potential components indicate that *Sequoiadendron* consistently maintained positive Ψ_p against gravity, but Ψ_w routinely hovered close to the TLP (Fig. 8). This "risky" behavior underscores the functional significance of several water relations traits. First, decreasing $\Psi_{\pi ft}$ with height maintained TLP below minimum Ψ_w that were more negative with height. Second, the passive concentration of these osmotica toward midday as the shoots desiccated additionally promoted positive Ψ_p. Third, our large values of C_{area} indicate the ability to release ample quantities of water to the transpiration stream over small changes in Ψ_w to buffer diurnal variation in environmental conditions that become increasingly threatening as midday Ψ_w approach TLP. Finally, subjecting shoots in the lower crowns to Ψ_w experienced in the upper crowns would have resulted in turgor loss for each of the four trees, thus emphasizing the functional importance of variation in water relations traits with height that successfully prevented the typical range of Ψ_w from sinking below TLP under gravitational constraints. Operating close to the TLP while also having tight stomatal regulation may allow *Sequoiadendron* to survive short-term drought by maximizing the functional range of water potentials while avoiding rapid hydraulic failure, in which case overall drier climates should result in carbon starvation (McDowell *et al*., 2008; Ambrose *et al*., 2009, 2015). Such an

isohydric strategy may explain why the species appeared to tolerate the recent 2012-2017 California drought that killed more than 100 million other trees (USDA, 2016), yet it succumbed to more extensive climatic shifts in the past 2.3 million years (Davis, 1999a, 1999b; Dodd & DeSilva, 2016).

Contrasting strategies among tall conifers

Tall conifers potentially employ three contrasting shoot water relations strategies to maintain Ψ_p against height-related constraints. In the first strategy, TLP is uniform with height in the spring but progressively declines with height in the summer months via osmotic adjustment as observed in *Pseudotsuga menziesii* (Woodruff *et al*., 2004; Meinzer *et al*., 2008). Whether hydraulic capacitance plays a role alongside osmotic adjustment in this strategy remains unknown. In the second, the emphasis is on capacitive discharge of stored water. Both TLP and $\Psi_{\pi ft}$ are uniform with height, but increases in hydraulic capacitance and water storage may reduce height-related hydraulic constraints as suggested for *Sequoia* and *Cryptomeria* (Ishii *et al*., 2014; Azuma *et al*., 2016). Whether osmotic adjustment seasonally alters TLP with height in this strategy remains uncertain because a decrease in $\Psi_{\pi ft}$ with height has been documented for *Sequoia* (Koch *et al*., 2004). In the third strategy, $\Psi_{\pi ft}$ consistently maintains more negative TLP with height as we determined for *Sequoiadendron*, but hydraulic capacitance and water storage do not play a substantial role. These apparently contrasting strategies could be explained by seasonal osmotic adjustment with height. During the spring to summer shoot growth phase, osmotic concentrations increase with height perhaps to maintain sufficient Ψ_p required for foliar expansion against the gravitational potential gradient, as proposed by Woodruff *et al*. (2004). The resulting expectation is a steepening (more negative) slope in the relationship between $\Psi_{\pi ft}$ and height during the dry season, which would be mirrored in the relationship between TLP and height. Consistent with this expectation, data from *Pseudotsuga menziesii* measured during bud-break in May and from *Cryptomeria* in May yielded essentially unchanging $\Psi_{\pi ft}$ and TLP with height (Woodruff *et al*., 2004; Azuma *et al*., 2016). In addition, data from *Pseudotsuga menziesii*, *Sequoia*, and *Sequoiadendron* during the growing season well after bud-break yielded strongly negative slopes of $\Psi_{\pi ft}$ and TLP with height (Monteuuis, 1987; Koch *et al*., 2004; Woodruff *et al*., 2004). However, the fact that a relatively long period of seasonal osmotic adjustment with height in *Pseudotsuga menziesii* does not perfectly coincide with the shorter period of foliar expansion (Meinzer *et al*., 2008) indicates additional functions of seasonal osmotic adjustment with height. Similar measurements on additional tree species, especially tall angiosperms, are needed to further evaluate the commonness and function of seasonal osmotic adjustment with height, and to determine whether or not increasing hydraulic capacitance and water storage capacity with height are also seasonally regulated.

Conclusions

Gravity exerts a strong influence over foliar water relations of *Sequoiadendron*, yet positive turgor pressures and high water contents were maintained along a height gradient extending nearly 95 m above the ground. With increasing height in tree, higher osmotic concentrations drove a reduction in TLP that matched the gravitational potential gradient. Water contents were maintained above dangerous levels and controlled by a balance between tissue elasticity and the proportion of less mobile apoplastic water. Hydraulic capacitance was nearly twice as large as previously reported for other trees, indicating great potential to stabilize water potentials against short-term fluctuations vapor pressure deficits. However, a seasonal shift

toward less mobile apoplastic water helped maintain high water content as environmental conditions became increasingly desiccating. This suite of foliar water relations traits, which may be unique among tall trees, permits minimum midday water potentials to operate close to the TLP, and may also enable the Earth's largest tree species to survive short-term drought.

ACKNOWLEDGEMENTS

This project was funded in part by Save The Redwoods League through the Redwoods and Climate Change Initiative. Christina Bentrup and Becket DeChant collected shoots for diurnal water potential measurements. Anthony R. Ambrose, Koren R. Nydick, Heather M. Reith, Steve C. Sillett, Christopher S. Wong, and Robert A. York assisted with field logistics. John J. Battles, W. Jesse Hahm, George W. Koch, Cindy V. Looy, Stefania Mambelli, and four anonymous reviewers provided constructive comments on the manuscript. We are grateful to Calaveras Big Trees State Park, Kings Canyon National Park, Mountain Home State Demonstration Forest, and Sequoia National Forest for research permissions.

REFERENCES

Ambrose AR, Sillett SC, Dawson TE. 2009. Effects of tree height on branch hydraulics, leaf structure and gas exchange in California redwoods. *Plant, Cell & Environment* 32: 743–757.

Ambrose AR, Sillett SC, Koch GW, Van Pelt R, Antoine ME, Dawson TE. 2010. Effects of height on treetop transpiration and stomatal conductance in coast redwood (*Sequoia sempervirens*). *Tree Physiology* 30: 1260–1272.

Ambrose AR, Baxter WL, Wong CS, Næsborg RR, Williams CB, Dawson TE. 2015. Contrasting drought-response strategies in California redwoods. *Tree Physiology* 35: 453–69.

Ambrose AR, Baxter WL, Wong CS, Burgess SS, Williams CB, Næsborg RR, Koch GW, Dawson TE. 2016. Hydraulic constraints modify optimal photosynthetic profiles in giant sequoia trees. *Oecologia* 23: 1–8.

Anderson MA, Graham RC, Alyanakian GJ, Martynn DZ. 1995. Late summer water status of soils and weathered bedrock in a giant sequoia grove. *Soil Science* 160: 415–422.

Anderson RS, Smith SJ. 1994. Paleoclimatic interpretations of meadow sediment and pollen stratigraphies from California. *Geology* 22: 723–726.

Azuma W, Ishii HR, Kuroda K, Kuroda K. 2016. Function and structure of leaves contributing to increasing water storage with height in the tallest *Cryptomeria japonica* trees of Japan. *Trees* 30: 141–152.

Bacelar EA, Correia CM, Moutinho-Pereira JM, Gonçalves BC, Lopes JI, Torres-Pereira JM. 2004. Sclerophylly and leaf anatomical traits of five field-grown olive cultivars growing under drought conditions. *Tree Physiology* 24: 233–239.

Bales RC, Hopmans JW, O'Geen AT, Meadows M, Hartsough PC, Kirchner P, Hunsaker CT, Beaudette D. 2011. Soil moisture response to snowmelt and rainfall in a Sierra Nevada mixed-conifer forest. *Vadose Zone Journal* 10: 786–799.

Bartlett MK, Scoffoni C, Sack L. 2012. The determinants of leaf turgor loss point and prediction of drought tolerance of species and biomes: a global meta-analysis. *Ecology Letters* 15: 393–405.
Bartlett MK, Zhang Y, Kreidler N, Sun S, Ardy R, Cao K, Sack L. 2014. Global analysis of plasticity in turgor loss point, a key drought tolerance trait. *Ecology Letters* 17: 1580–1590.
Belmecheri S, Babst F, Wahl ER, Stahle DW, Trouet V. 2016. Multi-century evaluation of Sierra Nevada snowpack. *Nature Climate Change* 6: 2–3.
Blackman CJ, Brodribb TJ, Jordan GJ. 2010. Leaf hydraulic vulnerability is related to conduit dimensions and drought resistance across a diverse range of woody angiosperms. *New Phytologist* 188: 1113–1123.
Brodribb TJ, Holbrook NM, Edwards EJ, Gutierrez MV. 2003. Relations between stomatal closure, leaf turgor and xylem vulnerability in eight tropical dry forest trees. *Plant, Cell & Environment* 26: 443–450.
Brodribb TJ, Holbrook NM. 2005. Water stress deforms tracheids peripheral to the leaf vein of a tropical conifer. *Plant Physiology* 137: 1139–1146.
Bucci SJ, Goldstein G, Meinzer FC, Scholz FG, Franco AC, Bustamante M. 2004. Functional convergence in hydraulic architecture and water relations of tropical savanna trees: from leaf to whole plant. *Tree Physiology* 24: 891–899.
Buckley TN. 2014. The contributions of apoplastic, symplastic and gas phase pathways for water transport outside the bundle sheath in leaves. *Plant, Cell & Environment* 38: 7–22.
Cayan DR, Maurer EP, Dettinger MD, Tyree M, Hayhoe K. 2008. Climate change scenarios for the California region. *Climate Change* 87: 21–42.
Célino A, Fréour S, Jacquemin F, Casari P. 2013. The hygroscopic behavior of plant fibers: A review. *Frontiers in Chemistry*. doi: 10.3389/fchem.2013.00043.
Cheung YNS, Tyree MT, Dainty J. 1975. Water relations parameters on single leaves obtained in a pressure bomb and some ecological interpretations. *Canadian Journal of Botany* 53: 1342–1346.
Chin ARO, Sillett SC. 2016. Phenotypic plasticity of leaves enhances water-stress tolerance and promotes hydraulic conductivity in a tall conifer. *American Journal of Botany* 103: 796–807.
Connor DJ, Legge NJ, Turner NC. 1977. Water relations of mountain ash (*Eucalyptus regnans* F. Muell.) forests. *Functional Plant Biology* 4: 753–762.
Davis OK. 1999a. Pollen analysis of a late-glacial and Holocene sediment core from Mono Lake, Mono County, California. *Quaternary Research* 52: 243–249.
Davis OK. 1999b. Pollen analysis of Tulare Lake, California: Great-Basin-like vegetation in Central California during the full glacial and early Holocene. *Review of Palaeobotany & Palynology* 107: 249–257.
Dawson TE. 1990. Spatial and physiological overlap of three co-occurring alpine willows. *Funcional Ecology* 4: 13–25.
Dixon HH, Joly J. 1895. On the ascent of sap. *Philosophical Transactions of the Royal Society, B* 186: 563–576.
Dodd RS, DeSilva R. 2016. Long-term demographic decline and late glacial divergence in a Californian paleoendemic: *Sequoiadendron giganteum* (giant sequoia). *Ecology & Evolution* 6: 3342–3355.

Edwards WR, Jarvis PG, Landsberg JJ, Talbot H. 1986. A dynamic model for studying flow of water in single trees. *Tree Physiology* 3: 309–324.
Goulden ML, Anderson RG, Bales RC, Kelly AE, Meadows M, Winston GC. 2012. Evapotranspiration along an elevation gradient in California's Sierra Nevada. *Journal of Geophysical Research* 117: G3.
Griffin D, Anchukaitis KJ. 2014. How unusual is the 2012–2014 California drought? *Geophysical Research Letters* 41: 9017–9023.
Hacke UG (ed). 2015. Functional and ecological xylem anatomy. Springer, Cham, Switzerland.
Hamby DM. 1994. A review of techniques for parameter sensitivity analysis of environmental models. *Environmental Monitoring & Assessment* 32: 135–154.
Hao GY, Sack L, Wang AY, Cao KF, Goldstein G. 2010. Differentiation of leaf water flux and drought tolerance traits in hemiepiphytic and non-hemiepiphytic Ficus tree species. *Functional Ecology* 24: 731–740.
Hinckley TM, Duhme F, Hinckley AR, Richter H. 1980. Water relations of drought hardy shrubs: osmotic potential and stomatal reactivity. *Plant, Cell & Environment* 3: 131–140.
Hinckley TM, Lachenbruch B, Meinzer FC, Dawson TE. 2011. A lifespan perspective on integrating structure and function in trees. In: Meinzer FC, Lachenbruch B, Dawson TE (eds) Size-and age-related changes in tree structure and function. Springer, The Netherlands, pp 3–30.
Hunsaker CT, Whitaker TW, Bales RC. 2012. Snowmelt runoff and water yield along elevation and temperature gradients in California's southern Sierra Nevada. *Journal of the American Water Resources Association* 48: 667–678.
Ishii H, Jennings G, Sillett S, Koch G. 2008. Hydrostatic constraints on morphological exploitation of light in tall *Sequoia sempervirens* trees. *Oecologia* 156: 751–763.
Ishii HR, Azuma W, Kuroda K, Sillett SC. 2014. Pushing the limits to tree height: could foliar water storage compensate for hydraulic constraints in *Sequoia sempervirens*? *Functional Ecology* 28: 1087–1093.
Jepson J. 2000. The tree climber's companion: a reference and training manual for professional tree climbers. Beaver Tree Publishing, Longville, MN.
Koch GW, Sillett SC, Jennings GM, Davis SD. 2004. The limits to tree height. *Nature* 428: 851–854.
Koide RT, Robichaux RH, Morse SR, Smith CM. 2000. Plant water status, hydraulic resistance and capacitance. In: Pearcy RW, Ehleringer JR, Mooney HA, Rundel, PW (eds) Plant physiological ecology: field methods and instrumentation. Kluwer Dordrecht, The Netherlands, pp 161–183.
Kozlowski TT, Pallardy SG. 2002. Acclimation and adaptive responses of woody plants to environmental stresses. *Botanical Review* 68: 270–334.
Kramer PJ, Boyer JS. 1995. Water relations of plants and soils. Academic press, San Diego, CA.
Kubiske ME, Abrams MD. 1991. Rehydration effects on pressure-volume relationships in four temperate woody species: variability with site, time of season and drought conditions. *Oecologia* 85: 537–542.
Kubiske ME, Abrams MD. 1994. Ecophysiological analysis of woody species in contrasting temperate communities during wet and dry years. *Oecologia* 98: 303–312.
Ladiges PY. 1975. Some aspects of tissue water relations in three populations of *Eucalyptus viminalis* Labill. *New Phytologist* 75: 53–62.
Lambers H, Chapin III FS, Pons TL. 2008. Plant physiological ecology. Springer, New York.

Lamont BB, Lamont HC. 2000. Utilizable water in leaves of 8 arid species as derived from pressure-volume curves and chlorophyll fluorescence. *Physiologica Plantarum* 110: 64–71.
Lawlor DW, Cornic G. 2002. Photosynthetic carbon assimilation and associated metabolism in relation to water deficits in higher plants. *Plant Cell & Environment* 25: 275–294.
Marcott SA, Shakun JD, Clark PU, Mix AC. 2013. A reconstruction of regional and global temperature for the past 11,300 years. *Science* 339: 1198–1201.
Martins SCV, McAdam SAM, Deans RM, DaMatta FM, Broadribb TJ. 2016. Stomatal dynamics are limited by leaf hydraulics in ferns and conifers: results from simultaneous measurements of liquid and vapour fluxes in leaves. *Plant Cell & Environment* 39: 694–705.
McDowell N, Pockman WT, Allen CD, Breshears DD, Cobb N, Kolb T, Plaut J, Sperry J, West A, Williams DG, Yepez EA. 2008. Mechanisms of plant survival and mortality during drought: why do some plants survive while others succumb to drought? *New Phytologist* 178: 719–739.
Meinzer FC, Bond BJ, Karanian JA. 2008. Biophysical constraints on leaf expansion in a tall conifer. *Tree Physiology* 28: 197–206.
Mencuccini M. 2003. The ecological significance of long-distance water transport: short-term regulation, long-term acclimation and the hydraulic costs of stature across plant life forms. *Plant Cell & Environment* 26: 163–182.
Merchant A, Callister A, Arndt S, Tausz M, Adams. 2007. Contrasting physiological responses of six *Eucalyptus* species to water deficit. *Annals of Botany* 100: 1507–1515.
Mitchell, PJ, Veneklaas EJ, Lambers H, Burgess SSO. 2008. Leaf water relations during summer water deficit: differential responses in turgor maintenance and variation in leaf structure among different plant communities in southwestern Australia. *Plant Cell & Environment* 31: 1791–1802.
Monteuuis O. 1987. In vitro meristem culture of juvenile and mature *Sequoiadendron giganteum*. *Tree Physiology* 3: 265–272.
Niinemets Ü. 2001. Global-scale climatic controls of leaf dry mass per area, density, and thickness in trees and shrubs. *Ecology* 82: 453–469.
Nobel PS. 1983. Biophysical Plant Physiology and Ecology. W.H. Freeman and Company, San Francisco, CA.
Oldham AR, Sillett SC, Tomescu AMF, Koch GW. 2010. The hydrostatic gradient, not light availability, drives height-related variation in *Sequoia sempervirens* (Cupressaceae) leaf anatomy. *American Journal of Botany* 97: 1087–1097.
Parker GG. 1995. Structure and microclimate of forest canopies. In: Lowman MD, Nadkarni NM (eds) Forest canopies. Academic Press, San Diego, CA, pp 73–106.
Petit G, Pfautsch S, Anfodillo T, Adams MA. 2010. The challenge of tree height in *Eucalyptus regnans*: when xylem tapering overcomes hydraulic resistance. *New Phytologist* 187: 1146–1153.
Philip JR. 1966. Plant water relations: some physical aspects. *Annual Review of Plant Physiology* 17: 245–268.
Pittermann J, Stuart SA, Dawson TE, Moreau A. 2012. Cenozoic climate change shaped the evolutionary ecophysiology of the Cupressaceae conifers. *Proceedings of the National Acadamy of Sciences, USA* 109: 9647–9652.

R Development Core Team. 2016. R: a language and environment for statistical computing. R Foundation for Statistical Computing, Vienna, Austria.
Richter H. 1978. Diagram for description of water relations in plant cells and organs. J*ournal of Experimental Botany* 29: 1197–1203.
Rocky Mountain Tree-Ring Research. 2016. OLDLIST. www.rmtrr.org/oldlist.htm (28 September 2016, date last accessed).
Robichaux RH. 1984. Variation in the tissue water relations of two sympatric Hawaiian *Dubautia* species and their natural hybrid. *Oecologia* 65: 75–81.
Rundel PW. 1972. Habitat restriction in giant sequoia: the environmental control of grove boundaries. *American Midland Naturalist* 1: 81–99.
Sack L, Cowan PD, Jaikumar N, Holbrook NM. 2003. The 'hydrology' of leaves: co-ordination of structure and function in temperate woody species. *Plant, Cell & Environment* 26: 1343–1356.
Sanders GJ, Arndt SK. 2012. Osmotic adjustment under drought conditions. In: Aroca R (ed) Responses to drought stress: from morphological to molecular features. Springer, Berlin, Germany, pp 199–229.
Scholz FG, Phillips NG, Bucci SJ, Meinzer FC, Goldstein G. 2011. Hydraulic capacitance: biophysics and functional significance of internal water sources in relation to tree size. In: Meinzer FC, Lachenbruch B, Dawson TE (eds) Size-and age-related changes in tree structure and function. Springer, The Netherlands, pp 341–361.
Scoffoni C. 2015. Modelling the outside-xylem hydraulic conductance: towards a new understanding of leaf water relations. *Plant, Cell & Environment* 38: 4–6.
Sillett SC, Van Pelt R, Carroll AL, Kramer RD, Ambrose AR, Trask DA. 2015. How do tree structure and old age affect growth potential of California redwoods? *Ecological Monographs* 85: 181–212.
Smith ED, Szidarovszky F, Karnavas WJ, Bahill A. 2008. Sensitivity analysis, a powerful system validation technique. *Open Cybernetics & Systemics Journal* 2: 39–56.
Sokal RR, Rohlf FJ. 1995. Biometry (3rd edition). WH Freeman and Company, New York.
Steponkus PL. 1984. Role of the plasma-membrane in freezing-injury and cold acclimation. *Annual Review of Plant Physiology & Plant Molecular Biology* 35: 543–584.
Tng DY, Williamson GJ, Jordan GJ, Bowman DM. 2012. Giant eucalypts–globally unique fire-adapted rain-forest trees? *New Phytologist* 196: 1001–1014.
Turner NC. 1988. Measurement of plant water status by the pressure chamber technique. *Irrigation Science* 9: 289–308.
Tyree MT. 1976. Negative turgor pressure in plant cells: fact or fallacy? *Canadian Journal of Botany* 54: 2738–2746.
Tyree MT. 1988. A dynamic model for water flow in a single tree: evidence that models must account for hydraulic architecture. *Tree Physiology* 4: 195–217.
Tyree MT, Hammel HT. 1972. Measurement of turgor pressure and water relations of plants by pressure-bomb technique. *Journal Experimental Botany* 23: 267–282.
Tyree MT, Zimmermann MH. 2002. Xylem structure and the ascent of sap, 2nd edition. Springer-Verlag, Berlin, Germany.
Tyree MT, Sperry JS. 1989. Vulnerability of xylem to cavitation and embolism. *Annual Review of Plant Biology* 40: 19–36.
United States Department of Agriculture. 2016. New aerial survey identifies more than 100 million dead trees in California. USDA Office of Communications:

http://www.fs.fed.us/news/releases/new-aerial-survey-identifies-more-100-million-dead-trees-californiairma.nps.gov/Stats/Reports/SEQU (30 November 2016, date last accessed).
Van Pelt R. 2001. Forest Giants of the Pacific Coast. University of Washington Press, Seattle, WA.
Willard D. 2000. A Guide to the Sequoia Groves of California. Yosemite Natural History Association, Yosemite National Park, CA.
Woodruff DR, Bond BJ, Meinzer FC. 2004. Does turgor limit growth in tall trees? *Plant, Cell & Environment* 27: 229–236.
Woodruff DR, McCulloh KA, Warren JM, Meinzer FC, Lachenbruch B. 2007. Impacts of tree height on leaf hydraulic architecture and stomatal control in Douglas-fir. *Plant, Cell & Environment* 30: 559–569.
Yaaran A, Moshelion M. 2016. Role of aquaporins in a composite model of water transport in the leaf. Int J Mol Sci 17: 1045. doi:10.3390/ijms17071045.
York RA, Stephenson NL, Meyer M, Hanna S, Tadashi M, Caprio AC, Battles JJ. 2013. A natural resource condition assessment for Sequoia and Kings Canyon National Parks: Appendix 11: giant sequoia. National Park Service, Natural Resource Report NPS/SEKI/NRR—2013/665.11.
Zweifel R, Item H, Häsler R. 2001. Link between diurnal stem radius changes and tree water relations. *Tree Physiology* 21: 869–877.
Zwieniecki MA, Boyce CK. 2014. The role of cellulose fibers in *Gnetum gnemon* leaf hydraulics. *International Journal of Plant Sciences* 175: 1054–1061.

CHAPTER 3

Stem water storage in giant sequoia tree tops

ABSTRACT

Nonsteady-state conditions within large trees generate water potential gradients that release and absorb water from internal storage compartments. In such trees, water stored in stems is an important contributor to transpiration that can reduce the probability of hydraulic dysfunction as well as improve photosynthetic carbon gain. However, the dynamics of water storage may be dampened with height in tree because of chronically low water potentials associated with the gravitational potential gradient. I quantified the importance of elastic stem water storage in the top 5 to 6 m of large *Sequoiadendron giganteum* (giant sequoia) trees using a combination of detailed architectural measurements and automated sensors that monitored diurnal fluxes in sap flow, stem diameter, and water potential. Relative water storage capacity in stems contributed less than 2% of water transpired at the tree tops, and hydraulic capacitance was similarly low, ranging from just 3 to 4 L MPa^{-1} m^{-3}. These low values may be associated with the chronically low water potentials imposed by gravity, and could indicate a trend of decreasing water storage dynamics with height in tree. Branch diameter flux consistently and substantially lagged behind fluxes in water potential and sap flow, which occurred in sync. This lag suggests that the inner bark, which consists mostly of live secondary phloem tissue, was an important hydraulic capacitor, and that hydraulic resistance between the xylem and phloem retards water transfer between these tissues. Tree tops transpired an average of 114 L d^{-1}, while whole-tree water use ranged from 2227 to 3752 L d^{-1} and corroborated previous measurements for similar-sized giant sequoia. Despite transpiring more water than any other tree species on Earth, I estimate that giant sequoia relies minimally on water stored in stems and foliage to augment daily water use by 8 to 9% on warm and sunny summertime days. Extending this study to the whole-tree level will be a challenging endeavor because of the nonsteady-state conditions that are omnipresent within large trees.

INTRODUCTION

A central principal of the cohesion-tension theory is that water travels skyward via water potential gradient of sequentially lower pressures along the soil–plant–atmosphere continuum (Dixon & Joly 1895, Philip 1966). This simplified model can be modified by the addition of nonsteady-state conditions in which water entering the roots does not match the amount exiting the stomata (Hinckley et al. 2011). Such an imbalance between influx and efflux allows for reversals of the normal pressure gradient that can cause water to flow into the plant directly from the atmosphere (Burgess & Dawson 2004; Goldsmith et al. 2013; Dawson & Goldsmith 2018). Nonsteady states routinely occur within plants, too, and water potential gradients largely dictate the direction of flow among organs and tissues (Goldsmith 2013). Therefore, most plant parts have the ability to serve as storage reservoirs by releasing or absorbing water according to the distribution of water potentials within the whole plant. A truly steady-state system lacking these

hydraulic buffering effects would be decidedly inflexible and consequently prone to hydraulic dysfunction (Scholz et al. 2011).

Several metrics are commonly used to describe water storage dynamics in plants. Water storage capacity is defined as the quantity of stored water that can be released to the transpiration stream on a daily basis, and can be expressed in absolute liters or on a relative scale as a percent of daily transpiration. Hydraulic capacitance is the ability for stored water to be released and is expressed as the change in water content per change in water potential, normalized by tissue volume (i.e., L MPa^{-1} m^{-3}). These two metrics are related by an amount of releasable water, but they reflect fundamentally different biological properties (Scholz et al. 2011). A hydraulic capacitor is any plant component that can serve a water storage function and whose water content changes as water potential gradients dictate.

In trees, all three organs—roots, stems, and leaves—can function as hydraulic capacitors and therefore provide sources of water for transpiration (Waring & Running 1978; Waring et al. 1979; Goldstein et al. 1984; Holbrook & Sinclair 1992; Stratton et al. 2000; Meinzer et al. 2001). Root water storage dynamics are rarely studied (Domec et al. 2006; Scholz et al. 2007, 2008) perhaps because the small range of water potentials over which roots operate inhibits their ability to release stored water compared to leaves and stems. Leaves, on the other hand, experience large diurnal swings in water potential, but the relative contribution of leaf water storage to total daily transpiration is generally lower than that of stems (Scholz et al. 2011), although this pattern may be reversed in young saplings when foliage comprises a higher proportion of the total biomass (Zweifel et al. 2001). In large trees, stems contain the vast majority of the total plant volume (e.g., Wickens 2008; Sillett et al. 2015) and therefore represent potentially enormous reservoirs for water storage. For example, wood of the famed Madagascar baobab trees (*Adansonia* spp.) contains up to 79% water (Chapotin et al. 2006a). Stem water storage has long been considered an important contributor to tree transpiration (Reynolds 1965; Waring & Running 1978; Nielsen et al. 1990; Zweifel et al. 2001; Pfautsch et al. 2015a), and mobilization of water stored in stems is particularly well suited for buffering transpiration–induced xylem tension to reduce cavitation and loss of hydraulic conductivity (Meinzer et al. 2009). It can also prolong stomatal opening and enable early flushing of leaves, thus increasing carbon gain (Borchert 1994; Goldstein et al. 1998; Phillips et al. 2003; Chapotin et al. 2006b).

Stem water storage capacity scales positively with tree size (Scholz et al. 2011), but relative water storage capacity appears to be size-independent as values range widely from 4% in mature *Pinus ponderosa* to over 50% in saplings of *Picea abies* (Phillips et al. 2003; Zweifel et al. 2001). Reliance on stem water storage increases during dry periods when water potential flux is greatest, which underscores the physiological importance of water storage dynamics both in dry environments and also seasonally when water is limited (Phillips et al. 1997, 2003; Chapotin et al. 2006b; Bucci et al. 2008). Tall trees must cope with a different kind of water limitation because the gravitational potential gradient imposes lower water potentials with height in tree at a rate of –0.0098 MPa m^{-1} (Nobel 1983). In principal, higher capacitances with height in tree should be particularly beneficial for reducing the probability of cavitation by releasing stored water when midday water potentials, which are also influenced by gravity, are lowest (Meinzer et al. 2009). Indeed, stem hydraulic capacitance increases with total tree height, varying by more than an order of magnitude from about 20 to 500 L MPa^{-1} m^{-3} (Scholz et al. 2011). However, this relationship at the whole-tree level may be misleading because water storage capacity as well as hydraulic capacitance may be limited by chronically low water potentials that occur at the tops of tall trees (e.g., Koch et al. 2004; Woodruff et al. 2004) where full tissue hydration

might rarely occur. In foliage, for example, gravity-corrected relative water content decreased well below 100% along height gradient in tall *Sequoiadendron giganteum* trees (Williams et al. 2017). Studying hydraulic capacitance along a height gradient within trees or at the tops of tall trees could reveal that the dynamics of stem water storage are subdued by gravity.

Both wood and bark can serve as hydraulic capacitors in stems. In secondary xylem at very high water potentials (e.g., 0 to –0.05 MPa), stored water is released from the long tapered ends of conduits that have already embolized (Tyree & Zimmermann 2002). Then from high to moderate water potentials, elastic shrinkage of the sapwood releases water primarily from ray parenchyma cells (Tyree & Yang 1990; Holbrook 1995). Finally, inelastic displacement of water occurs by the formation of new embolisms during low water potentials (Tyree & Yang 1990). The inner bark, classically defined as the live components of the bark and consisting mostly of secondary phloem tissue (Evert 2006), may also release water via elastic shrinkage and thus serve as a hydraulic capacitor (Pfautsch et al. 2015a). Secondary phloem and the sugary phloate it transports can exceed the water storage capacity of the xylem (Sevanto et al. 2002, 2003, 2011; Mencuccini et al. 2013). The cohesion-tension theory of water flow (Dixon & Joly 1895) and the pressure-flow model of phloate transport (Münch 1930) are currently the best supported models for transport through plant vascular tissue (Tyree & Zimmermann 2002; Holbrook & Zwieniecki 2011), but xylem and phloem tissues have primarily been studied as separate systems. The physiological importance of a direct hydraulic connection between these two transport tissues was only recently realized (Zweifel et al. 2001; Hölttä et al. 2006, 2009; Stroock et al. 2014), and experimental confirmation of xylem-phloem water transfer has now been provided (Pfautsch et al. 2015b). The direction and rate of water transfer into or out of the transpiration stream is driven by a difference in water potentials between xylem and phloem tissues (Pfautsch et al. 2015a). That is, nonsteady-state conditions inside stems allow both the wood and bark to serve as hydraulic capacitors.

California's giant sequoia (*Sequoiadendron giganteum* (Lindley) J. Buchholz) has great potential for reliance on stem water storage. First, its massive trunks and immense crowns that can support 1400 m^3 of wood and 6700 m^2 of leaf area (Van Pelt 2001, Sillett et al. 2015) have the capacity to store large volumes of water, especially since absolute water storage capacity increases with tree size (Scholz et al. 2011). Second, the species is restricted to basin-like topographies in the southern Sierra Nevada Mountains where summertime atmospheric conditions are typically warm and dry, yet the soils contain abundant subsurface groundwater (Rundel 1972; Anderson et al. 1995; Willard 2000). This combination of environmental conditions could foster highly dynamic recharge-discharge cycles because hydraulic capacitors that are depleted in the daytime have the potential to completely refill at night. Third, water storage is typically greater in stems than in foliage (Scholz et al. 2011) which in large *Sequoiadendron* trees can release as much as 150 L d^{-1} (Williams et al. 2017), so stems of this species could contribute substantially to water storage capacity. Fourth, the combination of *Sequoiadendron*'s large size and the environmental conditions in which the species lives supports very large demands for water, with 2220 and 2720 L d^{-1} reported for two large individuals during warm and dry summertime conditions (Ambrose et al. 2016). Such copious water demands must be partly satisfied by water stored in stems, but the importance of this contribution in *Sequoiadendron* remains unknown.

This investigation assessed dynamic water storage in the stems of large trees. The primary objective was to quantify the elastic component of stem water storage at the tops of large *Sequoiadendron*. Efforts were focused at the tree tops in order to capture water potentials that

were chronically low but had pronounced diurnal variation to drive flux in elastic water storage under gravitational constraints. Although it was not one of the initial objectives, data generated at the tree top also allowed qualitative evaluation of the hydraulic connection between secondary xylem and inner bark tissues. The secondary objective was to provide context for tree-top water use and storage, which I accomplished by quantifying volumetric sap flow at the whole-tree level. This quantification enabled us to corroborate previous estimates of daily water use in two *Sequoiadendron* trees, as these estimates were the largest reported for any trees on Earth (Ambrose et al. 2016).

MATERIALS & METHODS

Study location, tree selection, and study design

Three study trees were selected from Whitaker's Forest Research Station (36°41'60"N 118°55'50"W; 1740 m elevation) which is located in California's Sierra Nevada Mountains and owned by the University of California, Berkeley. The site is dominated by mature and second-growth mixed conifer forest and contains exceptionally tall *Sequoiadendron* trees (Willard et al. 2000). Trees were considered for the study if they were at least 80 m tall, supported fully emergent and intact tops, reached apparent maximum height, and had no evidence of major fire damage at their bases (Table 1).

Table 1. Characteristics of *Sequoiadendron giganteum* trees used to estimate the importance of stem water storage in tree tops. Leaf area and minimum age were calculated according to Sillett et al. (2015).

Tree	DBH (cm)	Height (m)	Main trunk volume (m^3)	Sapwood area (m^2)	Leaf area (m^2)	Minimum age (yr)
1	438	82.1	290	1.22	3744	556
2	496	86.3	413	1.23	4102	708
3	424	85.7	259	0.71	3827	619

Tree crowns were accessed using arborist techniques (Jepson 2000). Tree tops were defined as distal to an unbranched and undamaged section of trunk between 30 and 40 cm in diameter, which corresponded to 76.1 to 81.1 m above ground level. These clear sections of trunk facilitated installation of sensors as well as measurements of stem diameter needed for estimation of stem volumes. From each tree top, three representative branches were selected for detailed study based on their size, azimuthal trajectory, and apparent vigor. The demarcation of tree tops focused the study to the distal 5.2 to 6.0 m of each tree and a total of nine branches that were 7.1 to 12.0 cm basal diameter (mean 9.8 cm) and supported 12.0 to 41.0 m of total stem path length (mean 28.6 m).

Four types of automated sensors were deployed in each tree (Figure 1). Temperature and relative humidity sensors were placed at the tree tops. Sap flow gauges were installed at the tree base, at the base of the tree top, and at the base of the three representative branches to monitor the rate of water use at each of these levels. A set of dendrometers was paired with the tree-top

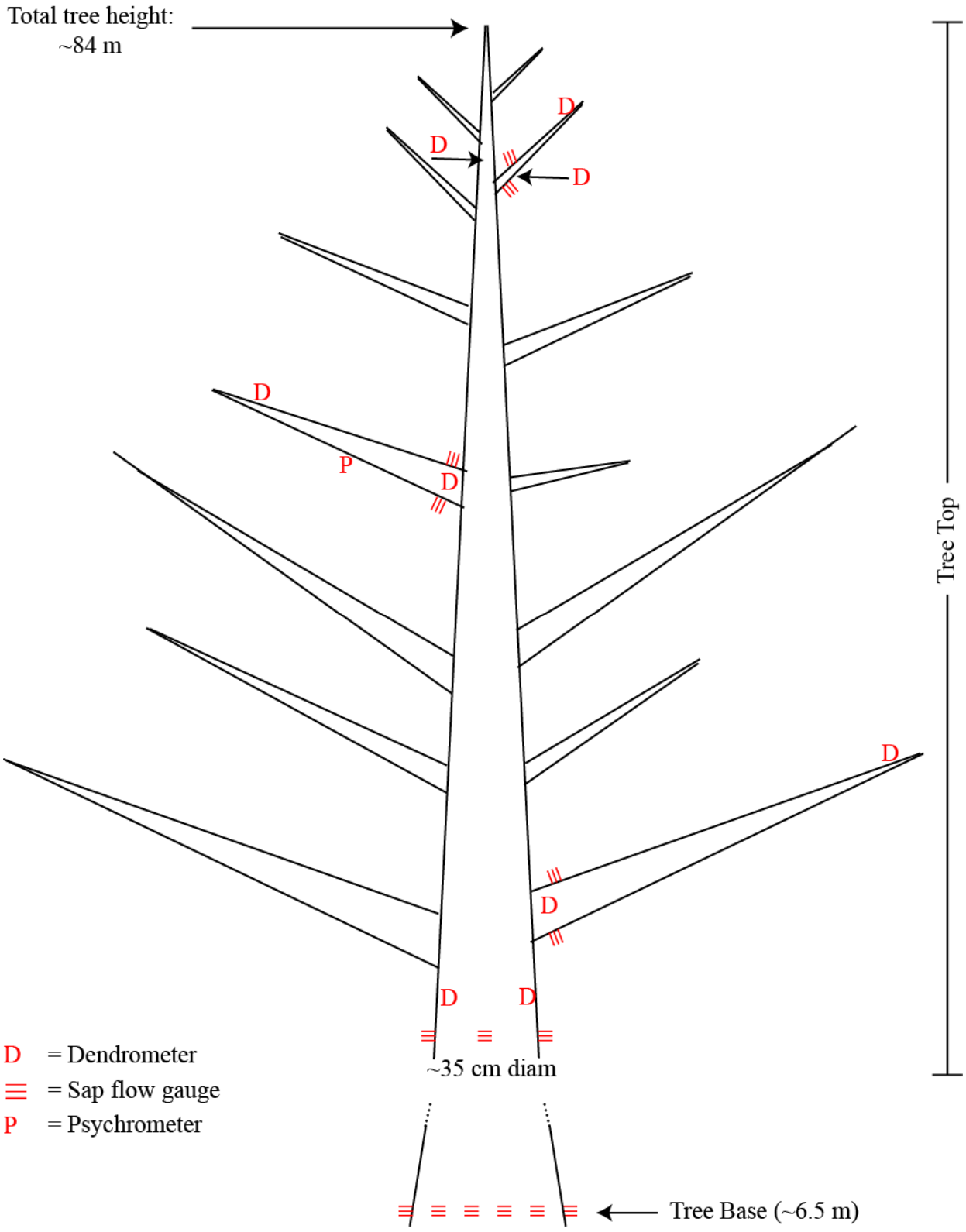

Figure 1. Distribution of physiological sensors deployed in three large *Sequoiadendron giganteum* trees to quantify the importance of stem water storage.

sap flow gauges to monitor changes in stem diameter. Stem psychrometers, which measured xylem water potential, were installed on one study branch in each tree. A tree's sensor array combined with detailed measurements of stem volume allowed quantifying water use at the whole-tree, tree-top, and whole-branch levels; estimating displacement of stored stem water at the tree-top and whole-branch levels; and evaluating sources of stem water storage. All sensor arrays were powered by sealed lead-acid batteries that were charged by solar panels. Dataloggers were programmed to record data on a 20-min schedule continuously from mid-July through September 2013. Although 2.5 months of data were collected in total, wound responses, power failures, and sensor malfunctions interrupted periods of otherwise continuous data. I therefore selected the most continuous and highest quality data from a 7-day period extending August 1st to August 7th for analysis.

Stem volume estimates

Two separate protocols were followed to estimate total stem volume in each tree top. First, the main trunk as well as accessory trunks and their connecting limbs were each divided into segments in which proximal and distal positions corresponded with stem junctions or termini. Height above ground, azimuth and distance from main trunk, and stem diameter were recorded for each position, thus allowing the stem segments to be modeled in three dimensional space as conical frusta whose volumes could be calculated. A separate protocol was used to predict each of the remaining stem volumes (*V)* which all occurred in branches. Branch *V* was predicted from simple field estimates of branch parameters using the equation,

$$V = 0.00014158*D^{2.1864} + 0.0073865*P^{0.79304} + 0.0020964*F^{1.1408} \quad \text{(Equation 1)}$$

where *D* is branch basal diameter (cm), *P* is live stem path length >7 cm diameter (m), and *F* is the count of foliar units ($R^2 = 0.9781$; Sillett et al. 2015). A foliar unit was defined as a typical quantity of foliage occupying an intact branch with a basal diameter of 7.0 cm. The number of these repeating clusters of foliage on each branch was estimated to 0.1 *F*. Since the standard errors for each component of Equation 1 were unavailable (Sillett et al. 2015), I conservatively estimated the uncertainty for each variable based on the difficulty of making field measurements, using 5% for *D*, 20% for *P*, and 50% for *F*. Propagation of uncertainties followed standard practices (Bevington & Robinson 2002) to obtain *V*. In addition to estimating *V* for each stem segment, the nine branches from each tree that were selected for detailed study were dissected to obtain high-resolution estimates of stem *V*. These dissected stems were cut at whole cm diameter increments yielding 344 total segments that were modeled as conical frusta. Field measurements used to obtain estimates of stem *V* were made with clinometers, compasses, measuring tapes, and an Impulse® laser range finder (Laser Technology, Inc.). Heights and distances were measured to 0.1 m resolution, diameters to 0.1 cm, and azimuths to the nearest degree.

Environmental conditions

Air temperature and relative humidity were recorded using two USB-programmable dataloggers (model EL-USB-2; Lascar Electronics Inc., Erie, PA, USA) secured to each of the study branches. Each logger was suspended inside a foil-covered cap to shield it from direct sunlight. Vapor pressure deficit was calculated using Tetens' equation (Buck 1981). I provided context for these summertime conditions by comparing them to a full year (2013) of data

generated from a weather station perched atop another *Sequoiadendron* of similar height located 23 km to the southeast in Sequoia National Park in Giant Forest at 2131 m elevation.

Sap flow

In each study tree, sap flow was measured using the heat ratio method (HRM; Burgess et al. 2001) in the trunk at tree-base and tree-top positions as well as in the three branches selected for detailed study. At a tree's base just above the trunk buttresses, which corresponded to about 6.5 m above ground level, six HRM probesets were inserted into the wood with equal azimuthal spacing between sets. Two custom-built 110-mm long probesets each connected to a datalogger via a relay multiplexer (models CR10x, AM16/32; Campbell Scientific, Logan, UT, USA) were installed at 90º and 270º. These custom probesets captured the radial profile of heat pulse velocity across the thick layer of sapwood by measuring the velocity at ten equally spaced radial depths from 12.5 to 100.0 mm. Four additional 35-mm long HRM probe sets connected to dataloggers (SmartLogger; ICT International Ltd., Armidale, NSW, Australia) measured heat pulse velocity at 12.5 and 27.5-mm depths and were installed at 30º, 150º, 210º, and 330º to sample additional circumferential variation in the velocity at the bases of the large main trunks. Tree-top heat pulse velocity was measured in the trunk using three 35-mm long HRM probes installed with equal azimuthal spacing, while in branches it was measured using two 35-mm long HRM probes installed at opposite sides of the main stem axis at approximately 45º from vertical. All probesets were installed with 6 mm spacing between probes.

At the end of the field campaign, a zero reference heat pulse velocity was obtained by severing the xylem at each sap flow measurement position and recording the sap flow for an additional 48 hours. For trunks, 5 and 12-mm diameter increment cores were extracted directly below and above each of the HRM probesets, and the cores were used to determine bark and sapwood radii as well as wood density and water content using the water-immersion method. For branches, the primary stem axes were cut 5 cm distal to the HRM probesets, and the cut ends were sealed in plastic bags to prevent evaporation. The harvested branches were then lowered to the ground where 12 mm diameter cores were extracted to determine wood density and water content, and stem volumes were measured during dissection. At each measurement position, a transverse section of wood was sawn from the branch, sanded with 600 grit sandpaper, and digitally scanned at 600 dpi so that high resolution measurements of sapwood cross-sectional area could be obtained using Adobe PhotoShop (Adobe Systems, San Jose, California). The bark and sapwood radii along with stem diameters provided the geometric inputs for calculating sapwood cross-sectional areas at each measurement point on a trunk. Each of the sapwood cross-sectional areas for trunks and branches was then divided into concentric annuli delineated by the midpoint between HRM measurement depths.

Missing data points that spanned up to 10 consecutive 20-min intervals rendered several of the sap flow datasets unusable, so a data cleaning procedure was applied. All sap flow datasets were gap-filled using a Hampel Filter with $k = 10$ and $t = 1$, in which values within a sliding window of $2k+1$ time stamps that differed from the median of the window by more than t standard deviations were replaced with the median value (Pearson 2002). Each time series dataset was then smoothed using a 60-minute moving average. These data cleaning procedures were implemented using the R package 'pracma' (Borchers 2017; R Core Development Team 2017). The cleaned heat pulse velocities were corrected for probe misalignment errors using the zero reference values and for wounding errors assuming a 0.17 cm wound response (Burgess et al. 2001), and then converted to sap velocities using the wood properties obtained from

increment cores (Becker & Edwards 1999). Scaling from sap velocities to volumetric flow rates at a measurement position was accomplished by multiplying the average sap velocity of all replicate depths by the cross-sectional area of the corresponding annulus and then summing across all annuli (Hatton et al. 1990). Standard errors were estimated for each 20-minute interval using the velocities obtained across the depth profile of all sap flow gauges at a measurement position. For the tree bases, these scaling and error propagation procedures were performed separately for the 35 mm versus 110 mm probesets to enable comparisons between the two methodologies.

Dendrometry

Point dendrometers consisting of pressure transducers mounted to temperature-insensitive carbon fiber frames (models ZN11-T-WP, ZN11-Ox-WP; Natkon.ch, Oetwil am See, Switzerland) were installed onto the trunk and branches in each tree top to measure radial changes in stem size. On trunks, two dendrometers facing opposite azimuths were positioned at the base of the tree top and another about 1.5 m from the tree apex. On branches, one dendrometer was paired with the sap flow gages near a branch's base and another about 1.5 m from its terminus. Dead bark tissues were removed at the point of contact between the sensor head and the stem prior to installation. The dendrometers were wired to dataloggers (model CR23x; Campbell Scientific, Logan, UT, USA) and yielded a resolution of less than 1 μm. Temperature was recorded using a USB-programmable datalogger (model EL-USB-2; Lascar Electronics Inc., Erie, PA, USA) positioned immediately adjacent to each dendrometer, so that a correction factor of -0.28 μm $°C^{-1}$ could be applied. Stem diameter was recorded at each dendrometer position and used as a baseline from which changes in diameter were added. Diurnal changes in stem diameter were assumed to reflect physical deformation due to discharge-recharge cycles of water storage.

Psychrometry

Stem psychrometers connected to microvolt dataloggers (model PSY1; ICT International Ltd., Armidale, NSW, Australia) provided measurements of stem xylem water potential to 0.01 MPa resolution for branch in each tree. Psychrometers were cleaned, calibrated, and installed following the manufacturer's instructions, except that self-fusing silicone tape (Rescue Tape; Harbor Products Inc., Carson City, NV, USA), not vacuum grease, was used to hermetically seal the chamber against the stem. This modification prevented grease from leaking into the chamber and contaminating the delicate thermocouples under warm conditions. Plastic C-clamps were used to firmly secure the psychrometers to the selected branches, which were 3 to 4 cm diameter at the point of installation. Pre-dawn and mid-day water potentials measured on nearby shoots with a Scholander pressure chamber (model 1000, PMS Instrument Co., Corvallis, OR) validated the stem psychrometer measurements.

Scaling stem water storage to the tree top

A two-step process was used to scale stem water storage to entire tree tops. In the first step, a relationship was developed to predict diurnal change in stem volume (ΔV) from stem V. The tree-top trunks and main stem axes of branches selected for detailed study were partitioned into conical frusta delimited by dendrometer positions. Daily average maximum and average minimum diameters measured by the dendrometers at those positions were used to calculate a maximum diurnal change in frustum volume for each stem segment. This provided 12 pairs of V

and ΔV for a predictive relationship (i.e., 1 trunk segment and 3 branch segments from each of 3 trees) but did not consider small stem segments beyond the distalmost dendrometers. Therefore, I assumed that a stem of 0 cm diameter yielded 0 ΔV which provided an additional set of stem segments for the predictive relationship; that is, the trunk or branch stem segment beyond a stem's distalmost dendrometer was modeled as a cone whose base fluctuated in diameter but whose top did not. Exercising this assumption doubled the number of points for deriving a relationship for predicting ΔV from V. These two variables were $\log_{10}$-transformed to comply with assumptions of normality and homoscedasticity (Sokal & Rohlf, 1995) prior to fitting a power function using ordinary least squares regression that yielded a predictive relationship in which 98.59% of the variation in ΔV was explained by V,

$$\Delta V = 1.4295 * V^{0.8622} \quad \text{(Equation 2)}$$

Uncertainty in predicting ΔV from Equation 2 assumed 5% error in estimating stem volume from field measurements. In the second step, this power function was applied to the remaining stem segments, which included accessory trunks and their connecting limb segments as well as components of the dissected branches for which dendrometer data were lacking. Equation 2 was also applied to whole branches whose total stem volumes were predicted from Equation 1, and the uncertainty in estimating V from Equation 1 was carried forward. Finally, total tree-top ΔV was summed across all components to arrive at a final estimate for diurnal tree-top stem water storage capacity, and the component uncertainties were added in quadrature. The importance of stored stem water was then expressed as the quotient of tree-top stem water storage per daily summertime water use.

Time lags

Sources of water storage in trees may be identified by comparing the timing of peaks and troughs in different time series datasets such that time lags indicate water storage (Scholz et al. 2011). Hydraulic resistance between xylem and inner bark tissues decouples the diurnal size fluctuations of these tissues (Zweifel et al. 2014), leading to a predictable lag in water potentials between them (Pfautsch et al. 2015a). To evaluate whether water storage was sourced from inner bark, I used a cross-correlation analysis to identify lags among fluxes in branch sap flow, stem size, and stem water potential. Cross-correlation analysis slides one time series over a second, calculating the product and then the integral of that product at each time step; the largest integral is accepted as the final best alignment, and a correlation coefficient is calculated (Chatfield 1996). The number of lagged time steps to obtain the largest integral indicates the direction and duration of lag between fluxes. Stem size flux that lagged behind sap flow and water potential was considered evidence that the inner bark served a hydraulic capacitance function. Cross-correlation analyses were performed in R (R Core Development Team 2017).

RESULTS

Environmental conditions

The intensive study period extending August 1-7 captured warm and dry conditions typical for summertime in the Southern Sierra Nevada Mountains (Figure 2). Few clouds were observed. Average temperature was 18.6 ºC (range 13.6 to 22.9), relative humidity was 38.9%

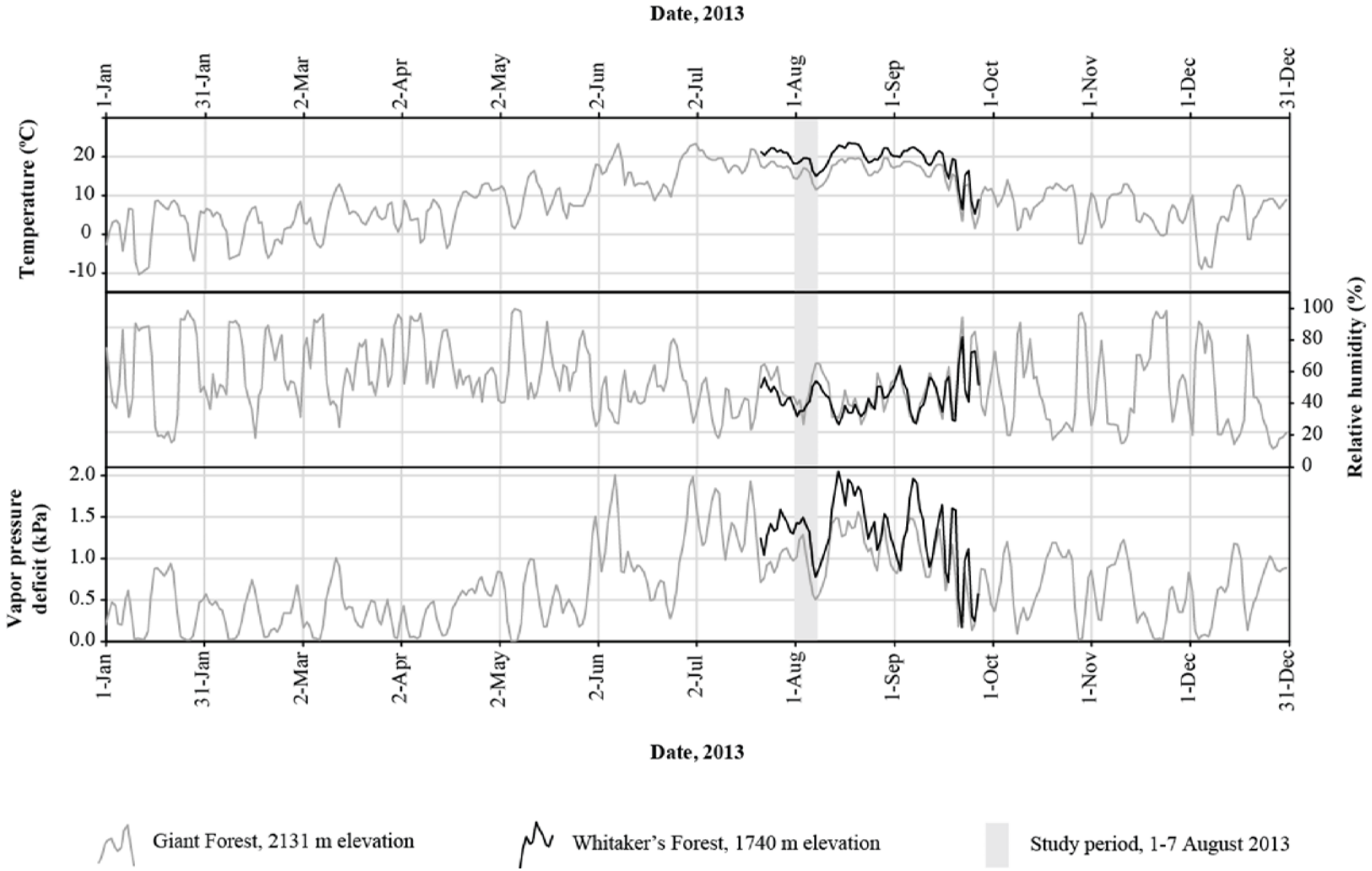

Figure 2. Weather data from the tops of large *Sequoiadendron giganteum* trees at Whitaker's Forest during a summertime field campaign to quantify the importance of stem water storage. Context for these environmental conditions was provided by comparing to a full year (2013) of data generated from a weather station perched atop another *Sequoiadendron* of similar height located nearby in Giant Forest, Sequoia National Park.

(range 26.4 to 58.1), and vapor pressure deficit was 1.3 kPa (range 0.7 to 1.9). Compared to Giant Forest, conditions at Whitaker's Forest were generally warmer and drier with higher vapor pressure deficits, but the two sites experienced similar trajectories in these variables (Figure 2).

Daily water use

Volumetric sap flow rates measured at tree-base and tree-top positions followed clear diurnal cycles, with lowest rates between 6:00 and 6:30 and highest rates in the early to late afternoon (Figures 3, 4). Among tree bases, the outermost 1-2 cm of the sapwood had consistently lower sap flow rates (Figure 4), but the remaining radial profile failed to show a consistent pattern. Whole-tree water use measured for five complete days via the 110-mm long probes was slightly larger but within one standard error of the 35-mm long probes also positioned at tree bases. Average daily volumetric sap flow measured with the long probes was 2227 ± 181 to 3752 ± 177 L d^{-1}, which corresponded to 0.582 ± 0.124 to 0.915 ± 0.105 L d^{-1} m^{-2} when expressed per unit of leaf area (Table 2). Tree top volumetric sap flow measured with the 35-mm long probes averaged 98 ± 15 to 134 ± 22 L d^{-1}, and ranged 0.670 ± 0.151 to 0.830 ± 0.165 L d^{-1} when expressed per unit of leaf area. Daily water use per unit of leaf area was not different at tree base and tree top positions (one-tailed t-test, P=0.22).

Elastic water storage

Dendrometers installed onto trunks and branches at the tree top positions registered maximum stem sizes around 8:00 and minima in the early evening (Figure 3). These daily fluxes in stem diameter were just a fraction of a millimeter, but were larger in trunks (0.235 ± 0.008 mm d^{-1}) than in branches (0.1105 ± 0.004 mm d^{-1}). Overall larger stems yielded larger fluxes in stem volumes (Figure 5). Combining the stem size flux data with stem geometries, I estimated elastic stem water storage at the tree tops to range from 1.49 ± 0.03 L d^{-1} to 2.47 ± 0.035 L d^{-1}, which corresponded to 1.52 ± 0.15% to 1.84 ± 0.16% of daily sap flow through the tree tops (Table 3). Thus, water stored in stems contributed less than 2% of daily tree top water use.

Xylem water potential

Stem psychrometers applied to the xylem of the study branches showed that daily fluxes in water potentials were routinely 0.75 to 0.90 MPa and displayed clear diurnal courses (Figure 3). Maximum values averaged over the 7-day study period occurred between 5:00 and 7:00 and ranged from –0.90 to –1.04 MPa, while minimum values occurred between 17:00 and 18:00 and ranged from –1.79 to –1.84 MPa. A slight mid-day increase in water potentials was observed in the early afternoon in some branches.

Time lags

Among the three trees, I observed several consistent hysteresis-like behaviors and time lags between sensor positions and types of sensors over the seven days of measurements (Figure 3, Table 4). For example, in each of the nine study branches and in each of the three tree-top trunks, diameter flux measured via dendrometry lagged behind sap flow by 1 hr to 5 hrs 20 min. Flux in branch diameter also consistently lagged behind branch water potential measured with the stem psychrometers. However, fluxes in branch sap flow and water potential were not consistently offset in time. Sap flow at trunk bases did not lag behind trunk sap flow at the tree tops, while lags in sap flow among branches as well as between branches and trunks were inconsistent (data not shown).

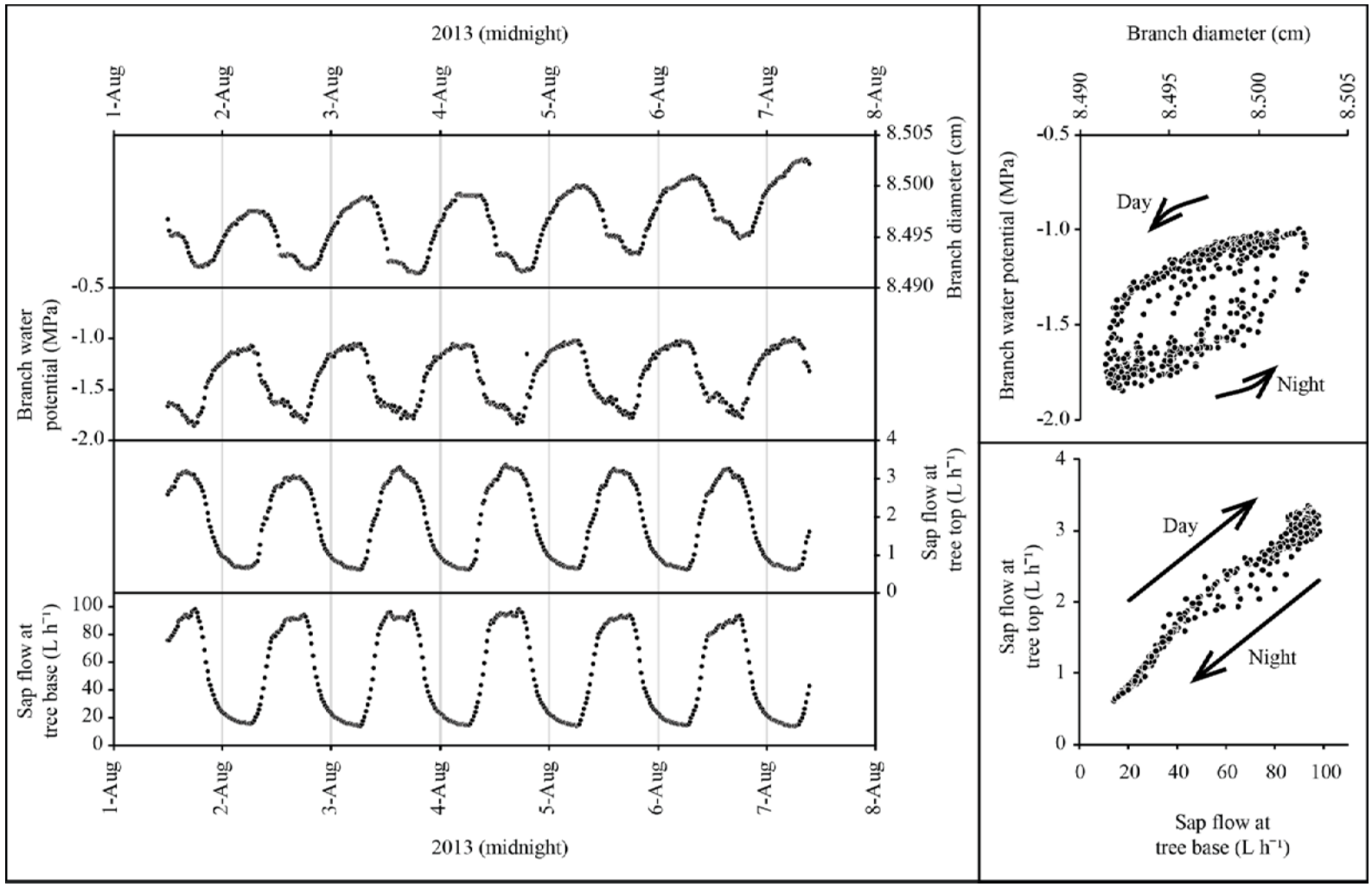

Figure 3. Example fluxes of tree-top branch water potential and branch diameter as well as volumetric sap flow at tree-base and tree-top positions for a large *Sequoiadendron giganteum* tree. Flux in branch diameter lagged behind branch water potential, causing hysteresis-like behavior. Sap flux in trunks at the tree top was coordinated in time with sap flow in trunks at the tree base, causing linear behavior.

Table 2. Average daily volumetric sap flow rates ± 1 SE expressed in absolute terms as well as normalized by leaf area, measured at the whole-tree level and the top 5 to 6 m for three large *Sequoiadendron giganteum* trees.

	Whole tree		Tree top	
Tree	**L d^{-1}**	**L d^{-1} m^2**	**L d^{-1}**	**L d^{-1} m^2**
1	3538 ± 168	0.945 ± 0.105	109 ± 18	0.830 ± 0.165
2	3752 ± 177	0.915 ± 0.105	134 ± 22	0.641 ± 0.162
3	2227 ± 181	0.582 ± 0.124	98 ± 15	0.670 ± 0.151

DISCUSSION

The objectives were to quantify the importance of elastic stem water storage at the tops of large *Sequoiadendron* trees and to provide context for tree top water use and storage by estimating whole-tree daily water use. Results were consistent with the notion that chronically low water potentials may subdue water storage dynamics, and suggest that a hydraulic connection between secondary xylem and inner bark allows stored water to be released from the live phloem tissues. Water storage capacity in stems contributed a small amount to daily whole-tree water use, which exceeded 3000 L d^{-1}.

Water storage capacity and hydraulic capacitance

Absolute water storage capacity was larger in more voluminous stems, consistent with the positive relationship between stem diameter and amount of stored water used commonly observed in both angiosperms and conifers (Scholz et al. 2011). Extrapolating this trend to the enormous sizes of *Sequoiadendron* trunks would suggest great potential for large amounts of water storage, but the water storage volume alone does not necessarily convey its importance. For example, I estimated that the elastic component of stem water storage contributed less than 2% to daily transpired water on warm and sunny summertime days. Adding the contribution from inelastic displacement of water associated with the formation of new embolisms during low water potentials (Tyree & Yang 1990) would likely impart a minimal effect given the very high retention of hydraulic conductivities that occur under normal operating water potentials at the tops of tall *Sequoiadendron* (Ambrose et al. 2009). The small contribution of stem water storage leads us to conclude that this storage reservoir is of less relative importance than foliage, which contributes approximately 7% of daily water use in *Sequoiadendron* (Williams et al. 2017). This means that stems contributed about 29% of the aboveground stored water, which fits within the 15 to 35% predicted for stems using modelling approaches (Edwards et al. 1986, Tyree 1988, Zweifel & Häsler 2001). Combined, the relative importance of the stems and the foliage in *Sequoiadendron* (8 to 9%) provides estimates close to that reported for potted *Picea abies* saplings (Zweifel et al. 2001) and within the range reported for larger conifers (Phillips et al. 2003). However, values up to 50% have been reported (Scholz et al. 2011), some of which may reflect a choice of methods. For example, sap flux in trunks that lags behind canopy branches has been attributed to water storage (Phillips et al. 1997; Goldstein et al. 1998, Meinzer et al. 2004, Čermák et al. 2007, Scholz et al. 2008; Köcher et al. 2013), but variable illumination patterns among branches over the course of a day can translate into variation in the timing of

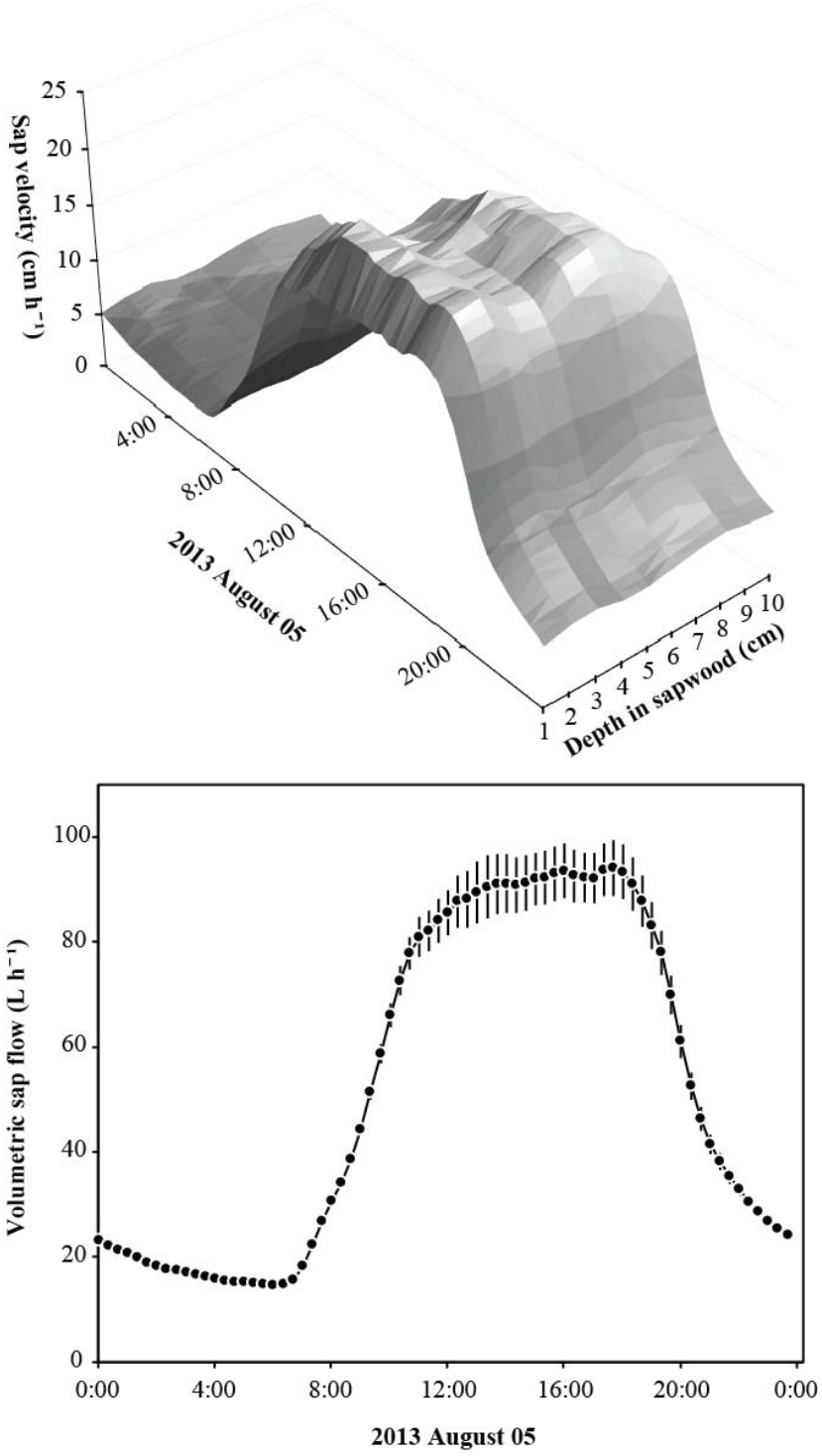

Figure 4. Example diurnal course of sap flow in a large *Sequoiadendron giganteum* tree averaged from two probesets positioned at opposite sides of the tree base. Upper panel: average sap velocity across the radial profile of sapwood at 10 equally spaced depths. Lower panel: diurnal course of volumetric flow sap flow integrated across the sapwood. Vertical bars are ± 1 standard error.

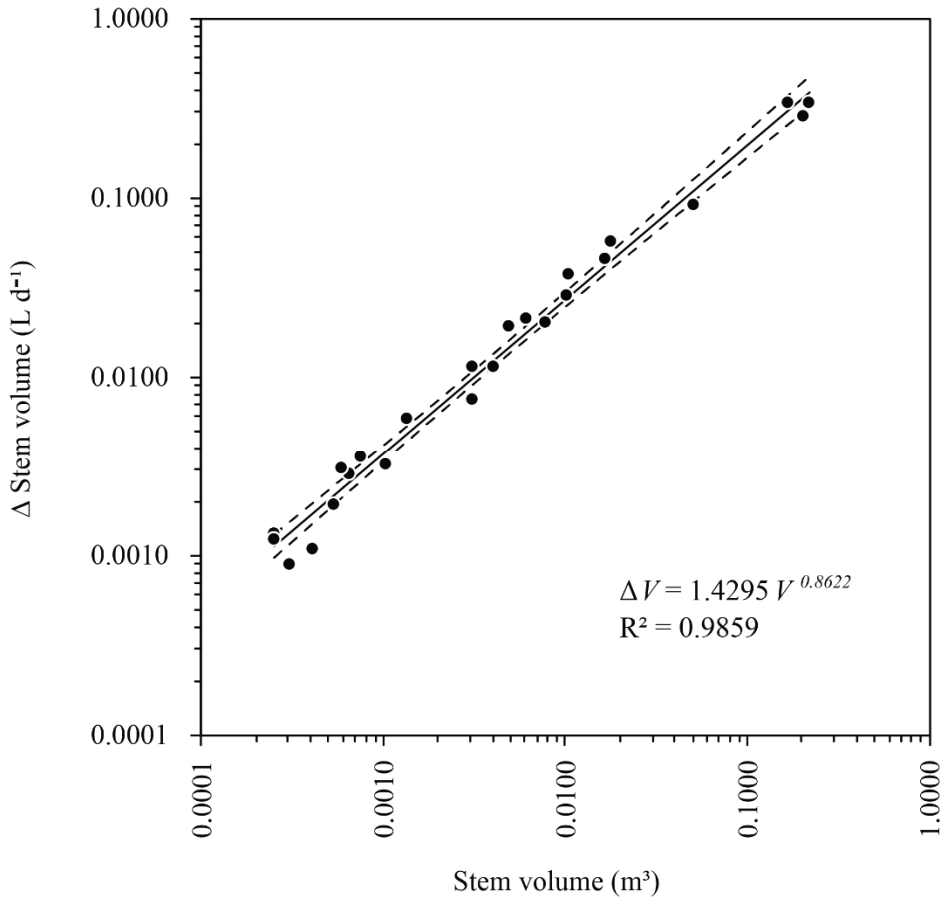

Figure 5. Water storage capacity, measured here as diurnal change in stem volume (ΔV), increased with stem volume (V) in the top 5-6 m of large *Sequoiadendron giganteum* trees. Solid line represents a power function derived via ordinary least squares regression of $\log_{10}$-transformed data. Dashed envelope represents 95% confidence interval.

transpirational demand and therefore obscure water storage dynamics (Burgess & Dawson 2008). The sap flux data underscore this methodological consideration because I observed highly variable time lags among sap flux measurements in branches but no differences in flux between upper and lower trunk positions. Therefore, the results support the tendency for larger stems to rely on larger absolute volumes of stored water, but the relative contribution of stored water does not appear to scale universally with tree size (Scholz et al. 2011).

The combination of dendrometry, geometry, and psychrometry enabled the calculation of hydraulic capacitance at the branch segment level for one branch in each tree. These values, which ranged from about 3 to 4 L MPa^{-1} m^{-3}, were one to two orders of magnitude smaller than previous reports for conifer sapwood (Scholz et al. 2011). This large discrepancy can be attributed to several factors. First, the gravitational potential gradient imposed chronically low water potentials in the branches studied here, which were 78 to 83 m above ground level. Moisture release curves generated for conifer sapwood prior to the inelastic release of stored water indicate that hydraulic capacitance decreases with more negative water potentials (Waring

Table 3. Stem volumes and water storage capacities ± 1 SE in the top 5 to 6 m of large *Sequoiadendron giganteum* trees.

Tree	Stem volume (m^3)	Absolute water storage capacity (L d^{-1})	Relative water storage capacity (%)
1	0.719 ± 0.013	1.707 ± 0.025	1.560 ± 0.164
2	1.095 ± 0.019	2.471 ± 0.035	1.840 ± 0.162
3	0.621 ± 0.014	1.493 ± 0.026	1.524 ± 0.150

et al. 1979; Tyree & Yang 1990; Barnard et al. 2011; McCulloh et al. 2014). Thus, while the *range* of water potentials over which hydraulic capacitance was measured may be similar among studies and controlled for in its calculation, the amount of releasable water is highly dependent upon the *absolute* water potentials one normally observes in the field. Second, high-density wood has low water content (Borchert 1994). The relatively high wood density in the study branches (mean 0.448 g cm^{-3}) indicates correspondingly small proportions of ray parenchyma that are known to express high hydraulic capacitance (Holbrook 1995; Meinzer et al. 2003, 2006, 2008; Scholz et al. 2007). I speculate that relatively high wood density explains the smaller hydraulic capacitances observed in branches versus trunks (McCulloh et al. 2014) as well as in the trunk near the tree tops versus tree bases (Domec & Gartner 2001) from which the majority of reported sapwood capacitance values have been derived (Scholz et al. 2011). Third, a difference in the types of tissues measured renders direct comparisons challenging. The methodology I used for estimating hydraulic capacitance included all tissues in a stem segment and did not allow for separating the contributions from inner bark versus secondary xylem, whereas others include only sapwood. Inner bark is known to function as a hydraulic capacitor (Pfautsch et al. 2015a), and the potential for heartwood capacitance remains unclear (White et al. 1985). Despite these differences, estimates of stem hydraulic capacitance suggest that very little water is expressed per volume of tissue under normal operating water potentials in tree-top branches of *Sequoiadendron*.

The notion that low water potentials could subdue water storage dynamics can in principal be extended beyond the tops of tall trees to include shorter statured woody plants that occupy dry environments. For example, predawn water potentials in *Juniperus monospera* that can remain between –2.0 and –4.0 MPa for months (Breshears et al. 2009) may inhibit capacitive release of water stored in stems. The fact that hydraulic capacitance decreases with more negative water potentials (Waring et al. 1979; Tyree & Yang 1990; Barnard et al. 2011; McCulloh et al. 2014) supports the extension of these results to short-statured woody plants that are under chronically low water potentials.

Support for xylem-phloem water transfer

The sequence of time lags and hysteresis-like behaviors I observed among fluxes in sap flow, water potential, and branch diameter enabled qualitative evaluation of the hydraulic connection between secondary xylem and secondary phloem. As proposed by Pfautsch et al. (2015a), a diurnal course of the hydraulic interaction between these tissues can be divided into four phases that are driven by transpiration-induced water potential flux and outwardly expressed as changes in stem diameter. Starting pre-dawn when transpiration is very slow, water potentials in the xylem and phloem tissues are relaxed and at equilibrium, and stem diameter is stable.

Table 4. Lag times among fluxes in sap flow, branch diameter, and xylem water potential measured in stems in the top 5 to 6 m of three large *Sequoiadendron giganteum* trees. Positive lags imply position 1, sensor 1 lagged behind position 2, sensor 2. Values were derived from cross-correlation analysis.

Tree	Position 1, sensor 1	Position 2, sensor 2	Lag time (h:mm)	Cross-correlation coeficient
1	Tree base trunk, sap flow	Tree top trunk, sap flow	-0:40 to 0:20	0.98
1	Branch 1, dendrometer	Branch 1, sap flow	2:00 to 2:40	0.96
1	Branch 2, dendrometer	Branch 2, sap flow	4:20 to 5:20	0.81
1	Branch 3, dendrometer	Branch 3, sap flow	1:00 to 1:40	0.96
1	Tree top trunk, dendrometer	Tree top trunk, sap flow	1:40 to 2:20	0.93
1	Branch 2, psychrometer	Branch 2, sap flow	0:20 to 1:00	0.77
1	Branch 2, dendrometer	Branch 2, psychrometer	2:40 to 3:20	0.95
2	Tree base trunk, sap flow	Tree top trunk, sap flow	-0:20 to 0:20	0.99
2	Branch 4, dendrometer	Branch 4, sap flow	1:40 to 2:20	0.86
2	Branch 5, dendrometer	Branch 5, sap flow	1:40 to 2:40	0.83
2	Branch 6, dendrometer	Branch 6, sap flow	1:40 to 2:00	0.81
2	Tree top trunk, dendrometer	Tree top trunk, sap flow	1:40 to 2:40	0.93
2	Branch 5, psychrometer	Branch 5, sap flow	-0:20 to 0:20	0.93
2	Branch 5, dendrometer	Branch 5, psychrometer	2:00 to 2:40	0.92
3	Tree base trunk, sap flow	Tree top trunk, sap flow	-0:20 to 0:20	0.97
3	Branch 7, dendrometer	Branch 7, sap flow	3:40 to 4:20	0.96
3	Branch 8, dendrometer	Branch 8, sap flow	1:20 to 2:20	0.83
3	Branch 9, dendrometer	Branch 9, sap flow	4:20 to 5:20	0.72
3	Tree top trunk, dendrometer	Tree top trunk, sap flow	2:20 to 3:20	0.93
3	Branch 8, psychrometer	Branch 8, sap flow	-0:40 to 0:00	0.96
3	Branch 8, dendrometer	Branch 8, psychrometer	2:00 to 2:40	0.86

During the daytime as transpiration increases, xylem water potential sinks below that of the phloem, thereby drawing water from phloem tissues which results in stem contraction. Toward dusk as transpiration begins to slow, xylem water potential rises to equilibrium with the phloem, so phloem-to-xylem water transfer stops and stem diameter stabilizes. At nighttime when transpiration is very slow, xylem water potential rises above that of the phloem and causes xylem-to-phloem water transfer that results in stem expansion. Since hydraulic resistance between xylem and phloem decouples the diurnal size fluctuations of these tissues (Zweifel et al. 2014), water potential of the phloem is predicted to lag behind that of the xylem (Pfautsch et al. 2015a). This explains observations of fluxes in transpiration and water potential that precede changes in stem diameter (Lassoie 1973; Parlange et al. 1975; Edwards et al. 1986; Perämäki et al. 2001, 2005; Sevanto et al. 2002; Steppe & Lemeur 2004; Steppe et al. 2006; Drew et al. 2008). Consistent with these observations, I found that fluxes in sap flow and xylem water potential occurred in sync while stem diameter flux consistently and substantially lagged behind (Table 4; Figure 3). These data therefore provide support for water transfer between xylem and phloem tissues that is driven by nonsteady-state conditions manifest as water potential gradients within branches.

This sequence of time lags suggests that water extracted from phloem tissues is responsible for the flux in stem diameter, but the sequence alone does not exclude the possibility that the xylem tissues themselves also contracted. Models indicate that diurnal flux in phloem osmotic concentration could cause detectable physical deformations of both phloem and xylem tissues (Genard et al. 2001; Hölttä et al. 2006; De Schepper & Steppe 2010). However, the modulus of elasticity for inner bark is about 10 to 100 MPa while that for wood is far greater at about 1000 MPa (Irvine & Grace 1997; Alméras 2008; Sevanto et al. 2011; Mencuccini et al. 2013; Giroud et al. 2017), demonstrating that changes in water potential much more strongly deform the flexible phloem compared to the rigid xylem. Moreover, applying pairs of point dendrometers simultaneously to inner bark and xylem tissues typically indicates that phloem tissue carries the vast majority of the diurnal flux in stem diameter (Sevanto et al. 2002, 2003, 2011; Mencuccini et al. 2013), the exception being *Eucalyptus globulus* saplings that had a very thin layer of bark and a thick layer of juvenile sapwood which was not fully lignified and therefore highly flexible (Zweifel et al. 2014). These observations suggest that the diurnal stem flux I measured in *Sequoiadendron* tree tops was caused primarily by phloem water extraction driven by transpiration-induced changes in water potential. Therefore, the growing body of evidence that phloem serves an important hydraulic capacitance function (Pfautsch et al. 2015a) now includes stems under gravity-induced, chronically low water potentials at the tops of tall trees.

Daily water use

Estimates of whole-tree daily water use in *Sequoiadendron* corroborate those previously reported for similar sized trees the same site (Ambrose et al. 2016), and to my knowledge are the largest yet measured for any individual tree (Wullschleger et al. 1998; Meinzer et al. 2005; Zeppel 2013). Tree size explains substantial variation in daily water use (Meinzer et al. 2005), and the large trunks and sapwood cross-sectional areas of *Sequoiadendron* clearly extend this trend. However, tree size alone cannot fully account for such copious water demands because scaling daily water use by sapwood cross-sectional area across a large range of conifer sizes varies more than one order of magnitude from about 100 to 1800 L d^{-1} m^{-2} (Meinzer et al. 2005), and approximately 3000 L d^{-1} m^{-2} for the trees studied here. *Sequoiadendron*'s relatively wide tracheid lumens, which range from about 40 to 50 μm at the bases of tall individuals (Williams et al., *in review*) likely permit high axial permeability (Tyree & Zimmermann 2002) compared to the smaller diameter tracheids found in many other conifer stems (e.g., Pittermann et al. 2006). In addition, the topographic basins to which *Sequoiadendron* is restricted supply abundant soil moisture (Rundel 1972, Anderson et al. 1995, Willard 2000) that sustains the high transpirational rates inherent with these very large trees with large leaf areas. Given that the trees studied here contain less than 25% of the main trunk volume and support just 60% of the leaf area of the largest *Sequoiadendron* tree (Van Pelt 2000; Sillett et al. 2015), the species has great potential for even higher rates of daily water use as pointed out by Ambrose et al. (2016).

Tree tops on average used just 3.7% of the total daily water budget, but I observed no difference between tree-top and tree-base positions when daily water use was scaled per unit leaf area. This result might at first appear surprising given that height in forest canopy is associated with increasingly desiccating microclimatic conditions, including higher sunlight intensity and wind speed as well as lower relative humidity (Parker 1995; Niinemets 2007) that together have the potential to increase transpiration. However, height-related hydraulic constraints such as the gravitational potential gradient and the accumulation of hydraulic resistance over long transport

paths may explain this result. The lack of vertical trends in branch-averaged transpiration and stomatal conductance previously observed in *Sequoiadendron* was attributed to hydraulic constraints on the ability to optimize photosynthesis with the brighter conditions available in the upper crowns of tall trees (Ambrose et al. 2016). If daily water use per leaf area is truly constant with height in tree, models incorporating transpiration rates for *Sequoiadendron* groves or trees of different sizes will be simplified.

Using dendrometry to predict xylem water potential

High resolution point dendrometers are potentially a useful tool for low-impact monitoring of flux in xylem water potential, among other uses (Drew & Downes 2009). Other methods of obtaining accurate water potential measurements are complimentary but have individual limitations. Pressure chambers are easy to use and rugged, but they are unsuitable for high-frequency monitoring of water potentials (Turner 1981). Stem psychrometers, on the other hand, are well suited for high-frequency and long-term monitoring, but they are delicate, thermally sensitive, and require invasive removal of bark and some xylem for installation (Martinez et al. 2011). Microtensiometers are a promising new approach, but installation requires boring a small hole into the xylem (Pagay et al. 2014). After correcting for lags in the time series, I found good agreement (high cross correlation coefficients) between fluxes in stem size and water potential for the three branches on which I applied both dendrometers and psychrometers. The overall half-dome shape in daily fluxes even appeared similar, with an abrupt and steep decline in the early morning followed by a stable period, then an abrupt relaxation that continued at a decelerating rate into the nighttime (Figure 5). Both of these diurnal courses match the four-phase hydraulic interaction proposed between bark and xylem described above (Pfautsch et al. 2015a). The disadvantage in using dendrometry to predict xylem water potential would be developing a calibration that includes a time lag. However, assuming diameter flux does occur at low levels in the sapwood (Zweifel et al. 2000, Sevanto et al. 2002, 2008, 2011; Zweifel et al. 2014; Pfautsch et al. 2015a), applying dendrometers radially to the xylem surface may enable high-frequency and real-time estimates of xylem water potential with little damage to the stem as demonstrated by Offenthaler et al. (2001).

Conclusions and future directions

Large *Sequoiadendron* trees contain expansive sapwood cross-sectional areas, wide tracheids, and abundant foliage that in combination can support water budgets exceeding 3000 L d^{-1}. The relatively small water storage capacities and hydraulic capacitances I observed among tree-top stems may be associated with chronically low water potentials imposed by gravity, which I hypothesize is caused by a trend of decreasing water storage dynamics with height in tree. Nonetheless, *Sequoiadendron* relies on water stored in stems and foliage to augment daily water use by 8 to 9% on warm and sunny summertime days. In agreement with a growing body of evidence, the time lags I observed among fluxes in sap flow, water potential, and stem diameter indicate that a large portion of the available water stored in upper crown branches is carried by secondary phloem tissues comprising the majority of the inner bark. The high-resolution point dendrometer is a promising and low-impact tool for quantifying xylem water potential that will foster a deeper understanding of the dynamics of water storage and nonsteady-state conditions omnipresent within large trees.

ACKNOWLEDGEMENTS

This project was funded in part by Save The Redwoods League through the Redwoods and Climate Change Initiative and also by a Save The Redwoods League Research Grant. Collaborators Rikke Reese Næsborg, Anthony Ambrose, Wendy Baxter, George Koch, and Todd Dawson provided critical guidance and assistance at multiple stages that will be rewarded with coauthorship when this manuscript is published. Thanks to Roman Zweifel and Alec Downey for providing guidance on using dendrometers and psychrometers, Steve Burgess for writing the program that ran the long sap flow probes, Chris Wong for helping to install sensors and dissect branches, Steve Sillett for loaning sap flow equipment and determining the ages of study trees, and Rob York for aiding with field logistics. Autumn Amici, John Battles, Cindy Looy, Sybil Gotsch, and Emily Heyne provided constructive comments on the manuscript. I am grateful to the Center for Forestry at UC Berkeley for research permissions and use of the Whitaker's Forest Research Station.

REFERENCES

Alméras T. 2008. Mechanical analysis of the strains generated by water tension in plant stems. Part II: strains in wood and bark and apparent compliance. *Tree Physiology* 28: 1513–1523.

Ambrose AR, Sillett SC, Dawson TE. 2009. Effects of tree height on branch hydraulic, leaf structure and gas exchange in California redwoods. *Plant, Cell & Environment* 32: 743–757.

Ambrose AR, Baxter WL, Wong CS, Burgess SS, Williams CB, Næsborg RR, Koch GW, Dawson TE. 2016. Hydraulic constraints modify optimal photosynthetic profiles in giant sequoia trees. *Oecologia* 23: 1–8.

Anderson MA, Graham RC, Alyanakian GJ, Martynn DZ. 1995. Late summer water status of soils and weathered bedrock in a giant sequoia grove. *Soil Science* 160: 415–422.

Barnard DM, Meinzer FC, Lachenbruch B, McCulloh KA, Johnson DM, Woodruff DR. 2011. Climate-related trends in sapwood biophysical properties in two conifers: avoidance of hydraulic dysfunction through coordinated adjustments in xylem efficiency, safety and capacitance. *Plant, Cell & Environment* 34: 643–654.

Becker P, Edwards WR. 1999. Corrected heat capacity of wood for sap flow calculations. *Tree Physiology* 19: 767–768.

Bevington PR, Robinson DK. 2002. Data Reduction and Error Analysis for the Physical Sciences 3rd edn, McGraw-Hill, New York.

Borchert R. 1994. Soil and stem water storage determine phenology and distribution of tropical dry forest trees. *Ecology* 75: 1437–1449.

Borchers HW. 2017. pracma: Practical numerical math functions. R package version 2.0.7. [WWW document] URL https://CRAN.R-project.org/package=pracma. [accessed 15 Oct 2017]

Breshears DD, Myers OB, Meyer CW, Barnes FJ, Zou CB, Allen CD, McDowell NG, Pockman WT. 2009. Tree die-off in response to global change-type drought: Mortality insights from a decade of plant water potential measurements. *Frontiers in Ecology and the Environment* 7: 185–189.

Bucci SJ, Scholz FG, Goldstein G, Meinzer FC, Franco AC, Zhang Y, Hao GY. 2008. Water relations and hydraulic architecture in Cerrado trees: adjustments to seasonal changes in water availability and evaporative demand. *Brazilian Journal of Plant Physiology* 20: 233–245.

Buck AL. 1981. New equations for computing vapor pressure and enhancement factor. *Journal of Applied Meteorology* 20: 1527–1532.

Burgess SS, Dawson TE. 2004. The contribution of fog to the water relations of Sequoia sempervirens (D. Don): foliar uptake and prevention of dehydration. *Plant, Cell & Environment* 27: 1023–1034.

Burgess SS, Dawson TE. 2008. Using branch and basal trunk sap flow measurements to estimate whole-plant water capacitance: a caution. *Plant and Soil* 305: 5–13.

Burgess SS, Adams MA, Turner NC, Beverly CR, Ong CK, Khan AA, Bleby TM. 2001. An improved heat pulse method to measure low and reverse rates of sap flow in woody plants. *Tree Physiology* 21: 589–598.

Čermák J, Kučera J, Bauerle WL, Phillips N, Hinckley TM. 2007. Tree water storage and its diurnal dynamics related to sap flow and changes in stem volume in old-growth Douglas-fir trees. *Tree Physiology* 27: 181–198.

Chapotin SM, Razanameharizaka JH, Holbrook NM. 2006*a*. A biomechanical perspective on the role of large stem volume and high water content in baobab trees (*Adansonia* spp.; Bombacaceae). *American Journal of Botany* 93: 1251–1264.

Chapotin S, Razanameharizaka JH, Holbrook NM. 2006*b*. Baobab trees (*Adansonia*) in Madagascar use stored water to flush new leaves but not to support stomatal opening prior to the rainy season. *New Phytologist* 169: 549–559.

Chatfield C. 1996. The Analysis of Time Series: An Introduction (sixth ed.), Chapman & Hall/CRC.

Dawson TE, Goldsmith GR. 2018. The value of wet leaves. *New Phytologist* (in press).

De Schepper V, Steppe K,Van Labeke M-C & Lemeur R. 2010. Detailed analysis of double girdling effects on stem diameter variations and sap flow in young oak trees. *Environmental and Experimental Botany* 68: 149–156.

Dixon HH, Joly J. 1895. On the ascent of sap. *Philosophical Transactions of the Royal Society, B* 186: 563–576.

Domec JC & Gartner BL. 2001. Embolism and water storage capacity in bole xylem segments of mature and young Douglas-fir trees. *Trees* 15: 204–214.

Domec J-C, Scholz FG, Bucci SJ, Meinzer FC, Goldstein G, Villalobos-Vega R. 2006. Diurnal and seasonal variation in root xylem embolism in neotropical savanna woody species: impact on stomatal control of plant water status. *Plant, Cell & Environment* 29: 26–35.

Drew DM, Downes GM. 2009. The use of precision dendrometers in research on daily stem size and wood property variation: a review. *Dendrochronologia* 27: 159–172.

Drew DM, O'Grady AP, Downes GM, Read J, Worledge D. 2008. Daily patterns of stem size variation in irrigated and unirrigated *Eucalyptus globulus*. *Tree Physiology* 28: 1573–1581.

Edwards WRN, Jarvis PG, Landsberg JJ, Talbot H. 1986. A dynamic model for studying flow of water in single trees. *Tree Physiology* 1: 309–324.

Evert, RF. 2006. Esau's Plant Anatomy: Meristems, Cells, and Tissues of the Plant Body: Their Structure, Function, and Development. Hoboken, NJ: John Wiley & Sons, Inc.

Génard M, Fishman S, Vercambre G, Huguet JG, Bussi C, Besset J, Habib R. 2001. A biophysical analysis of stem and root diameter variations in woody plants. *Plant Physiology* 126: 188–202.
Giroud G, Bégin J, Defo M, Ung CH. 2017. Regional variation in wood density and modulus of elasticity of Quebec's main boreal tree species. *Forest Ecology and Management* 400: 289–299.
Goldsmith GR. 2013. Changing directions: the atmosphere–plant–soil continuum. *New Phytologist* 199: 4–6.
Goldsmith GR, Matzke NJ, Dawson TE. 2013. The incidence and implications of clouds for cloud forest plant water relations. *Ecology Letters* 16: 307–314.
Goldstein G, Meinzer FC, Monasterio M. 1984. The role of capacitance in the water balance of Andean giant rosette species. *Plant, Cell & Environment* 7: 179–186.
Goldstein G, Andrade JL, Meinzer FC, Holbrook NM, Cavelier J, Jackson P, Celis A. 1998. Stem water storage and diurnal patterns of water use in tropical forest canopy trees. *Plant, Cell & Environment* 21: 397–406.
Hatton TJ, Catchpole EA, Vertessy RA. 1990. Integration of sapflow velocity to estimate plant water use. *Tree Physiology* 6: 201–209.
Hinckley TM, Lachenbruch B, Meinzer FC, Dawson TE. 2011. A lifespan perspective on integrating structure and function in trees. In: Size-and age-related changes in tree structure and function (pp. 3–30). Springer Netherlands.
Holbrook NM. 1995. Stem water storage. In BL Gartner, ed, Plant Stems: Physiology and Functional Morphology. Academic Press, San Diego, pp 151–174.
Holbrook NM, Sinclair TR. 1992. Water balance in the arborescent palm, Sabal palmetto. II. Transpiration and stem water storage. *Plant, Cell & Environment* 15: 401–409.
Holbrook NM, Zwieniecki MA. 2011. Vascular transport in plants. Academic Press, Burlington, MA, USA.
Hölttä T, Vesala T, Sevanto S, Perämäki M, Nikinmaa E. 2006. Modeling xylem and phloem water flows in trees according to cohesion theory and Münch hypothesis. *Trees* 20: 67–78.
Hölttä T, Mencuccini M, Nikinmaa E. 2009. Linking phloem function to structure: analysis with a coupled xylem-phloem transport model. *Journal of Theoretical Biology* 259: 325–337.
Irvine J. & Grace J. 1997. Continuous measurement of water tensions in the xylem of trees based on the elastic properties of wood. *Planta* 202: 455–461.
Jepson J. 2000. The tree climber's companion: a reference and training manual for professional tree climbers. Beaver Tree Publishing, Longville, MN.
Koch GW, Sillett SC, Jennings GM, Davis SD. 2004. The limits to tree height. *Nature* 428: 851–854.
Köcher P, Horna V, Leuschner C. 2013. Stem water storage in five coexisting temperate broad-leaved tree species: significance, temporal dynamics and dependence on tree functional traits. *Tree Physiology* 33: 817–832.
Lassoie JP. 1973. Diurnal dimensional fluctuations in a Douglas-fir stem in response to tree water status. *Forest Science* 19: 251–255.
Martinez EM, Cancela JJ, Cuesta TS, Neira XX. 2011. Use of psychrometers in field measurements of plant material: accuracy and handling difficulties. *Spanish Journal of Agricultural Research* 9: 313–328.

McCulloh KA, Johnson DM, Meinzer FC, Woodruff DR. 2014. The dynamic pipeline: hydraulic capacitance and xylem hydraulic safety in four tall conifer species. *Plant, Cell & Environment* 37: 1171–1183.
Meinzer FC, Clearwater MJ, Goldstein G. 2001. Water transport in trees: current perspectives, new insights and some controversies. *Environmental and Experimental Botany* 45: 239–262.
Meinzer FC, James SA, Goldstein G, Woodruff D. 2003. Whole-tree water transport scales with sapwood capacitance in tropical forest canopy trees. *Plant, Cell & Environment* 26: 1147–1155.
Meinzer FC, James SA, Goldstein G. 2004. Dynamics of transpiration, sap flow and use of stored water in tropical forest canopy trees. *Tree Physiology* 24: 901–909.
Meinzer FC, Bond BJ, Warren JM, Woodruff DR. 2005. Does water transport scale universally with tree size? *Functional Ecology* 19: 558–565.
Meinzer FC, Brooks JR, Domec J-C, Gartner BL, Warren JL, Woodruff D, Bible K, Shaw DC. 2006. Dynamics of water transport and storage in conifers studied with deuterium and heat tracing techniques. *Plant, Cell & Environment* 29: 105–114.
Meinzer FC, Woodruff DR, Domec J-C, Goldstein G, Campanello PI, Gatti MG, Villalobos-Vega R. 2008. Coordination of leaf and stem water transport properties in tropical forest trees. *Oecologia* 156: 31–41.
Meinzer FC, Johnson DM, Lachenbruch B, McCulloh KA, Woodruff DR. 2009. Xylem hydraulic safety margins in woody plants: coordination of stomatal control of xylem tension with hydraulic capacitance. *Functional Ecology* 23: 922–930.
Mencuccini M, Hölttä T, Sevanto S, Nikinmaa E. 2013. Concurrent measurements of change in the bark and xylem diameters of trees reveal a phloem-generated turgor signal. *New Phytologist* 198: 1143–1154.
Münch E. 1930. Die Stoffbewegungen in der Pflanze. Fischer, Jena.
Nielsen ET, Sharifi MR, Rundel PW, Forseth IN, Ehleringer J. 1990. Water relations of stem succulent trees in north central Baja California. *Oecologia* 82: 299–303.
Niinemets Ü. 2007. Photosynthesis and resource distribution through plant canopies. *Plant Cell Environ* 30: 1052–1071.
Nobel PS. 1983. Biophysical plant physiology and ecology. W.H. Freeman and Company, San Francisco, CA.
Offenthaler I, Hietz P, Richter H. 2001. Wood diameter indicates diurnal and long-term patterns of xylem potential in Norway spruce. *Trees* 15: 215–221.
Parker GG. 1995. Structure and microclimate of forest canopies. In: Lowman MD, Nadkarni NM (eds) Forest canopies. Academic Press, San Diego, CA, pp 73–106.
Parlange J-Y, Turner NC, Waggoner PE. 1975. Water uptake, diameter change, and nonlinear diffusion in tree stems. *Plant Physiology* 55: 247–250.
Pagay V, Santiago M, Sessoms DA, Huber EJ, Vincent O, Pharkya A, Corso TN, Lakso AN, Stroock AD. 2014. A microtensiometer capable of measuring water potentials below −10 MPa. *Lab on a Chip* 14: 2806−2817.
Pearson RK. 2002. Outliers in process modeling and identification. *IEEE Transactions on Control Systems Technology* 10: 55–63.
Perämäki M, Nikinmaa E, Sevanto S, Ilvesniemi H, Siivola E, Harti P, Vesala T. 2001. Tree stem diameter variations and transpiration in scots pine: an analysis using a dynamic sap flow model. *Tree Physiology* 21: 889–987.

Perämäki M, Vesala T, Nikinmaa E. 2005. Modelling the dynamics of pressure propagation and diameter variation in sapwood. *Tree Physiology* 25: 1091–1099.
Pfautsch S, Hölttä T, Mencuccini M. 2015a. Hydraulic functioning of tree stems—fusing ray anatomy, radial transfer and capacitance. *Tree Physiology* 35: 706–722.
Pfautsch S, Renard J, Tjoelker MG, Salih A. 2015b. Phloem as capacitor: radial transfer of water into xylem of tree stems occurs via symplastic transport in ray parenchyma. *Plant Physiology* 167: 963–971.
Philip JR. 1966. Plant water relations: some physical aspects. *Annual Review Plant Physiology* 17: 245–268.
Phillips N, Nagchaudhuri A, Oren R, Katul G. 1997. Time constant for water transport in loblolly pine trees estimated from time series of evaporative demand and stem sapflow. *Trees* 11: 412–419.
Phillips NG, Ryan MG, Bond BJ, McDowell NG, Hinckley TM, Čermák J. 2003. Reliance on stored water increases with tree size in three species in the Pacific Northwest. *Tree Physiology* 23: 237–245.
Pittermann J, Sperry JS, Hacke UG, Wheeler JK, Sikkema EH. 2006. Inter-tracheid pitting and the hydraulic efficiency of conifer wood: the role of tracheid allometry and cavitation protection. *American Journal of Botany* 93: 1265–1273.
Reynolds ERC. 1965. Transpiration as related to internal water content. *Nature* 207: 1001–1002.
Rundel PW. 1972. Habitat restriction in giant sequoia: the environmental control of grove boundaries. *American Midland Naturalist* 1: 81–99.
Scholz FG, Bucci SJ, Goldstein G, Meinzer FC, Franco AC, Miralles-Wilhelm F. 2007. Biophysical properties and functional significance of stem water storage tissues in neo-tropical savanna trees. *Plant, Cell & Environment* 30: 236–248.
Scholz FC, Bucci SJ, Goldstein G, Meinzer FC, Franco AC, Miralles-Wilhelm F. 2008. Temporal dynamics of stem expansion and contraction in savanna trees: withdrawal and recharge of stored water. *Tree Physiology* 28: 469–480.
Scholz FG, Phillips NG, Bucci SJ, Meinzer FC, Goldstein G. 2011. Hydraulic capacitance: biophysics and functional significance of internal water sources in relation to tree size. In:
Meinzer FC, Lachenbruch B, Dawson TE (eds) Size-and age-related changes in tree structure and function. Springer, The Netherlands, pp 341–361.
Sevanto S, Vesala T, Perämäki M, Nikinmaa E. 2002. Time lags for xylem and stem diameter variations in a scots pine tree. *Plant, Cell & Environment* 25: 1071–1077.
Sevanto S, Vesala T, Perämäki M, Nikinmaa E. 2003. Sugar transport together with environmental conditions controls time lags between xylem and stem diameter changes. *Plant, Cell & Environment* 26: 1257–1265.
Sevanto S, Nikinmaa E, Riikonen A, Daley M, Pettijohn JC, Mikkelsen TN, Phillips N, Holbrook NM. 2008. Linking xylem diameter variations with sap flow measurements. *Plant and Soil* 305: 77–90.
Sevanto S, Hölttä T, Holbrook NM. 2011. Effects of the hydraulic coupling between xylem and phloem on diurnal phloem diameter variation. *Plant, Cell & Environment* 34: 690–703.
Sillett SC, Van Pelt R, Carroll AL, Kramer RD, Ambrose AR, Trask D. 2015. How do tree structure and old age affect growth potential of California redwoods? *Ecological Monographs* 85: 181–212.
Sokal RR, Rohlf FJ. 1995. Biometry (3rd edition). New York, USA: WH Freeman and Company.

Steppe K, De Pauw DJ, Lemeur R, Vanrolleghem PA. 2006. A mathematical model linking tree sap flow dynamics to daily stem diameter fluctuations and radial stem growth. *Tree Physiology* 26: 257–273.
Steppe K, Lemeur R. 2004. An experimental system for analysis of the dynamic sap-flow characteristics in young trees: results of a beech tree. *Functional Plant Biology* 31: 83–92.
Stratton L, Goldstein G, Meinzer FC. 2000. Stem water storage capacity and efficiency of water transport: their functional significance in a Hawaiian dry forest. *Plant, Cell & Environment* 23: 99–106.
Stroock AD, Pagay VV, Zwieniecki MA, Holbrook NM. 2014. The physicochemical hydrodynamics of vascular plants. *Annual Review of Fluid Mechanics* 46: 615–642.
Turner NC. 1981. Techniques and experimental approaches for the measurement of plant water status. *Plant and soil* 58: 339–366.
Tyree MT. 1988. A dynamic model for water flow in a single tree: evidence that models must account for hydraulic architecture. *Tree Physiology* 4: 195–217.
Tyree MT, Yang S. 1990. Water storage capacity of *Thuja*, *Tsuga* and *Acer* stems measured by dehydration isotherms: the contribution of capillary water and cavitation. *Planta* 182: 420–426.
Tyree MT, Zimmermann MH. 2002. Xylem structure and the ascent of sap, 2nd edition. Springer-Verlag, Berlin, Germany.
Van Pelt R. 2001. Forest giants of the Pacific Coast. University of Washington Press, Seattle, WA.
Waring RH, Running SW. 1978. Sapwood water storage: its contribution to transpiration and effect upon water conductance through the stems of old-growth Douglas-fir. *Plant, Cell & Environment* 1: 131–140.
Waring RH, Whitehead D, Jarvis PG. 1979. The contribution of stored water to transpiration in Scots pine. *Plant, Cell & Environment* 2: 309–317.
White JW, Cook ER, Lawrence JR. 1985. The D/H ratios of sap in trees: implications for water sources and tree ring D/H ratios. *Geochimica et Cosmochimica Acta* 49: 237–246.
Wickens GE. 2008. The baobabs: pachycauls of Africa, Madagascar and Australia. Springer Science & Business Media.
Willard D. 2000. A Guide to the Sequoia Groves of California. Yosemite Natural History Association, Yosemite National Park, CA.
Williams CB, Anfodillo T, Crivellaro A, Dawson TE, Koch GW. *In review*. Constraints on hydraulic compensation in the Earth's tallest trees. Submitted to *New Phytologist*.
Williams CB, Reese Næsborg R, Dawson TE. 2017. Coping with gravity: the foliar water relations of giant sequoia. *Tree Physiology* 37: 1312–1326.
Woodruff DR, Bond BJ, Meinzer FC. 2004. Does turgor limit growth in tall trees? *Plant, Cell & Environment* 27: 229–236.
Wullschleger SD, Meinzer FC, Vertessey RA. 1998. A review of whole-plant water use studies in trees. *Tree Physiology* 18: 499–512.
Zeppel M. 2013. Convergence of tree water use and hydraulic architecture in water-limited regions: a review and synthesis. *Ecohydrology* 6: 889–900.
Zweifel R, Item H, Häsler R. 2000. Stem radius changes and their relation to stored water in stems of young Norway spruce trees. *Trees* 15: 50–57.

Zweifel R, Item H, Häsler R. 2001. Link between diurnal stem radius changes and tree water relations. *Tree Physiology* 21: 869–877.
Zweifel R, Drew D, Schweingruber F, Downes GM. 2014. Xylem as the main origin of stem radius changes in *Eucalyptus*. *Functional Plant Biology* 41: 520–534.